

รายงานวิจัยฉบับสมบูรณ์

การศึกษาคุณลักษณะ การกระจาย และการประยุกต์ใช้ฮอร์โมนที่ควบคุมการหลั่งฮอร์โมนกระตุ้นต่อมเพศของกุ้งขาว

Characterizations, Localization, and Possible applications of gonadotropin-releasing hormone (GnRHs) for stimulating ovarian maturation and spawning in the Pacific white shrimp, *Litopenaeus vannamei*

โดย

ผศ.ดร.ยสวันต์ ตินิกุล และคณะ
มหาวิทยาลัยมหิดล วิทยาเขตนครสวรรค์

มิถุนายน 2556

สัญญาเลขที่ MRG5480061

รายงานวิจัยฉบับสมบูรณ์

โครงการ: การศึกษาคุณลักษณะ การกระจาย และการประยุกต์ใช้ฮอร์โมนที่ควบคุมการหลั่งฮอร์โมนกระตุ้นต่อมเพศของกุ้งขาว

Characterizations, Localization, and Possible applications of gonadotropin-releasing hormone (GnRHs) for stimulating ovarian maturation and spawning in the Pacific white shrimp, *Litopenaeus vannamei*

หัวหน้าโครงการวิจัย:

ผศ.ดร. ยสวันต์ ตินิกุล

มหาวิทยาลัยมหิดล วิทยาเขตนครสวรรค์

นักวิจัยที่ปรึกษาโครงการวิจัย:

ศ.ดร.ประเสริฐ โศภน

ภาควิชากายวิภาคศาสตร์ คณะวิทยาศาสตร์ มหาวิทยาลัยมหิดล

ระยะเวลาโครงการ: 15 มิถุนายน 2554 ถึง 15 มิถุนายน 2556

สนับสนุนโดยสำนักงานคณะกรรมการการอุดมศึกษา สำนักงานกองทุนสนับสนุนการวิจัย
และมหาวิทยาลัยมหิดล
(ความเห็นในรายงานนี้เป็นของผู้วิจัย สกอ. และ สกว. ไม่จำเป็นต้องเห็นด้วยเสมอไป)

ACKNOWLEDGEMENTS

I would like to acknowledge the support of many people, without whom this project would not have been accomplished. First, I would like to express my gratefulness and deep appreciation to my major mentor, Prof. Dr. Prasert Sobhon, for his kindness, encouragement, excellent suggestions, counseling, support throughout this project, and for the revision of my manuscripts. My grateful appreciation is also extended to Prof. Dr. Peter J Hanna for their constructive comments, valuable guidance, research directions, and for the revision of my manuscripts. As well, I wish to express my gratefulness to Dr. Sompong Yoongtong, Vice President of Mahidol University, Nakhonsawan Campus, Nakhonsawan province, for providing the opportunities for me to conduct researches and valuable advices. Moreover, I would also like to express my gratefulness to Assoc. Prof. Dr. Chaitip Wanichanon for their valuable advices. I am extremely grateful to my oversea mentor, Assoc. Prof. Dr. Scott Cummins, at the Faculty of Science, Health and Education, University of the Sunshine Coast, Queensland, Australia, for his kindness, encouragement, precious mentoring, sharing his knowledge, and constructive advice on my works during my project.

My special thank is expressed to Dr. Ruchanok Tinikul for her kindness, helpful suggestions, patience, and supportive encouragement. In addition, my special gratitude is also extended to Dr. Jaruwan Ponjaroen, Dr. Charoonroj Chotwiwatthanakun, Dr. Panat Anuracpreeda, Dr. Napamanee Kornthong, Dr. Piyachat Chansela, Dr. Parinyaporn Nuurai and Dr. Ittipon Phoungpetchara for their helps, valuable advices, and companionships. I would also like to thank Mr. Tanes Poomtong, Mr. Nipon Senin, Mr. Li and Mrs. Ping, Ms. Nattakarn, Ms. Samaitong Ciangjen and Mr. Anurak Prabyai for their help and useful suggestions. I also thank Center of Nanoimaging (CNI) and Olympus Bioimaging Centers, Faculty of Science, Mahidol University for the use of a confocal microscope and technical assistance. I would like to thank members at the Electron Microscopy and Cell Biology Laboratories (EM), and all staffs at Department of Anatomy, Faculty of Science, Mahidol University, for their infinite help and sharing a good time together. My special gratitude is also extended to all staffs at Central Instrument Facility (CIF), Faculty of Science, Mahidol University.

I would like to acknowledge the financial support from a Research Grant for New Scholar to me (co-funded by the Thailand Research Fund, the Commission on Higher Education and Mahidol University, grant no. MRG5480061), and a Distinguished Research Professor Grant to Prof. Prasert Sobhon (jointly funded by the Thailand Research Fund, the Commission on Higher Education, and Mahidol University). Last of all, but the most on my mind, I am wholeheartedly grateful to my dearest mother, Mrs. Sirikul Tinikul and my family for their endless love, trust, and encouragement during my project study, which enables me to carry out and overcome all obstacles. Words are never enough to express how grateful I am for what they have done for me.

Assist. Prof. Dr. Yotsawan Tinikul

June 2013

บทคัดย่อ

รหัสโครงการ : MRG5480061

ชื่อโครงการ : การศึกษาคุณลักษณะ การกระจาย และการประยุกต์ใช้ฮอร์โมนที่ควบคุมการหลั่งฮอร์โมนกระตุ้นต่อมเพศของกุ้งขาว

ชื่อนักวิจัย: ผศ.ดร.ยสวันต์ ตินิกุล (หัวหน้าโครงการวิจัย)
ศ.ดร.ประเสริฐ โศภน (นักวิจัยที่ปรึกษาโครงการวิจัย)
อีเมล์ : anatch2002@yahoo.com

ระยะเวลาโครงการ : 15 มิถุนายน 2554 ถึง 15 มิถุนายน 2556

กุ้งขาว *(Litopenaeus vannamei)* เป็นสัตว์น้ำที่มีคุณค่าสูงทางเศรษฐกิจของประเทศไทย ซึ่งมีการเพาะเลี้ยงกันอย่างกว้างขวางในแถบภูมิภาคเอเชีย ปัญหาและอุปสรรคที่มักจะพบในการเพาะเลี้ยงกุ้งขาวในปัจจุบัน คือ การตัดตาแม่พันธุ์กุ้ง (eyestalk ablation) เพื่อกระตุ้นการพัฒนาของรังไข่ (ovarian maturation) และการฟักออกเป็นตัว (spawning) ของลูกกุ้งให้เร็วขึ้น ซึ่งวิธีการเหล่านี้นอกจากจะเป็นวิธีการทรมานกุ้งแล้ว ยังส่งผลต่ออายุขัยและจำนวนครั้งของการสืบพันธุ์ของแม่พันธุ์กุ้ง และปริมาณของลูกกุ้งในแต่ละครั้งด้วย ซึ่งวิธีการเหล่านี้อาจจะไม่เป็นที่ยอมรับในอนาคต ได้มีการรายงานมาก่อนว่า gonadotropin-releasing hormone (GnRH) มีผลต่อวงจรของการพัฒนาของรังไข่ของสัตว์น้ำกลุ่ม crustacean ชนิดอื่น และอาจจะมีผลต่อวงจรการพัฒนาของรังไข่ในกุ้งขาวด้วย ดังนั้นวัตถุประสงค์หลักของโครงการวิจัยนี้คือ ทำการตรวจสอบผลของ GnRH ต่อวงจรการพัฒนาของรังไข่และการตกไข่ นอกจากนี้เราได้ศึกษาระดับ การปรากฏและการกระจายของสารสื่อประสาทหลักและความสัมพันธ์ที่เป็นไปได้กับ GnRH ในกุ้งขาว เพื่อเป็นพื้นฐานนำไปสู่การศึกษาความสัมพันธ์ของการทำงานร่วมกันของสารนิวโรเปปไทด์และสารสื่อประสาท เราได้ทำการกระตุ้นพ่อแม่พันธุ์กุ้งขาวด้วย GnRH isoforms ซึ่งน่าจะมีคุณลักษณะที่ใกล้เคียงและอยู่ในสัตว์ที่มีระดับความสัมพันธ์เชิงวิวัฒนาการใกล้เคียงกับกุ้งขาวมากที่สุด คือ octopus-GnRH และ lampreyGnRH-III ต่อผลการพัฒนาของรังไข่และการตกไข่ การศึกษาการกระจายตัวของสารสื่อประสาทในเนื้อเยื่อระบบประสาทกลางและรังไข่ของกุ้งขาวด้วยกรรมวิธี HPLC และ immunohistochemistry เพื่อบ่งชี้ระดับและระบุตำแหน่งของเซลล์และโครงสร้างที่อยู่ในระบบประสาทส่วนกลางและรังไข่ จากการวิจัยในครั้งนี้มีประโยชน์ โดยอาจจะนำ GnRH มาใช้ในการกระตุ้นการพัฒนาของรังไข่และการฟักออกเป็นตัว (spawning) ของลูกกุ้งขาวให้เร็วขึ้นแทนการใช้วิธีตัดตาได้ในอนาคต

คำสำคัญ: โกนาโดโทรปินรีลิสซิ่งฮอร์โมน, ซีโรโทนิน, โดพามีน, ระบบประสาทส่วนกลาง, รังไข่, วิธีอิมมูโนฮีสโตเคมีสทรี, กุ้งขาว

Abstract

Project Code : MRG5480061

Project Title : Characterizations, Localization, and Possible applications of gonadotropin-releasing hormone (GnRHs) for stimulating ovarian maturation and spawning in the Pacific white shrimp, *Litopenaeus vannamei*

Investigators : Assist. Prof. Dr. Yotsawan Tinikul (Principal investigator)
Prof. Dr. Prasert Sobhon (Mentor)

E-mail Address : anatch2002@yahoo.com

Project Period : 15 June 2011 to 15 June 2013

The Pacific white shrimp, *Litopenaeus vannamei*, is a commercially important species in Thailand. One major drawback in the aquaculture of this shrimp is that female broodstocks must have their eyestalks ablated to stimulate ovarian maturation of the ovary. Stimulation by gonadotropin-releasing hormone (GnRH) could conceivably avoid the eyestalk ablation as it could over-ride the inhibition of the gonad-inhibiting hormone (GIH) produced by the eyestalk. In this proposal, we investigated the effects of GnRHs (octopusGnRH (OctGnRH) and lampreyGnRH-III (lGnRH-III), and dopamine on ovarian maturation and spawning, and study of the existence and possible relationship of GnRH and major neurotransmitters in the CNS and ovaries during ovarian maturation in *L. vannamei.* We found that both GnRH groups showed significantly shortened ovarian maturation period, increased GSI and OD, whereas DA-injected groups exhibited significantly delayed ovarian maturation, decreased GSI and OD, compared with control groups. The numbers of eggs per spawn among experimental groups showed no statistical difference compared with the control group. Both GnRH-irs were more intense in the follicular cells surrounding Oc2 and Oc3. These findings also suggest that GnRHs have a stimulating effect in stimulating ovarian maturation, while DA may play opposite role. Furthermore, we studied the changes in serotonin (5-HT) and dopamine (DA) levels, and their distribution patterns, in regions of the central nervous system (CNS) and ovary, during the ovarian maturation cycle to better understanding about the relationship of neurotransmitters and GnRHs. 5-HT concentration exhibited a gradual increase in the brain and thoracic ganglia, and reaching a maximum at the mature ovarian stage IV. In contrast, DA showed the highest concentration at ovarian stage II in the brain and thoracic ganglia, and then declined to the lowest concentration at ovarian stage IV. In the ovaries, 5-HT was highest at ovarian stage IV, whereas the concentration of DA was highest at ovarian stage II. 5-HT-ir and DA-ir were distributed extensively in neurons, fibers, and neuropils in the brain, CEG, SEG, thoracic ganglia and abdominal ganglia. In the ovary, 5-HT-ir exhibited high intensity in late oocytes, whereas DA-ir was more intense in early oocytes. This work showed opposing changes in the levels of these two neurotransmitters, and their specific localizations in the CNS and ovary, during ovarian maturation. Overall, this research could provide a useful knowledge for important involvements of GnRH and neurotransmitters in enhancing female white shrimp reproduction.

Keywords: Gonadotropin-releasing hormone; Serotonin, Dopamine; Central nervous system; Ovary; Immunohistochemistry; Pacific white shrimp, *Litopenaeus vannamei*

1. Objectives

Overall Objectives: The aim of this project was to investigate the effects of GnRHs on ovarian maturation and spawning, and to study the existence, distribution and possible relationship of GnRH and major neurotransmitters in the central nervous system and ovaries during ovarian maturation in the Pacific white shrimp, *L. vannamei.*

Specific Objectives: In order to reach the above goals, the following specific objectives are defined as follows:

1.1 Investigating the effects of GnRHs on ovarian maturation and spawning in the white shrimp, *L. vannamei*.

1.2 Studying the existence, distribution and possible relationship of GnRH and major neurotransmitters in the central nervous system and ovaries during ovarian maturation.

PART I. Investigation of the effects of GnRHs on ovarian maturation and spawning in the white shrimp, *L. vannamei*

1. Introduction

The Pacific white shrimp, *Litopenaeus vannamei*, is a major seafood that is cultured worldwide in Thailand and other Asian countries (Tsukimura and Kamemoto, 1991). Eyestalk ablation of this, and other decapod crustaceans, was practiced to increase the production through induction of gonad maturation and spawning. Therefore, attempts have been made in using various neurotransmitters and neuropeptides to prime female broodstocks in order to avoid this damaging practice. The synthesis and release of neurohormones in crustaceans are believed to be controlled by biogenic amines (Richardson et al., 1991), two of which are the neurotransmitters, serotonin (5-HT) and dopamine (DA). 5-HT has been

reported as having a role in the regulation of crustacean reproduction, especially ovarian maturation, in which it shortens the ovarian maturation period in the crayfish, *P. clarkii* (Kulkarni et al., 1992), the white shrimp*, L. vannamei* (Vaca and Alfaro, 2000; Alfaro et al., 2004), the black tiger shrimp, *Penaeus monodon* (Wongprasert et al., 2006), and the giant freshwater prawn, *M. rosenbergii* (Tinikul et al., 2009a). As well, 5-HT has been shown to induce vitellogenin (Vg) levels in the hemolymph of the Indian white shrimp, *Fenneropenaeus indicus* (Santhoshi et al., 2009), and the giant freshwater prawn, *M. rosenbergii* (Tinikul et al., 2008). DA is another major neurotransmitter present in the central nervous system (CNS) and ovaries of crustaceans, including many decapods (Tierney et al., 2003; Tinikul et al 2009b, 2011b). In addition, there have been reports regarding the inhibitory effect of DA on gonadal maturation in decapod crustacans, including the crayfish, *P. clarkii* (Sarojini et al., 1995a), and the freshwater prawn, *M. rosenbergii* (Tinikul et al., 2009a). DA has been thought to have an inhibitory effect on gonadal maturation by stimulating the release of gonad-inhibiting hormone (GIH), and/or by inhibiting the release of a putative gonad-stimulating hormone (GSH) (Fingerman 1997; Tinikul et al., 2008). Furthermore, a DA antagonist, spiperone (SP), increases the gonadosomatic (GSI) index in *P. clarkii,* when injecting during early vitellogenesis (Rodríguez et al., 2002). In male *M. rosenbergii*, DA also inhibits testicular maturation and spermatogenesis (Poljaroen et al., 2011). The inhibitory effects of DA in *M. rosenbergii* on gonad maruration would appear to be opposite to the positive stimulatory effects of 5-HT, but this needs to be tested.

Gonadotropin-releasing hormone (GnRH) is a decapeptide present in both vertebrates and invertebrates (Tsai, 2006). In vertebrates, GnRH regulates the synthesis and release of luteinizing hormone (LH) and follicle-stimulating hormone (FSH) from the pituitary gland, thereby regulating steroidogenesis and

gametogenesis (Tsai, 2006; Sower et al., 2009). GnRHs have recently been investigated in invertebrates, and appear to be both functionally and structurally homologous to vertebrate GnRHs, and some have been found to serve as reproduction-related neuropeptides (Terakado, 2001; Gorbman and Sower, 2003). Although there are reports of the absence of GnRHs in crustaceans (Lindemans et al., 2009; Tsai, 2006), there are an increasing number of reports regarding stimulatory effects of GnRHs on gonad maturation. Female broodstocks of *M. rosenbergii* treated with octopusGnRH, lamprey GnRH-I, or lamprey GnRH-III, showed significantly shortened ovarian maturation than those of control groups (Ngernsoungnern et al., 2009), and similar result was reported in *P. monodon* (Ngernsoungnern et al., 2008a). As well, there have been immunohistochemical based reports regarding the existence of GnRHs in various decapod crustacean tissues, including the CNS and gonads of *M. rosenbergii* (Ngernsoungnern et al., 2008b), *P. monodon* (Ngernsoungnern et al., 2008a), and *L. vannamei* (Tinikul et al., 2011a). Hence, GnRH-like peptides may exist in the white shrimp and play an important role in inducing ovarian maturation. The testing of GnRHs on ovarian maturation and spawning in *L. vannamei* have not been performed, and positive results could lead to enhanced reproduction in this species.

There is a current lack of knowledge regarding the roles of GnRHs and DA in controlling ovarian maturation in the Pacific white shrimp*, L. vannamei*. Some evidence from other important crustacean species indicates that they represent important mediators in reproduction. Therefore, the aim of our study was to investigate the effects of GnRHs and DA on ovarian maturation and spawning, as well as determine whether they are present in the ovaries in *L. vannamei*. In order to stimulate ovarian maturation, we applied 50% lower doses of GnRHs than had been used in other crustaceans, and this yielded significant results. Our study

represents an important step in determining the presence and effects of GnRH in the reproduction of the Pacific white shrimp, and the acquisition of data which could lead to changes in current spawning practices.

2. Materials and methods

2.1. Experimental animals

Male and female broodstocks of *L. vannamei*, weighing 50-60 g body weight (BW), were obtained from a commercial farm in Kui Buri district, Prachaubkirikhan, Thailand. The shrimps were kept in shaded concrete tanks filled to a depth of approximately 1 m with sea water at a temperature of approximately 28 °C, salinity between 30-32 ppt, and continuous aeration. Half the sea water was changed every day. The animals were fed twice daily with fresh squid, oysters and polychates. Male and female shrimps were stocked at a ratio of 1:4, respectively, in the same tank. Twenty plastic cages were added to every tank for molting animals to hide in. The shrimps were acclimatized under a photoperiod of 12:12 h light-dark for a week before beginning the experiments.

2.2. Histological observations of stages of ovaries

The ovarian stages during the maturation cycle were observed directly, and classified on the criteria described previously (Yano et al., 1988; Vaca and Alfaro, 2000; Tinikul et al., 2011a). In order to evaluate the histology after various treatments, pieces of ovaries were fixed in Bouin's fixative and processed for paraffin embedding, as described previously (Tinikul et al., 2011a). The sections were cut at a six-micron thickness from each ovary (n = 5), after which they were

deparaffinized and stained with hematoxylin and eosin (H&E). The sections were mounted with Permount (Bio-Optica, Milan, Italy) and viewed under a Nikon ECLIPSE E600 light microscope. Then images were photographed using a Nikon digital DXM1200 camera.

2.3. Peptides and antibodies

The DA used in this study was purchased (Sigma Chemical Company, St. Louis, MO). The GnRH peptides, octGnRH (pGlu-Asn-Tyr-His-Phe-Ser-Asn-Gly-Trp-His-Pro-Gly-NH_2) and lGnRH-III (pGlu-His-Trp-His-Asp-Trp-Lys-Pro-Gly-NH_2), were custom synthesized (GenScript, Piscataway, NJ, USA). The neurotransmitter and neuropeptides were dissolved in 0.9% normal saline. An antibody to octGnRH was produced previously and its specificity tested rigorously (Tinikul et al., 2011a). In addition, a polyclonal antibody against lGnRH-III was produced previously and its specificity was also tested rigorously (Saeton et al., in press). The female New Zealand white rabbits (8 week-old) used were obtained from the Animal Care Unit, Faculty of Science, Mahidol University, and used with the approval of Mahidol Animal Ethics Committee. In addition, the antidody against DA was purchased from Gemacbio, St. Jean d'Illac, France.

2.4. In vivo effects of GnRHs and DA on ovarian maturation and spawning

The doses of hormones used in this study were based on the positive effects of GnRHs in *M. rosenbergii* (Ngernsoungnern et al., 2009; Poljaroen et al., 2011), and for inhibitory effects of DA in *M. rosenbergii* (Tinikul et al., 2009a). We applied 50% lower doses of GnRHs (i.e., 25 and 250 ng/g BW) in this study, to

those used earlier, in an attempt to stimulate ovarian maturation and spawning at doses of GnRHs that may be used in aquaculture farm practice. All injections were performed at 7-day intervals. The shrimps were randomly divided into 7 groups of 40 animals each, and treated as follows: (1) a vehicle control group (C); (2 and 3) groups injected with octGnRH at 25 and 250 ng/g body weight (BW), respectively; (4 and 5) groups injected with lGnRH-III at 25 and 250 ng/g BW, respectively; and (6 and 7) groups injected with DA at 2.5 $x10^{-7}$ and 2.5 $x\ 10^{-6}$ mol/shrimp. Shrimps in each group were identified by tying plastic loops of different colors around one eyestalk. The injections were performed via an intramuscular site at the second abdominal segment using 1 ml syringes (NIPRO) fitted with a 26 G × 1⁄2 (0.45 × 12 mm) thin-wall needle (NIPRO).

The measurement of total length and weight of the shrimps were performed on every treatment day, prior to injections. Five shrimps in each group were randomly selected and sacrificed at days 0, 7, 14 and 21, to calculate a gonado-somatic index (GSI) and oocyte diameter for each. The GSI was calculated using the formula [ovarian weight (g)/body weight (g)] × 100. The experiment was performed in replicate. GSI values and oocyte diameters of the injected groups and the control groups were then analyzed for differences. The rest of the shrimps were allowed to proceed until they spawned. Pieces of ovary were subsequently fixed in Bouin's solution, paraffin embedded, sectioned, and stained with H&E, in order to determine the stages of ovarian maturation and oocyte diameters under the light microscope. Oocyte diameters were carefully measured as described previously (Tinikul et al., 2009a). Briefly, sixty randomly selected oocytes at each stage of development in each shrimp, and in three separate ovarian regions, were observed under the light microscope. Diameters of

the sixty oocytes that contained full nuclear profiles were measured, and the data expressed as a mean ± SD for each treatment group.

2.5. Evaluation of cell proliferation using antibody against a proliferating cell nuclear antigen (PCNA)

The ovaries from each of the shrimp at days 0, 7, 14, and 21 were dissected out and prepared for detection of the cellular proliferation of oocytes and histological evaluations. The cell proliferation evaluation used antibody against a proliferating cell nuclear antigen (anti-PCNA), and was based on a modified protocol described previously (Boglino et al., 2012). Ovarian sections were cut at a thickness of 6 μm and then rehydrated by washing 3 times in washing buffer (0.1 M phosphate buffered saline, PBS). Endogenous peroxidase activity was then blocked by immersing the sections in methanol containing 1% hydrogen peroxide (H_2O_2). The sections were immersed for 15 min in 1% glycine to block free aldehyde groups, and then washed three times with 0.1 M PBS plus 0.4% Triton-X 100 pH 7.4 (PBST). Subsequently, non-specific binding of proteins was blocked with 4% normal goat serum (NGS) in 0.1 M PBST, for 2 h at room temperature. The sections were washed three times with PBS, and incubated with anti-PCNA rabbit polyclonal antibody (Santa Cruz Biotechnology, CA, USA), at a dilution of 1:100 in PBS, overnight at room temperature. After washing three times, the sections were incubated in secondary antibody, HRP-conjugated goat anti-rabbit IgG (Southern Biotech, Birmingham, AL, USA), diluted 1:200 in blocking solution, for 2 h. The sections were then washed three times and the color reaction developed by adding NovaRed (Vector, Burlingame, CA, USA) until a red color was observed. The sections were washed with tap water for 10 min, and mounted

with the glycerol buffer. Finally, the sections were examined under a Nikon ECLIPSE E600 light microscope, and images were obtained using a Nikon digital DXM1200 camera.

The numbers of PCNA-labelled cells at each oocyte step were counted from 4-5 shrimps per group, using methods described previously (Poljaroen et al., 2011; Tinikul et al., 2011b). Digital images of ovaries at 20x and 40x magnifications were captured, with a resolution of at least 300 dpi. The numbers of PCNA-labelled cells were counted per visual field (mm^2 area) using a Cell Counter function in ImageJ software (version 1.43, NIH, Bethesda, MD, USA, available on the internet at http://rsb.info.nih.gov/ij/). At least five areas in each section, from both positive and negative areas, were counted to compare the numbers of PCNA-labelled cells. The counting was performed in triplicates, and the data expressed as a mean ± SD for each treatment group.

2.6. Processing of tissues for immunohistochemistry

Twenty female shrimps, with five (n = 5) at each of the four stages of the ovarian cycle (Tinikul et al., 2011a), were anesthetized on ice for 15-20 min and the ovaries were dissected out and immediately fixed with 4% paraformaldehyde in 0.1 M phosphate-buffered saline (PBS), for 12-16 h at 4 °C. After fixation and paraffin embedding, the tissue sections were cut at a 6 μm thickness and mounted on slides coated with 3-aminopropyl triethoxy-silane solution (Sigma-Aldrich Co., St. Louis, MO, USA). The sections were deparaffinized and rehydrated through a graded series of ethyl alcohol, for 5 min each, and then processed for immunoperoxidase and immunofluorescence detections.

The method for immunoperoxidase detection was based on that described previously (Tinikul et al., 2011a, 2011b). Rehydrated sections were immersed in 1% lithium carbonate in 70% ethanol, for 15-20 min, and then endogenous peroxidase was blocked by immersing the sections in 3% H_2O_2 in methanol for 45-60 min, and in 1% glycine in 0.1 M PBS for 15-20 min. The sections were washed four times with 0.4% Triton X-100 in 0.1 M PBS (PBST). Subsequently, the blocking of non-specific bindings was performed by incubating the sections in a blocking solution of 10% normal goat serum (NGS) in PBST for 2 h at room temperature. The sections were incubated with: (1) rabbit anti-DA (Gemacbio, St. Jean d'Illac, France) diluted 1:500 with 1% sodium meta-bisulfite, (2) rabbit anti-octGnRH diluted 1:100 in blocking solution, or (3) rabbit anti-lGnRH-III diluted 1:100 in blocking solution, at room temperature overnight. The sections were then incubated with secondary antibody, HRP-conjugated goat anti-rabbit IgG (SouthernBiotech, Birmingham, USA), at a 1:200 dilution in blocking solution, for 2 h. After washing three times, the immunoreactions were developed by immersing the sections in NovaRed substrate (Vector Laboratory, Burlingame, CA, USA), until a red color was observed. Finally, the sections were counterstained with Meyer hematoxylin for nuclei staining, dehydrated, and mounted with mounting reagent (Bio-Optica, Milan, Italy), prior to the examination of the sections under a Nikon ECLIPSE E600 light microscope. The images were photographed using a Nikon digital DXM1200 CCD camera.

In the immunofluorescence detection of GnRHs or DA, rehydrated sections were incubated with 1% glycine in PBS for 10 min, and non-specific binding was blocked by immersion in blocking solution containing 10% NGS in PBST, for 2 h at room temperature. The sections were then incubated with the primary antibody (rabbit anti-DA or rabbit anti-octGnRH, or rabbit anti-lGnRH-III), diluted 1:100 in

the blocking solution, overnight at room temperature. The sections were then incubated in secondary antibody, Alexa488-conjugated goat anti-rabbit IgG (Molecular Probes, Eugene, OR, USA), diluted 1:200 in blocking solution, for 2 h. In addition, the nuclei in sections of the CNS and ovaries were counterstained with ToPro-3 (Molecular Probes), diluted 1:3000 in blocking solution. The sections were mounted in Vectashield (Vector Laboratory, Burlingame, CA, USA). They were then viewed, and images captured, using an Olympus FV1000 confocal laser scanning microscope. Negative controls were performed by replacing the primary antibodies with pre-immune rabbit sera, or preabsorption of the primary antibodies with excess of synthetic GnRHs or DA.

2.7. Statistical analyses

Data were presented as means ± standard deviations. The data were then analyzed for statistical differences with a SPSS program, using one-way analysis of variance (ANOVA) and Duncan's multiple range test. A probability value less than 0.05 (P<0.05) indicated a significant difference.

3. Results

3.1. Effects of GnRH and DA on ovarian maturation and spawning

All shrimps tolerated the injected doses of neuropeptides and neurotransmitter without showing any abnormal behavior. The ovarian maturation periods of shrimps that received octGnRH at doses of 25 and 250 ng/g BW (i.e., 29.30 ± 3.24 and 28.54 ± 2.65 days, respectively), and lGnRH-III at doses of 25 and 250 ng/g BW (i.e., 25.76 ± 3.1 and 23.03 ± 2.02 days, respectively), were all

significantly shorter (P<0.05) than that of the controls (i.e., 38.75 ± 4.16 days) (Fig.1A). In contrast, the DA-injected groups at doses of 2.5 x 10^{-6} and 2.5 x 10^{-7} mol/shrimp showed significantly longer ovarian maturation periods (i.e., 60.8 ± 5.33 and 58.10 ± 5.67 days, respectively) than that of the control group (P<0.05). Moreover, the shrimps injected with octGnRH and lGnRH-III exhibited significantly higher GSI values compared with that of the control group (P<0.05), whereas the two shrimp groups injected with two doses of DA exhibited decreased GSI values compared with the control group (Fig. 1B).

Mean oocyte diameter (OD) of early pre-vitellogenic oocytes (Oc1, Oc2), vitellogenic oocytes (Oc3), and mature oocytes (Oc4), of all shrimp groups injected with octGnRH and lGnRH-III, increased significantly compared with the control group (P<0.05) (Fig. 2A). In contrast, all groups of shrimps injected with DA exhibited significantly decreased diameters of two steps of oocytes, namely Oc3 and Oc4, compared with the control group (P<0.05) (Fig. 2A). GnRH-induced shrimps, whose ovaries were determined to be at stage IV by external observations, underwent spawning on the following night or soon after.

The effect of GnRHs and DA on the quantity of spawned eggs was also evaluated. The number of eggs per spawn, after injections with octGnRH and lGnRH-III at doses of 25 and 250 ng/g BW, were approximately 98 x 10^{3} and 101 x 10^{3} eggs, respectively, and these values were not significantly different to the control group with 102 x 10^{3} eggs (P>0.05) (Fig. 2B). In contrast, the DA injected groups at doses of 2.5 x 10^{-6} and 2.5 x 10^{-7} mol/shrimp both yielded approximately 83 x 10^{3} eggs per prawn, which was lower compared with the control group, but not significantly different (P>0.05) (Fig. 2B). In addition, the number of spawners was 61.54% in the control group, compared with 69.23%,

76.92%, and 46.15% for the octGnRH, lGnRH-III, and DA -injected shrimps, respectively.

3.2. Histological evaluation of ovarian maturation

Histological evaluation of the diameters of oocytes detected after hormonal injections was performed to evaluate the ovarian maturation (Fig. 3). At days 0 and 7, there were no statistical differences among the injected groups and control group, as the ovaries contained mostly early previtellogenic oocytes (Oc1), and few late previtellogenic oocytes (Oc2). Distinct differences were observed at day 21, when the ovaries of the control group contained mostly early vitellogenic oocytes (Oc3), and few late previtellogenic oocytes (Oc2), whilst the ovaries of groups injected with octGnRH (at 250 ng/g BW) and lGnRH-III (at 25 and 250 ng/g BW) were mostly at stage IV of ovarian maturation, containing mostly mature oocytes (Oc4) with numerous cortical rods (CRs) (Fig. 3B-C). In addition, the diameters of mature oocytes in the GnRH-injected groups were greater than those of the control group (Fig. 3B-C). In contrast, the ovaries of two DA-injected groups on day 21 had only developed to stage II, and contained only a few early and late previtellogenic oocytes (Oc1 and Oc2) with decreased oocyte diameters, compared with the control group (Fig. 3D).

3.3. Determination of cell proliferation in early steps of oocytes

We selected and counted the PCNA-positive oogonia (Og), early previtellogenic oocytes (Oc1), and late previtellogenic oocytes (Oc2), as these three oocyte steps normally exhibited high rates cell proliferation (Fig. 4). At day 0,

PCNA-labeled cells of all groups were detected as oogonia and previtellogenic oocytes (Oc1), and these exhibited no statistical differences (P>0.05). At day 14, after injections with both doses of octGnRH and lGnRH-III, significantly greater numbers of PCNA-labeled oogonia and previtellogenic oocytes (Oc1-Oc2) were detected, compared with the control group (P<0.05) (Fig. 4). The numbers of PCNA-labeled cells decreased considerably, in particular the oogonia and previtellogenic oocytes, after injections with DA at the dose of 2.5×10^{-6} mol/shrimp (Fig. 4). No PCNA labeling was seen in mature oocytes (Oc3, Oc4).

3.4. The existence of octGnRH, lGnRH-III and DA immunoreactivities in the ovaries

In the ovaries, DA-ir was present in the cytoplasm of early and late previellogenic oocytes (Oc1 and Oc2) (Fig. 5B). In contrast, intense octGnRH-ir and lGnRH-III-ir was present in the follicular cells surrounding Oc2 and Oc3 (Fig. 5C-D). The control sections of the ovary showed no staining (Fig. 5A), and the oogonia were not immunoreactive (data not shown).

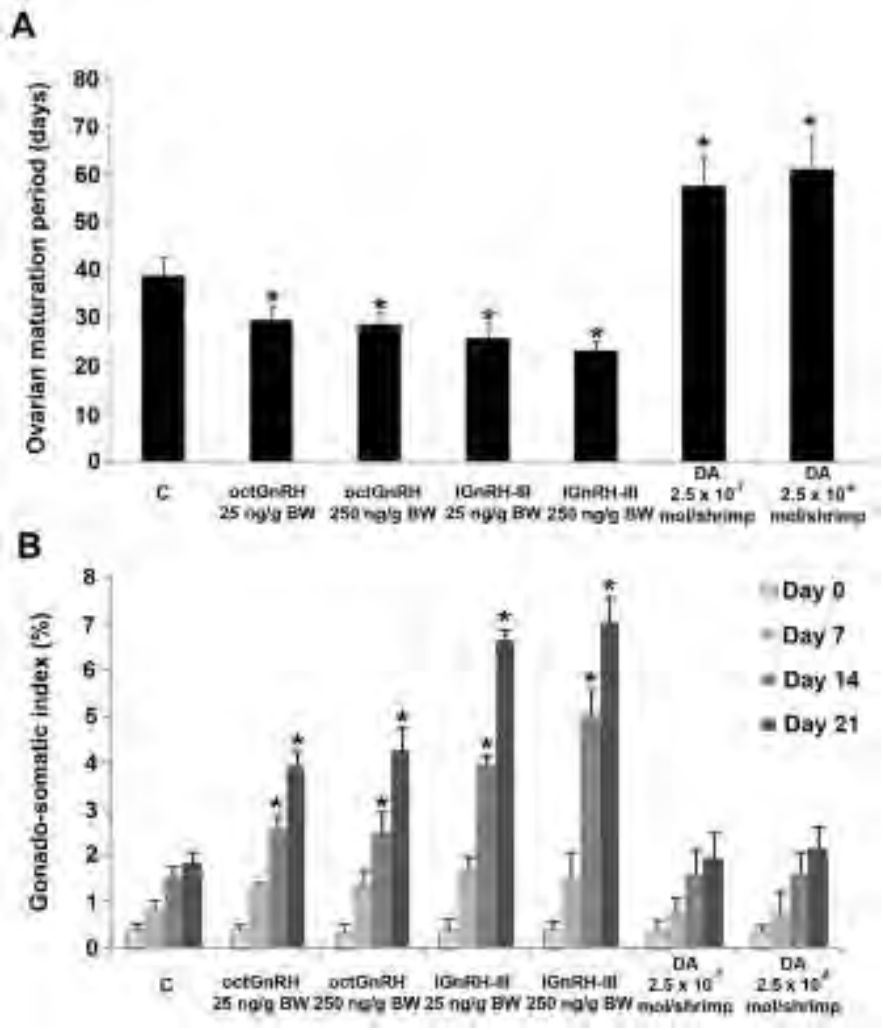

Fig. 1. Effects of GnRHs and DA on the ovarian maturation period in *L. vannamei*. (A) Histograms showing that shrimps injected with octGnRH, lGnRH-III exhibited significant shortening, while DA lengthening ovarian maturation period compared with the control group. (B) Mean gonado-somatic index (GSI) values after the same injections, evaluated at 0, 7, 14, and 21 days treatment.The groups injected with octGnRH (at 25 and 250 ng/g BW) and lGnRH-III (at 25 and 250 ng/g BW), showing significant increases of GSI by day 14 and 22, whereas DA showed no significant difference from the control group. GSI are presented as mean ± SD. Asterisks indicate significant differences (P<0.05).

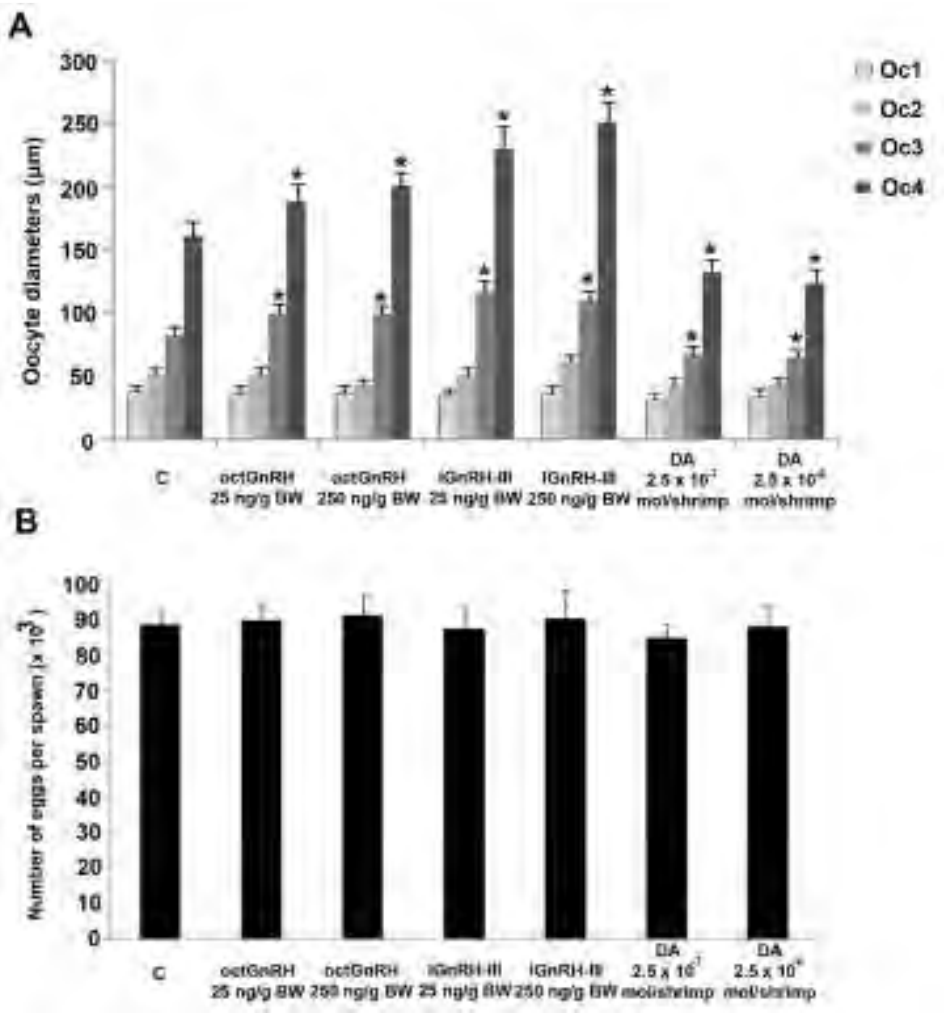

Fig. 2. (A) Histograms showing the diameters of oocytes 1 to 4 (Oc1-Oc4) after injections with octGnRH, lGnRH-III and DA compared with the control group. Columns represent mean ± SD of the diameters. Asterisks indicate significant differences, compared with the control group (P<0.05). (B) Numbers of eggs per spawned after injection with doses of octGnRH, lGnRH-III and DA, compared with the control (C).

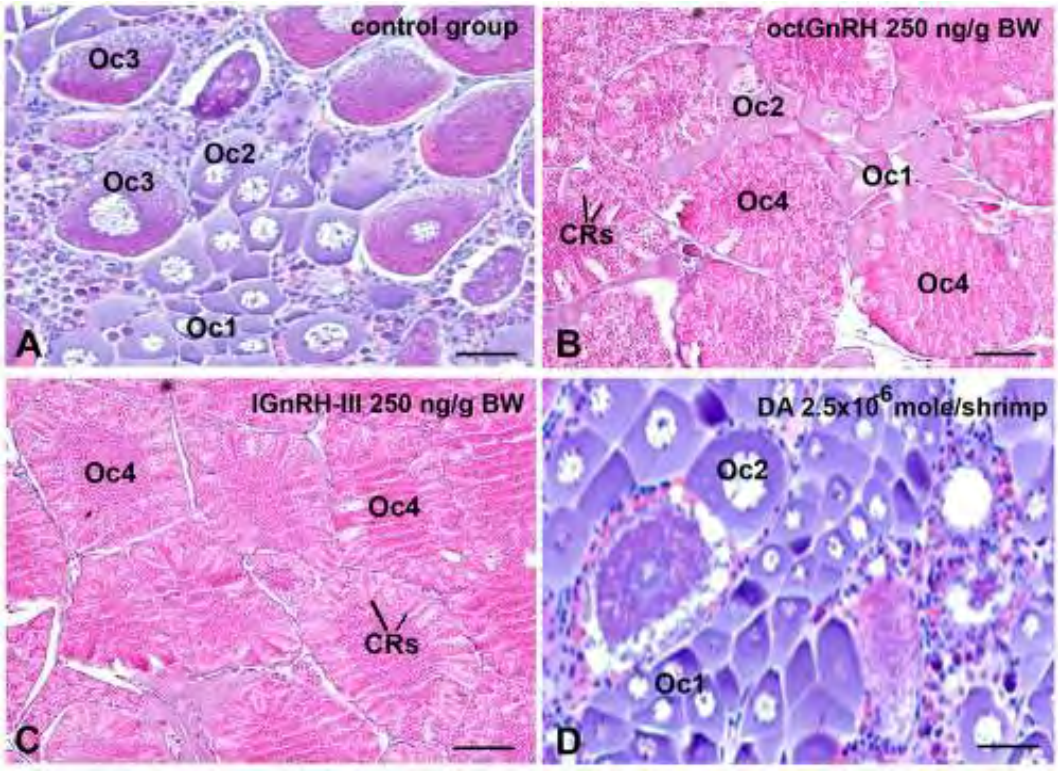

Fig. 3. Effects of octGnRH, lGnRH-III, and DA, on ovarian histology. (A) Ovaries of the control group on day 21 after injection with normal saline, showing characteristics of early ovarian stages II-III. (B-C) Ovaries of groups injected with octGnRH-injected (250 ng/g BW), lGnRH-III-injected (250 ng/g BW), on day 21 demonstrating characteristics of stage IV, containing fully mature oocytes with cortical rods. (D) DA-injected group (2.5 x 10^{-6} mol/shrimp) showing characteristics of stage I, contained mostly early previtellogenic oocytes. CRs, cortical rods; Oc1, early previtellogenic oocyte; Oc2, late previtellogenic oocyte; Oc3, early vitellogenic oocyte; Oc4, late vitellogenic oocyte; mOc, mature oocyte; Scale bars, 50 µm.

4. Discussion

Injecting octGnRH and lGnRH-III into mature female *L. vannamei* shortened the ovarian maturation period by about two weeks compared with that of the control group. In addition, the GnRHs caused significant increases in GSI and oocyte diameter values compared with the control group. The DA-injected groups showed the opposite results. DA-ir and GnRH-ir were present in different regions of the ovaries, with DA-ir located in the early oocytes and both GnRH immunoreactivities were intense in follicular cells surrounding Oc2 and Oc3.

There have been several reports investigating DA in regulating the ovarian maturation or embryonic development period. In the freshwater prawn, *M. rosenbergii*, DA lengthened ovarian maturation, spawning periods, and embryonic development (Tinikul et al., 2009a), and prolonged ovarian maturation and decreased GSI values of juvenile crayfish, *Cherax quadricarinatus* (Tropea and López Greco, in press). In the freshwater crab, *Oziotelphusa senex senex,* DA delayed ovarian maturation in eyestalk-ablated crabs. It was suggested that DA may control ovarian maturation by inhibiting the release of vitellogenin stimulating hormone (VSH) from the brain and thoracic ganglion, or having a possible direct action on ovaries (Sainath and Reddy, 2010, 2011). In *M. rosenbergii*, vitellogenin (Vg) concentrations of the shrimps treated with DA were lower at ovarian stage IV (Tinikul et al. 2008). Moreover, DA inhibits Vg concentrations in the fiddler crab, *Uca pugilator* (Sarojini et al., 1995c). These results also indicated a direct causal relationship, with DA preventing Vg synthesis by inhibiting the release of putative GSH, by stimulating the release of GIH from the eyestalks, or through a combination of these two mechanisms rather than directly on the target organ (Sarojini et al., 1995b; Chen et al., 1999, 2003). Our study is the first to report the negative effect of DA on ovarian maturation and spawning in *L. vannamei*. We

postulated that this neurotransmitter may act via the inhibition of putative GSH release and/or the stimulation of GIH release. Although the role of DA is not clearly known, it is also possible that DA might also delay oocyte maturation in *L. vannamei* by promoting meiotic arrest at the end of prophase stage, as our study showed that the oocytes of DA treated shrimp do not proliferate. However, this needs to be studied further.

Several studies have described the distribution and key roles for DA in oocyte maturation in decapod crustaceans. DA-ir is most intense in the ectoplasm of previtellogenic oocytes (Oc1, Oc2), but not in oogonia or follicular cells, indicating that DA plays a key role in regulating early oocyte development (Tinikul et al. 2009b). In the oyster, *C. angulata,* DA and a DA receptor were highly expressed in the early stages of ovarian cycle. It was suggested that the binding of DA to the *C. angulata*-DA1 receptor could play a major role in the early oocyte development (Yang et al., 2013). In the present study, we localized DA in the ovaries in order to confirm the existence and coincidental relationship of DA function on ovarian maturation. We found that DA-ir is more intense in the cytoplasm of the previtellogenic stage oocytes (Oc1, Oc2) in *L. vannamei* and this is in agreement with our previous report in *M. rosenbergii* (Tinikul et al., 2009b), in which it was suggested that DA might be taken up into the oocytes from the hemolymph, or this neurotransmitter might be synthesized within the oocytes. Previously, the concentration of DA in the ovary of *L. vannamei* was quantitated using HPLC analysis and the study showed that it was significantly higher in early ovarian stages (stages I–II) than in the late and mature stages (ovarian stages III–IV) (Tinikul et al., 2011b). In *M. rosenbergii*, DA concentrations in the ovary appear to be higher in the early stages (I and II), and DA-ir is more intense in early oocytes (Tinikul et al. 2009b). This implies that DA may play a major role in

regulating the early oocyte development. However, the precise actions of DA in oocyte development needed to be clarified by further studies.

Several studies have investigated the effects of GnRHs in decapod crustaceans. In female *M. rosenbergii* and *P. monodon,* injections with octGnRH and lGnRH-III shortened ovarian maturation period, increased GSI and oocyte diameter (Ngernsoungnern et al. 2008c, 2009). In male *M. rosenbergii,* GnRH also stimulated spermatogenesis and testicular maturation by increasing significantly testis-somatic index (TSI) and germ cell proliferation (Poljaroen et al. 2011). Our study is the first to report the positive effects of GnRHs on ovarian maturation development in *L. vannamei*. We used two times lower doses of GnRHs (i.e., 25 and 250 ng/g BW) than earlier reports (Ngernsoungnern et al., 2009; Poljaroen et al., 2011). Clearly, the use of lower doses of GnRHs in this study could still elicited positive results in shortening ovarian maturation periods in *L. vannamei*. The lowest GnRH dose of 25 ng/g BW was effective and could be tested in aquaculture farm practice.

In regard to oogenesis, PCNA-labelled cells were observed in a high number of oogonia and pre-vitellogenic oocytes in the groups receiving GnRH stimulation, while the groups injected with DA showed significantly lower number of PCNA-stained cells. This suggested that GnRH stimulates the early germ cell proliferation and differentiation, whereas DA inhibits the processes. The presence of PCNA may serve as a reliable marker of cell proliferation processes occurring in the ovaries. However, the mechanism of action of GnRH and DA on cell proliferation requires further studies.

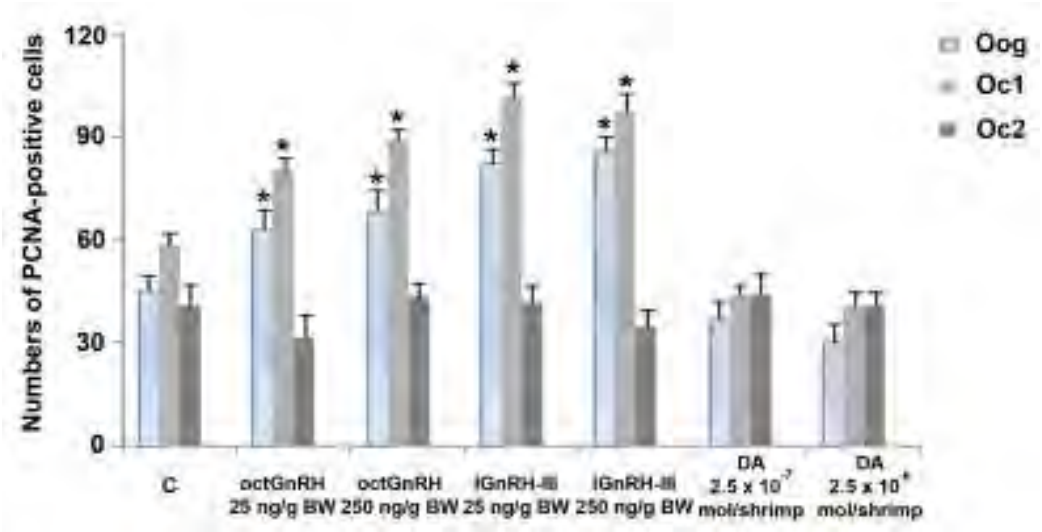

Fig. 4. Histograms showing the numbers of PCNA-labeled cells per mm^2 ($\bar{x}$ ± SD) in oogonia(Oog) and early oocytes (Oc1, and Oc2) at day 14 after injections with octGnRH, lGnRH-III, and DA. Each column represents the number of dividing cells as the mean ± SD. Asterisks indicate significant differences compared with the control group (P<0.05).

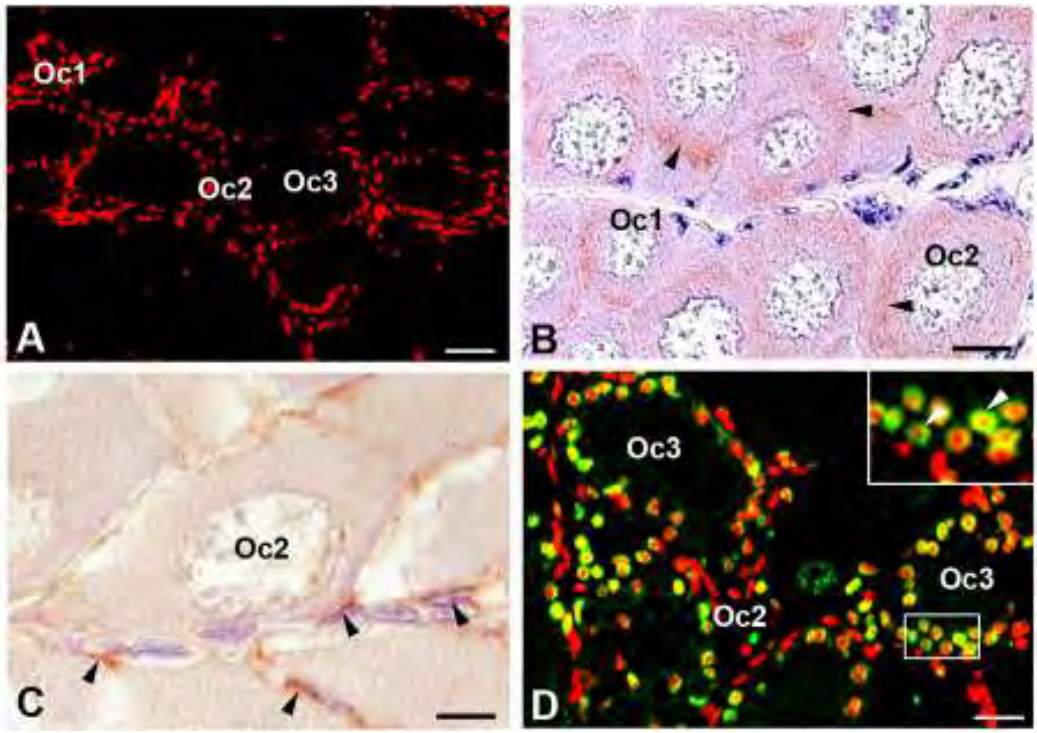

Fig. 5. Immunolocalization of immunoreactivities (-ir) of octGnRH, lGnRH-III and DA in the ovaries. (A) Control section of the oocytes showing no immunoreactivity. (B) DA-ir appeared intense in early oocytes (Oc1 and Oc2). (C) octGnRH-ir was detectd in the follicular cells surrounding early oocytes (Oc2 and Oc3). (D) Intense lGnRH-III-ir appeared in the follicular cells surrounding early oocytes (Oc2 and Oc3). The inset in D shows the immunoreactivity in follicular cells at high magnification (arrowheads).

Immunohistochemically, many studies have reported the presence of GnRH-like peptides in the ovaries of decapod crustaceans, including *P. monodon* and *M. rosenbergii*, using antibodies against octGnRH, lGnRH-I, and lGnRH-III. Strong lGnRH-I-ir was detected in the cytoplasm of late previtellogenic oocytes (Oc2) and in the cytoplasm of the follicular cells surrounding vitellogenic stage oocytes of *P. monodon* (Ngernsoungnern et al., 2008a), and of *M. rosenbergii* (Ngernsoungnern et al., 2008b). In *L. vannamei*, octGnRH-ir and tGnRH-I-ir was detected in both the cytoplasm of previtellogenic oocytes (Oc2), vitellogenic oocytes (Oc3), mature oocytes (Oc4), as well as in follicular cells, especially those surrounding the Oc2 and Oc3. It has been suggested that a GnRH-like peptide might be produced in both oocytes and in the follicular cells (Tinikul et al., 2011a). In our present study, we showed that both lGnRH-III and octGnRH-ir were more intense in the follicular cells surrounding previtellogenic oocytes. It is possible that GnRH may play a key role in controlling oocyte development and ovarian maturation in *L. vannamei* through synthesis within the follicular cells, and its local release may act in a paracrine fashion to induce ovarian maturation and spawning. However, the identity of a crustacean GnRH, and its possible applied benefits, is a high priority of our current research.

PART II. Study of the levels, existence, distribution and possible relationship of major neurotransmitters and GnRH in the CNS and ovaries during ovarian maturation

1. Introduction

In decapod crustaceans, major neurotransmitters that control ovarian maturation are serotonin (5-HT) and dopamine (DA): 5-HT has a stimulating effect on gonadal maturation, perhaps by inhibiting the release of gonad-inhibiting hormone (GIH), and/or by stimulating the release of gonad-stimulating hormone (GSH)/gonadotropins (GnRH), whereas DA plays the opposite role (Sarojini et al., 1995b; Fingerman, 1997). As our previous report (Tinikul et al. 2011), we found that GnRH immunoreactivity (ir) were detected in neurons of various clusters and in neuropils and fibers in the brain, SEG and thoracic ganglia. In the ovary, GnRH immunoreactivity-ir was also detected at medium intensity in the cytoplasm of early step oocytes (Oc2) and, at high intensity, in Oc3. Furthermore, GnRH immunoreactivity-ir was intense in follicular cells surrounding Oc2 and Oc3.

In this research, we have further investigated the possible relationship and actions between GnRH and major neurotransmitters such as 5-HT and DA in controlling reproduction, especially ovarian maturation. These two neurotransmitters may be involved in the synthesis and/or release of GnRH. Therefore, we have additionally determined changes in the levels of 5-HT and DA in various regions of the CNS and ovaries during various phases of the *L. vannamei* ovarian maturation cycle by HPLC. We also have reported the distribution patterns of 5-HT- and DA-ir structures in the CNS and ovary using immunohistochemistry. The implications of data on the opposing roles of the two neurotransmitters are shown. This part of study may provide us some knowledge

regarding the presence of these two neurotransmitters in the CNS and ovaries, and the possible co-actions between 5-HT/DA and GnRH in the white shrimp.

2. Materials and Methods

2.1 Chemicals and sample preparations

All chemicals used in the HPLC experiments, including 5-HT and DA, were obtained from Sigma-Aldrich (St. Louis, MO, USA). Standards of 5-HT and DA were dissolved in ice-cold 0.1 M perchloric acid on the day of analysis. They were then filtered through a 0.45 μm filter and stored on ice between injections into the HPLC system. The brain, subesophageal ganglion (SEG), five thoracic ganglia (combined), the six abdominal ganglia (combined), and the ovaries, were collected at mid-day from ten animals at each ovarian stage. Each organ was carefully dissected out, and its wet weight was determined before being prepared for analysis (see following sections).

2.2 Procedures for quantification of 5-HT and DA concentrations

Detection and quantification of 5-HT and DA in the CNS and ovaries were performed using a High Performance Liquid Chromatography with electrochemical detection (HPLC-ECD). The average concentrations of 5-HT and DA were estimated in three replicates. The quantifications of 5-HT and DA concentrations were based on the methods described previously by Mercier at al. (1991) and Tinikul et al. (2008). After being dissected out and weighed, each tissue of the CNS and ovary was placed in 50 μl of 0.1 M perchloric acid and homogenized at 4 °C. The concentrations of 5-HT and DA were detected electrochemically using a

completely isocratic mode. A glassy carbon electrode, serving as the working electrode was set with an Ag/AgCl reference electrode. The potential of the detector was set at a range between +0.7 to +0.8 V. The sensitivity of the detector was maintained at 100 nA with full scale deflection. The composition of mobile phase was 75 mM NaH_2PO_4, 50 μM EDTA, 0.3 mM sodium octylsulphate, 4% methanol, and 2.5% acetonitrile. The pH was adjusted to 2.75 with orthophosphoric acid. The flow rate was kept constant at 0.7 ml/min. The mixture was sonicated and centrifuged at 14,000 x *g* at 4 °C. The supernatants were collected and then filtered through a 0.22 μm Spin-x centrifugal filter tube (Corning, MA, USA) before injection. Samples were then injected into a 20 μl injection loop and passed onto a Brownlee C_{18}-Aquapore OD-300 HPLC column (250 x 4.6 mm i.d.) (Perkin-Elmer, CT, USA). The electrochemical signals were recorded and integrated using data analysis software (Millennium, Waters). The concentrations of 5-HT and DA were quantified using an external standard method in which peaks corresponding to the two neurotransmitters were detected in the extracts at the same elution times to their corresponding standards. Furthermore, the identities of the peaks were verified by spiking the tissue extracts with appropriate amounts of 5-HT and DA standards in repeated separations. The Bio-Rad Protein Assay System (Mississauga, Canada) was employed for protein determination in the extracts, following that described by Bradford (1976).

2.3 Processing of tissues for immunohistochemistry

Immunofluorescence and immunoperoxidase techniques were used for the detection of 5-HT immunoreactivity (5-HT-ir) and DA immunoreactivity (DA-ir) in neurons, fibers, and neuropils, in various parts of the CNS and ovaries, during

various stages of the ovarian cycle. The methods used were described previously (Mercier et al. 1991; Tinikul et al. 2009b, 2011). For observations of immunoreactivity in whole-mounts, the brain, circumesophageal ganglia (CEG), SEG, thoracic ganglia, abdominal ganglia, and ovaries, were obtained from 20 female shrimps at four stages of the ovarian cycle (n=5 animals per stage). Prior to dissection of the organs, the shrimps were anesthetized on ice for 15 min. The CNS and ovaries were fixed with 4% paraformaldehyde in 0.1 M phosphate-buffered saline (PBS) at 4 °C for 12 h, for 5-HT detection, whereas the CNS was fixed with 4% paraformaldehyde in Millonig's buffer (containing 120 mM NaH_2PO_4, 1% D-glucose, 0.005% $CaCl_2$, buffered with NaOH to pH 7.4) and 1% sodium meta-bisulfite in PBS at 4 °C for 12 h, for DA detection. For observation of the immunoreactivity in sections, another 20 female shrimps (n=5 animals per stage) were used, and organs were dissected out, fixed, and processed by the same protocols as described above. After fixation and paraffin embedding, the tissue sections were cut at 6 µm thickness, mounted on slides coated with 3-aminopropyl triethoxy-silane solution (Sigma-Aldrich Co., St. Louis, MO, USA), then processed for immunoperoxidase and immunofluorescence detections.

2.4 Immunoperoxidase detection

Sections of the CNS and ovaries were deparaffinized with xylene, and rehydrated through a graded series of ethyl alcohol (100%, 95%, 90%, 80%, and 70%), for 5 min each. The sections were then immersed in 1% lithium carbonate in 70% ethanol for 15 min. Subsequently, endogenous peroxidase and free aldehyde groups were removed by immersing the sections in 3% H_2O_2 in methanol for 45 min, followed by 1% glycine in 0.1 M PBS for 15 min. The

sections were then washed three times with 0.4% Triton X-100 with 1% sodium meta-bisulfite in 0.1 M PBS (PBST). Non-specific binding of proteins was blocked by incubating the sections in blocking solution (10% normal goat serum (NGS), 0.4% Triton X-100, 1% sodium meta-bisulfite in PBS), at room temperature for 2 h. The sections were subsequently incubated overnight in the primary antibodies, rabbit anti-5-HT (Chemicon International, USA), diluted 1:100 in blocking solution, or rabbit anti-DA (Gemacbio, St. Jean d'Illac, France), diluted 1:500 in blocking solution, at room temperature. After washing three times, the sections were incubated for 2 h in secondary antibody, HRP-conjugated goat anti-rabbit IgG (SouthernBiotech, Birmingham, AL, USA), diluted 1:200 in blocking solution, and then washed three times. The color reactions were developed by adding NovaRed (Vector, Burlingame, CA, USA) for 1-5 min, until a red color was observed. Subsequently, the sections were washed with tap water for 15 min, counterstained with Mayer's hematoxylin, dehydrated, and mounted with Permount (Bio-Optica, Milan, Italy). Finally, the sections were examined under a Nikon ECLIPSE E600 light microscope, and images were obtained using a Nikon digital DXM1200 camera.

2.5 Immunofluorescence detection

After fixation, the whole-mounts of the CNS were washed with 0.1 M PBS for 6 h, by changing the washing solution every 30 min. Each CNS was desheathed using microforceps and pre-incubated with 4% Triton X-100-PBS (10% NGS, 4% Triton X-100, 1% sodium meta-bisulfite in PBS) at 4 $^{\circ}$C for 24 h. The tissues were then washed three times with 0.1 M PBS, by changing the washing solution every 15 min. The CNS whole-mounts were then permeabilized

with Dent's solution (80% ethanol, 20% DMSO) at -20 ºC for 8 h, and washed five times with 0.1 M PBS by changing the washing solution every 15 min. The CNS whole-mounts were incubated in the primary antibodies (rabbit anti-5-HT diluted 1:100 or rabbit anti-DA diluted 1:500), in 2% NGS, 0.4% Triton X-100, 1% sodium meta-bisulfite in PBS, at 4 ºC for 6-7 days with gentle shaking. The CNS whole-mounts were then washed five times with PBST by changing the washing solution every 20 min, and followed by two washings with 0.1 M PBS by changing the washing solution every 15 min. The CNS whole-mounts were then incubated in the second antibody, Alexa 488-conjugated goat anti-rabbit IgG (Molecular Probes, Eugene, Oregon, USA), diluted 1:500 in 5% NGS, 0.4% Triton X-100, 1% sodium meta-bisulfite in 0.1 M PBS, at 4 ºC for 72 h, with gentle shaking. In addition, the nuclei of cells in the CNS and ovaries were counterstained with ToPro-3 (Molecular Probes, Eugene, Oregon, USA), diluted 1:2000 in blocking solution. ToPro-3 is either shown in red or blue. The whole-mounts were then washed with PBST for 2 h with six changes, and subsequently with PBS for 1 h with three changes. They were subsequently dehydrated through increasing concentrations of ethanol (50%, 70%, 80%, 90%, 95%, 3×100%), and cleared in methyl salicylate for 30-45 min.

The detection of immunofluorescence in tissue sections was based on the protocol of Tinikul et al. (2011). In brief, the sections were deparaffinized, rehydrated through a graded ethanol series, and incubated with 1% glycine in PBS for 10 min. Non-specific binding of proteins was blocked by immersing the sections in blocking solution (10% NGS and 1% sodium meta-bisulfite in PBST), at room temperature for 2 h. The sections were subsequently incubated overnight in the primary antibodies (rabbit anti-5-HT diluted 1:100 or rabbit anti-DA, diluted 1:500), in blocking solution, at room temperature. The sections were then

incubated in the secondary antibody, Alexa488-conjugated goat anti-rabbit IgG (Molecular Probes, Eugene, OR, USA), diluted at 1:500 in blocking solution, at room temperature for 2 h. In addition, the nuclei of cells were counterstained with ToPro-3 (Molecular Probes), diluted at 1:2000 in blocking solution. Finally, the sections were mounted in Vectashield (Vector Laboratory, Burlingame, CA, USA).

2.6 Confocal laser scanning microscopy and image analysis

The whole-mounts and sections of the CNS, as well as ovarian sections prepared for immunofluorescence detection, were viewed and photographed with an Olympus Fluoview 1000 laser-scanning confocal microscope (Olympus America, Center Valley, PA). The tissues were scanned sequentially for each fluorophore to obtain separate images for each label and an overlay image of all three channels for each optical section. These projected images were produced using subsets of the z-stacks. Furthermore, the digital images were exported and converted from the Olympus confocal system as .tiff images, and then transferred into Photoshop CS software (Adobe Systems Inc., San Jose, CA, USA) to adjust contrast and brightness to obtain optimal clarity. In addition, negative controls for each fluorochrome were scanned using the same parameter settings.

2.7 Estimating the numbers and staining intensities of 5-HT-ir and DA-ir neurons and fibers

The numbers of 5-HT-ir and DA-ir neurons in four whole-mounts of various regions of the brain (protocerebrum, deutocerebrum, and tritocerebrum), CEG, SEG (visceral sensory neuropil (VSN), first maxillary neuropil (MX-I), second maxillary neuropil (MX-II), first maxiliped (MP-I), second maxiliped (MP-II), third

maxiliped neuropils (MP-III)), thoracic ganglia 1-5, and abdominal ganglia 1-6, at each ovarian stage were determined. The methods used were described previously (Phoungpetchara et al. in press). The digital images of tissues at 20x and 40x magnifications were photographed. The images obtained were 512×512 or 1024×1024 pixels. Each image had a resolution of at least 300 dpi. The numbers of 5-HT-ir and DA-ir neurons were counted per visual field (mm^2 area) by using Cell Counter function in ImageJ software (version 1.43, NIH, Bethesda, MD, USA, available on the internet: http://rsb.info.nih.gov/ij/). At least ten areas in each section (15 random sections per organ) from both positive and negative areas were counted to compare the numbers of 5-HT-ir and DA-ir neurons during various stages of ovarian maturation cycle. The counting was performed in triplicates.

The intensities of 5-HT-ir and DA-ir in neurons and fibers in various CNS areas, and at each ovarian stage were quantified using computer image analysis ImageJ software (http://rsb.info.nih.gov/ij/) as described previously (Ngernsoungnern et al. 2008; Swayne et al. 2010). In brief, digital images of the whole-mounts and sections at 20x and 40x magnifications from five randomized sections of each area to be analyzed were obtained. The resolutions and pixels of images were defined as mentioned above, and images were then converted to a grayscale (*Image/Type/8-bit*). A box of 100 × 100 pixels was further generated and placed over the areas of neurons and fibers, to ensure equivalent areas for all analyzed images. Densitometric analysis of staining intensities was conducted using NIH ImageJ software. In addition, the subtract background function (*Process/Subtract Background*) in ImageJ software was used to minimize background signal. The examiners did not know to the identities of the sections to minimize bias in the analysis. Data are expressed as mean ± SEM.

2.8 Specificities of antibodies and controls

The specificities of the polyclonal antibodies against 5-HT and DA were tested by the manufacturer using standard immunohistochemical methods. The manufacturer has demonstrated that anti-5-HT and anti-DA antibodies did not cross-react with other biogenic amines. In the controls, the specificities of anti-5-HT and anti-DA were ascertained by omitting the primary antibodies from the staining, or by pre-absorption of the primary antibodies with 100 µg/ml of synthetic 5-HT or DA (Sigma-Aldrich, St. Louis, MO, USA) at 4 $^{\circ}$C for 16-18 h, before staining (Tierney et al. 1999). In these controls, no immunostaining was observed.

2.9 Statistical analyses

Experimental data were analyzed with the SPSS program for Windows software (version 12.0, SPSS Inc., Chicago, IL, USA) using a one-way analysis of variance (ANOVA) and Tukey's post hoc test. A probability value less than 0.05 ($P < 0.05$) indicated a statistical significance. Data were presented as $\overline{X}$ ± SEM.

3. Results

Stages of ovarian maturation cycle were identified by the appearance and size of ovaries that could be seen through the carapace in live females (Fig. 1a, c, e, g), and these were verified by histological examinations of the ovaries (Fig. 1b, d, f, h). There were four major ovarian stages which include: stage I containing mainly Oc1 (Fig. 1a, b), stage II containing previtellogenic oocytes (Oc1 and Oc2) (Fig. 1c, d), stage III comprising mostly pre-mature Oc3 (Fig. 1e, f), and stage IV containing mainly mature oocytes Oc4 (Fig. 1g, h). The mature Oc4 of stage IV

were characterized by the presence of cortical rods (CRs) around the periphery (Fig. 1h).

3.1 Changes of 5-HT and DA concentrations in the CNS and ovary

In the HPLC-ECD analyses, the standard peaks of DA and 5-HT showed elution times of about 10 and 25 min, respectively (Fig. 2a). The peaks of 5-HT and DA, in extracts of different parts of the CNS, and ovaries, at various reproductive stages, exhibited the same elution times as their corresponding standards (Fig. 2b). Moreover, when 5-HT and DA were added to each sample (repeated three times), higher spiked peaks appeared at the same positions as the standards (data not shown), thereby confirming that the peaks were 5-HT and DA in each of the organ extracts. The concentrations of 5-HT in the brain and thoracic ganglia showed a gradual increase from ovarian stage I, and reached the highest concentration at stage IV (Fig. 2c). The concentration of 5-HT at stage I in the brain was 0.15 ± 0.05 nmol/mg, and then it gradually increased through ovarian stage II (0.22 ± 0.06 nmol/mg) and ovarian stage III (0.45 ± 0.05 nmol/mg) to reach a maximum level (0.62 ± 0.08 nmol/mg) at stage IV. The 5-HT concentration in the brain at stage IV was approximately a 4-fold increase over stage I. The pattern was similar in the thoracic ganglia, where the 5-HT concentration was 0.21 ± 0.07 nmol/mg at ovarian stage I, 0.59 ± 0.12 nmol/mg at stage II, 1.37 ± 0.09 nmol/mg at stage III, and reached the highest level of 1.95 ± 0.12 nmol/mg at stage IV, exhibiting approximately a 9.5-fold increase. In the abdominal ganglia, there was little change in 5-HT concentrations from ovarian stage I to stage II (0.1 ± 0.02 to 0.17 ± 0.03 nmol/mg, respectively), and then a small decrease at ovarian stage III (0.09 ± 0.03 nmol/mg), and stage IV (0.11 ± 0.02 nmol/mg).

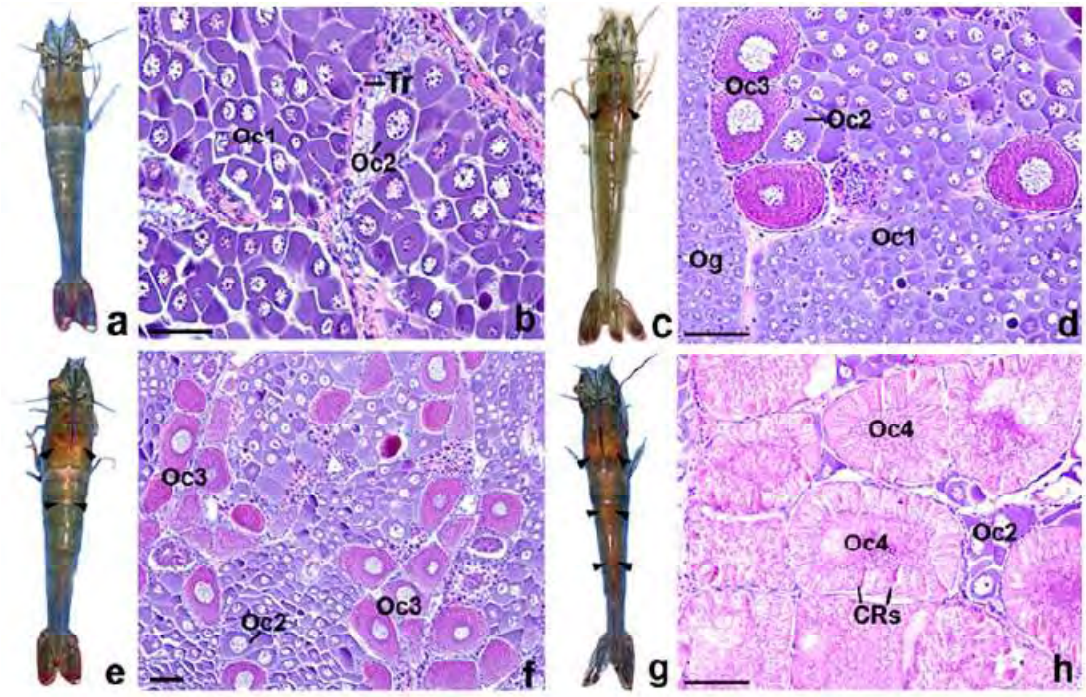

Fig. 1 a, c, e, g Dorsal views of female *L. vannamei*, showing the locations of ovaries (black arrowheads) at four stages of the ovarian maturation: stage I, stage II, stage III, and stage IV, respectively. **b, d, f, h** Light micrographs of H&E-stained sections of the ovarian stages I-IV, demonstrating histology of the oocyte development (Oc1 to Oc4). *CRs* cortical rods, *Og* oogonia, *Oc1* early previtellogenic oocyte, *Oc2* late previtellogenic oocytes, *Oc3* early vitellogenic oocytes, *Oc4* late vitellogenic (mature) oocytes, *Tr* trabeculae. *Bars* 50 μm (**b, d, f, h**)

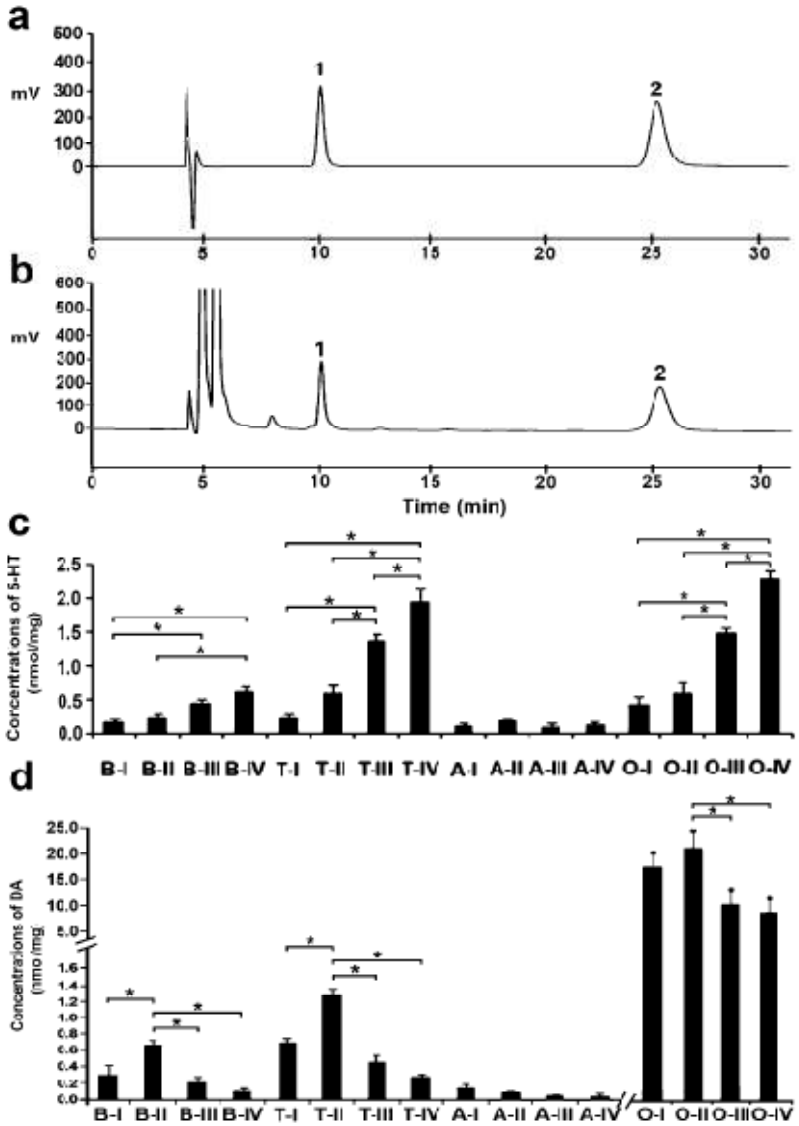

Fig. 2 a HPLC chromatograms of DA (1) and 5-HT (2) standards. The biphasic deflection just before 5 min indicates application of the standards. The standard peaks of DA and 5-HT showed elution times of about 10 and 25 min, respectively. **b** HPLC chromatogram of the brain extract showing DA (1) and 5-HT (2). **c, d** Concentrations of 5-HT and DA, in the brain, thoracic ganglia, abdominal ganglia, and ovary, at stages I-IV of ovarian maturation cycle. Concentrations are expressed as nmol/mg of protein in the organ extracts, and are presented as means ± SEM, with asterisks showing significant differences at $P<0.05$. *B* brain, *T* thoracic ganglia, *A* abdominal ganglia, *O* ovaries.

Interestingly, when various parts of the CNS were compared, the concentration of 5-HT was about 3-4 times higher in the brain at ovarian stage III and IV (P<0.05), respectively, than in the brain at ovarian stage I (Fig. 2c). The concentration of 5-HT was about 2.5, 7, 9.5 times higher in the thoracic ganglia at ovarian stage II, III and IV (P<0.05), respectively, than at stage I. The concentration of 5-HT in the thoracic ganglia at any ovarian stage was about 3 times higher than in the brain, and about 20 times higher than in abdominal ganglia. These results were statistically significant (P<0.05). There were significant increases in 5-HT concentrations in the brain and thoracic ganglia at stages III and IV, compared with stages I and II (P<0.05) (Fig. 2c). In the ovaries, the 5-HT concentration increased from ovarian stage I (0.42 ± 0.12 nmol/mg) to reach a maximum (2.28 ± 0.15 nmol/mg) at ovarian stage IV (P<0.05), exhibiting approximately a 5.5-fold increase (Fig. 2c).

The concentration of DA in the brain (Fig. 2d) increased slightly from ovarian stage I (0.35 ± 0.08 nmol/mg) to stage II (0.71 ± 0.06 nmol/mg), then declined by ovarian stage III (0.21 ± 0.07 nmol/mg), and was at a minimum by stage IV (0.11 ± 0.03 nmol/mg). As well, the concentration of DA in the thoracic ganglia increased from ovarian stage I (1.15 ± 0.06 nmol/mg) to be a little higher at stage II (1.88 ± 0.07 nmol/mg), and then declined during ovarian stages III and IV, (0.91 ± 0.07 and 0.60 ± 0.06 nmol/mg, respectively) (Fig. 2d). The pattern in the abdominal ganglia varied only slightly similar to that of 5-HT. The DA concentration was highest (0.16 ± 0.04 nmol/mg) at ovarian stage I and then decreased during ovarian stages II, III and IV (0.11 ± 0.03, 0.12 ± 0.02, 0.07 ± 0.02 nmol/mg, respectively). However, the minor variations in DA levels in the abdominal ganglia were not statistically significant. At ovarian stages I to IV, the concentrations of DA in the thoracic ganglia were about 3, 2.5, 4.5 and 5.5-fold

higher than in the brain (P<0.05). In addition, the DA concentrations in the thoracic ganglia were higher by 12-fold, 8.5-fold, 7-fold, and 10-fold increases at stages I, II, III, and IV, respectively, compared with the abdominal ganglia (P<0.05). When comparing within a tissue, the concentrations of DA were about 2, 3.5, and 7 times higher in the brain at ovarian stage II than in the brain at ovarian stage I, III, and IV. The DA concentration was about 1.6, 2, and 3 times higher in the thoracic ganglia at ovarian stage II (P<0.05) than in the thoracic ganglia at ovarian stage I, III and IV, respectively. The lowest and the highest concentrations of DA, in each part of the CNS at each ovarian stage, were the converse of those for 5-HT (Fig. 2d).

The concentration of DA in the ovaries (Fig. 2d) was high at ovarian stage I (17.92 ± 1.42 nmol/mg), then increased further to a maximum level at ovarian stage II (20.31 ± 1.94 nmol/mg), and subsequently decreased at ovarian stage III (11.03 ± 1.04 nmol/mg), reaching a minimum (9.71 ± 0.78 nmol/mg) at ovarian stage IV. The concentrations of DA at stages I and II were significantly higher by about 2 to 2.5 times than at stage III and IV (P<0.05). The concentration of DA in the ovary at ovarian stage II was about 10 times higher than 5-HT, but at stage IV, it was 5 times higher (P<0.05).

3.2 Distribution of 5-HT-ir and DA-ir in the CNS and the ovary

The distribution patterns of both neurotransmitters were similar in all stages of the ovarian cycle; however, the intensity of 5-HT-ir was highest at ovarian stage IV, and DA-ir at stage II. These results support the HPLC results. Hence the descriptions of the distribution patterns of 5-HT-ir and DA-ir neurons in the brain, CEG, SEG, thoracic ganglia, and abdominal ganglia illustrated here,

were from whole mounts taken at stage IV for 5-HT and from stage II for DA. However, the pictures of 5-HT-ir and DA-ir in the eyestalks and ovaries were obtained from the sections. In addition, the distribution patterns of 5-HT-ir and DA-ir in whole-mounts were also compared with 5-HT- and DA-ir in the sections (Figs. 3, 4, 5, 6, 7, 8, 9).

3.3 Distribution of 5-HT-ir in the CNS

We have previously classified neurons of *P. monodon* into three types, based on their distinct sizes (Ngernsoungnern et al. 2008). In *L. vannamei*, we also found three types of neurons with distinct sizes; the diameters of the small-, medium-, and large-sized neurons were 9 ± 2.5 μm, 28 ± 5.1 μm, and 68 ± 8.2 μm, respectively. These data represent mean ± SD of 30 cells. In the eyestalks, 5-HT-ir was detected in neurons of cluster 4 (X-organ), and fibers in the medulla externa (ME) and medulla interna (MI) (Fig. 3a, b). Intensely immunoreactive fibers were numerous in the sinus gland (SG) (Fig. 3a, b). In the median protocerebrum of the brain, strong 5-HT-ir was detected in many medium-sized neurons within cluster 6 (Fig. 3c, d). In addition, intense immunoreactive fibers were observed in the protocerebral bridge (PB), anterior medial protocerebral neuropil (AMPN), central body (CB), and posterior medial protocerebral neuropil (PMPN) (Fig. 3c, d). In the deutocerebrum, 5-HT-ir was detected in medium-sized neurons in cluster 11 and in the fibers of the olfactory neuropil (ON) (Fig. 3c). In the tritocerebrum, 5-HT-ir was detected in medium-sized neurons in cluster 17, fibers in the median antenna I neuropil (MAN), antenna II neuropil (AnN), and in the tegumentary neuropil (TN). Intense 5-HT-ir medium- and large-sized neurons as well as fibers were detected in the CEG (Fig. 3e).

In the SEG (Fig. 4a, b), intense 5-HT-ir neurons were distributed at the periphery of the MP-I to the MP-III segments of the ganglion. At the anterior end of the SEG, very intense 5-HT-ir fibers projected from the CEC to the SEG (Fig. 4a). These fibers extended along the midline, and branched at the MX-I to MP-III towards lateral margin of each ganglion. Paired 5-HT-ir fibers branched bilaterally from the MP-III to the SEG nerve roots (Fig. 4b). In the thoracic ganglia, most of 5-HT-ir neurons were localized in ventromedial cell clusters of the ganglia (Fig. 4c-f). Each of the thoracic ganglia contained intense 5-HT-ir neurons, as well as fibers which were more numerous and intensely stained, compared with those in other parts of the CNS. In the chain of thoracic ganglia, we could detect three major 5-HT-ir fiber bundles, namely, medial fiber bundles (MFB), central fiber bundles (CFB), and lateral fiber bundles (LFB). These fiber bundles were continuous from one ganglion to the next, passing within each intersegmental commissural fiber (IC) of the ventral nerve cord. The MFB and LFB were distinct in the T1 to T3 (Fig. 4c-f). As well, the CFB was located between the MFB and the LFB (Fig. 4d). The MFB and LFB then passed between T3 to T4 and T5 (Fig. 4g, h). In addition, a pair of 5-HT-ir neurons was detected at the dorsolateral cell cluster in T5 (Fig. 4i), and intense 5-HT-ir was also present throughout the T1-T5 neuropils (Fig. 4c-i).

In the abdominal ganglia, medium- and large-sized 5-HT-ir neurons were present in the dorso- and ventrolateral cell clusters, exemplified by 5-HT-ir neurons in A1 (Fig. 5a), and in A3 (Fig. 5b). The MFB and LFB also passed through the IC of all abdominal ganglia (Fig. 5c, d, e). Intensely immunoreactive punctate fibers were also detected in the neuropils of A1 to A6 (Fig. 5a, c, d). No 5-HT-ir was detected in control sections of any part of the CNS. The distribution of 5-HT-ir in the CNS is summarized in Fig. 9a, b, c, e, and Table 1.

3.4 Distribution of 5-HT-ir in the ovary

In the ovary, 5-HT-ir was intense in the cytoplasm of the late vitellogenic oocytes (Oc3 and Oc4) (Fig. 5f-h), and appeared much weaker in early oocytes (Oc1 and Oc2) (Fig. 5h). The oogonia were not immunoreactive (data not shown). No staining was observed in the control sections of the ovary (Fig. 5i). Other control sections using anti-5-HT pre-absorbed with synthetic 5-HT also showed no immunoreactivity. A summary of the distribution of 5-HT-ir in different steps of oocyte development is shown in Table 2.

The distribution patterns of 5-HT-ir in the CNS at stage IV were similar to the other stages, but the numbers and intensities of immunoreactive neurons and fibers in the latter were much lower (see Fig. 10a, c). This was confirmed in three replicated studies of each stage.

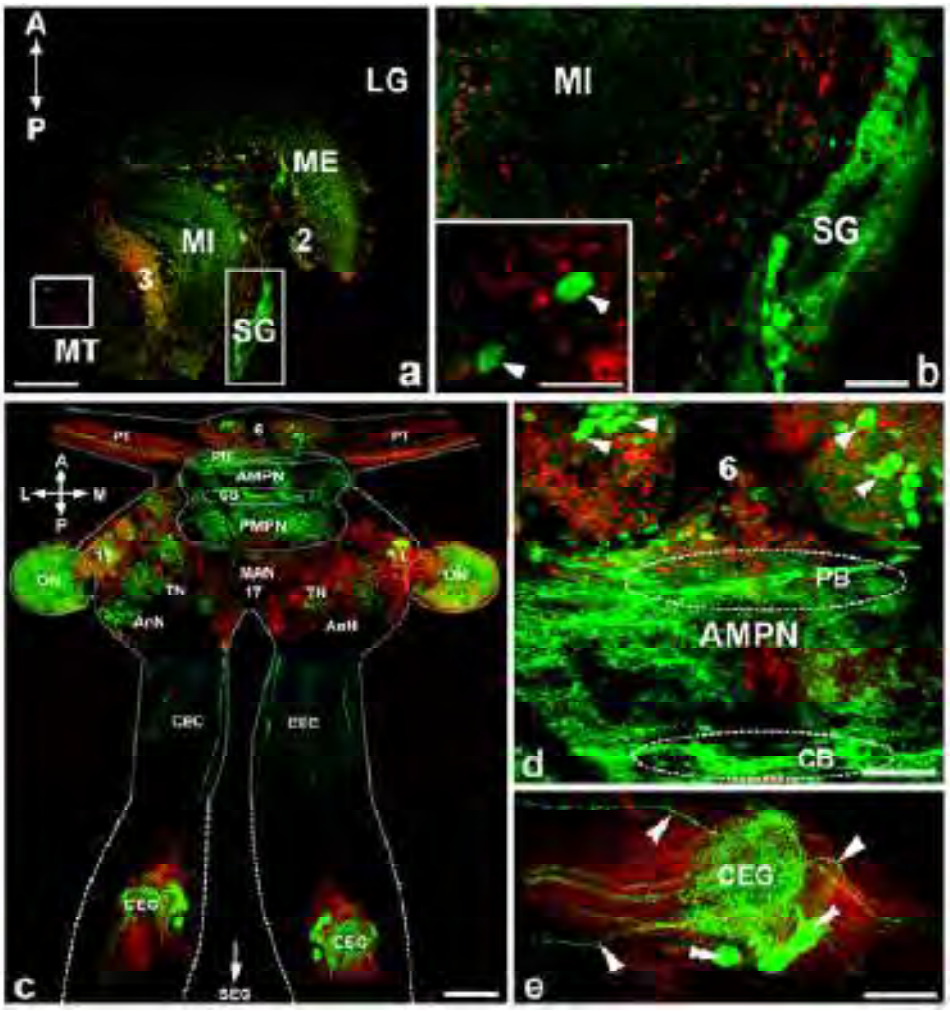

Fig. 3 Immunofluorescence detection of 5-HT-ir (green) in the CNS, with nuclei counterstained with ToPro-3 (red). **a** The eyestalk, with the orientation given at the top left, shows 5-HT-ir in the ME, MI, MT, and the SG (large boxed area). Some neurons in cluster 4 (small boxed area) exhibits a strong immunofluorescence. **b** High-power magnification of the boxed areas in **a,** showing the location of 5-HT-ir neurons in cluster 4 (inset, X-organ neurons, arrowheads) and very intense 5-HT-ir fibers in the SG. **c** Whole-mounts of the brain and CEG, with orientation given at the top left, exhibiting 5-HT-ir in neurons of clusters 6, 11, and 17, PB, AMPN, CB, PMPN, AnN, TN neuropils, and nearby fibers. **d** Numerous 5-HT-ir neurons in cluster 6 (arrows), and distinctive 5-HT-ir in the PB (dashed circles), AMPN, and the CB (dashed circles). **e** 5-HT-ir is very intense in a neuropil of the CEG, in neurons (double arrowheads), and in fibers (arrowheads) connecting the CEG with the brain. Numbers indicate neuronal clusters (*A* anterior, *AMPN* anterior medial protocerebral neuropil, *CB* central body, *CEC* circumesophageal connective, *CEG* circumesophageal ganglia, *L* lateral, *LG* lamina ganglionalis, *M* medial, *MAN* median antenna I neuropil, *ME* medulla externa, *MI* medulla interna, *MT* medulla terminalis, *ON* olfactory neuropils, *P* posterior, *PB* protocerebral bridge, *PMPN* posterior medial protocerebral neuropil, *PT* protocerebral tract, *SG* sinus gland, *TN* tegumentary neuropil). *Bars* 400 μm (**a, c**), 100 μm (**b**), 50 μm (**d, e**), 25 μm (inset in **b**)

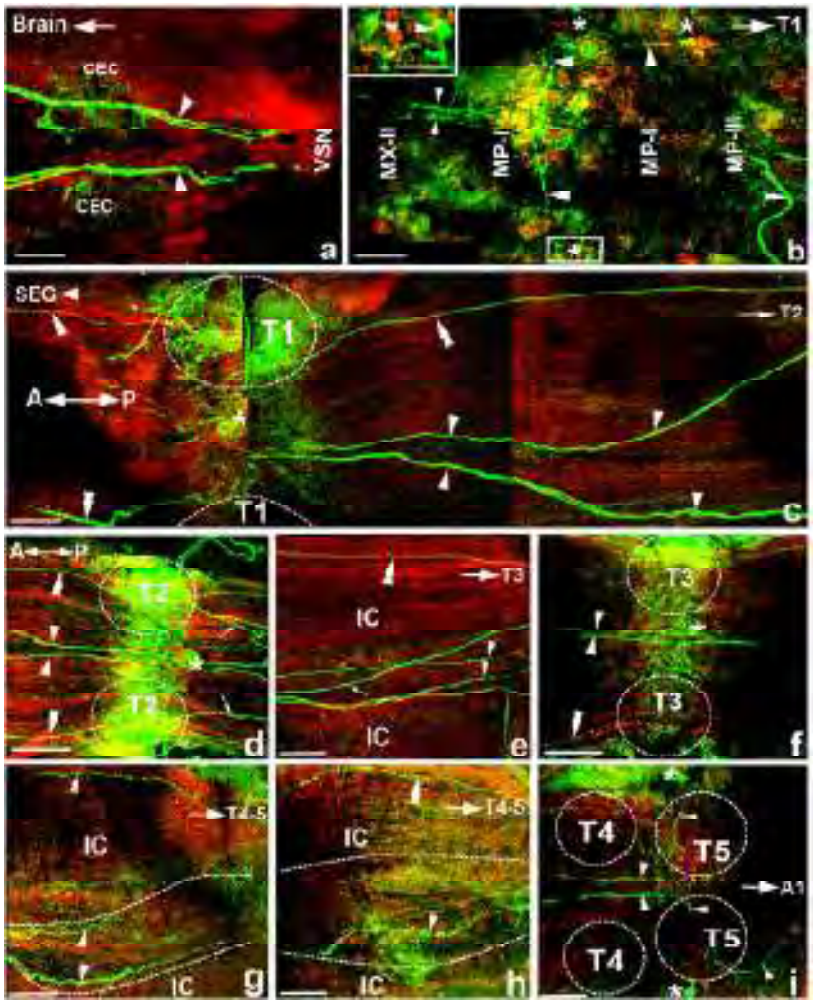

Fig. 4 Immunofluorescence detection of 5-HT-ir (green) in the CNS, with cell nuclei counterstained with ToPro-3 (red). **a** Intense 5-HT-ir fibers (arrowheads) run through the CEC to connect with the SEG. **b** 5-HT-ir neurons of the SEG are located at the periphery of MP-I to MP-III (asterisks). In addition, 5-HT-ir fibers run along the midline from the MX-II to MP-III (small arrowheads), at the MP-I (small arrowheads), they branch off laterally (large arrowheads). As well, the paired 5-HT-ir fibers branch out bilaterally at the MP-III to the SEG nerve root (double arrowheads). **b (inset)** High-power micrograph showing intense 5-HT-ir within neurons in the lateral clusters of the MP-I to MP-II. **c-f** The thoracic ganglia, with orientation shown at top left, show distinctive 5-HT-ir fiber bundles in the MFB (arrowheads) and LFB (double arrowheads) running from T1 to T3, with the CFB (arrows) lying lateral to the MFB and locating medial to the LFB. 5-HT-ir neurons in T2 are located at the ventromedial cell cluster in T1 to T3 (**c, d, f**, asterisks). Immunoreactive fibers are distinct in T1-T5 neuropils. **g, h** The MFB (arrowheads) and LFB (double arrowheads) extend from T3 to T5. **i** A pair of 5-HT-ir neurons are located at the dorsolateral cluster in T5 (asterisks). Dotted circles surround the neuropils of each thoracic ganglion. Dashed lines indicate each side of the IC. Asterisks represent the locations of 5-HT-ir neurons (*A* anterior, *CEC* circumesophageal connective, *CFB* central fiber bundle, *IC* intersegmental commissural fibers, *LFB* lateral fiber bundle, *MFB* medial fiber bundle, *MP-I*, *MP-II* and *MP-III* first, second and third maxilipeds, *MX-I* and *MX-II* first and second maxillary neuropils, *P* posterior, *SEG* subesophageal ganglion, *T1 to T5* thoracic ganglia 1 and 5, *VSN* visceral sensory neuropil). *Bars* 100 μm (**a-i**), 50 μm (**b, inset**)

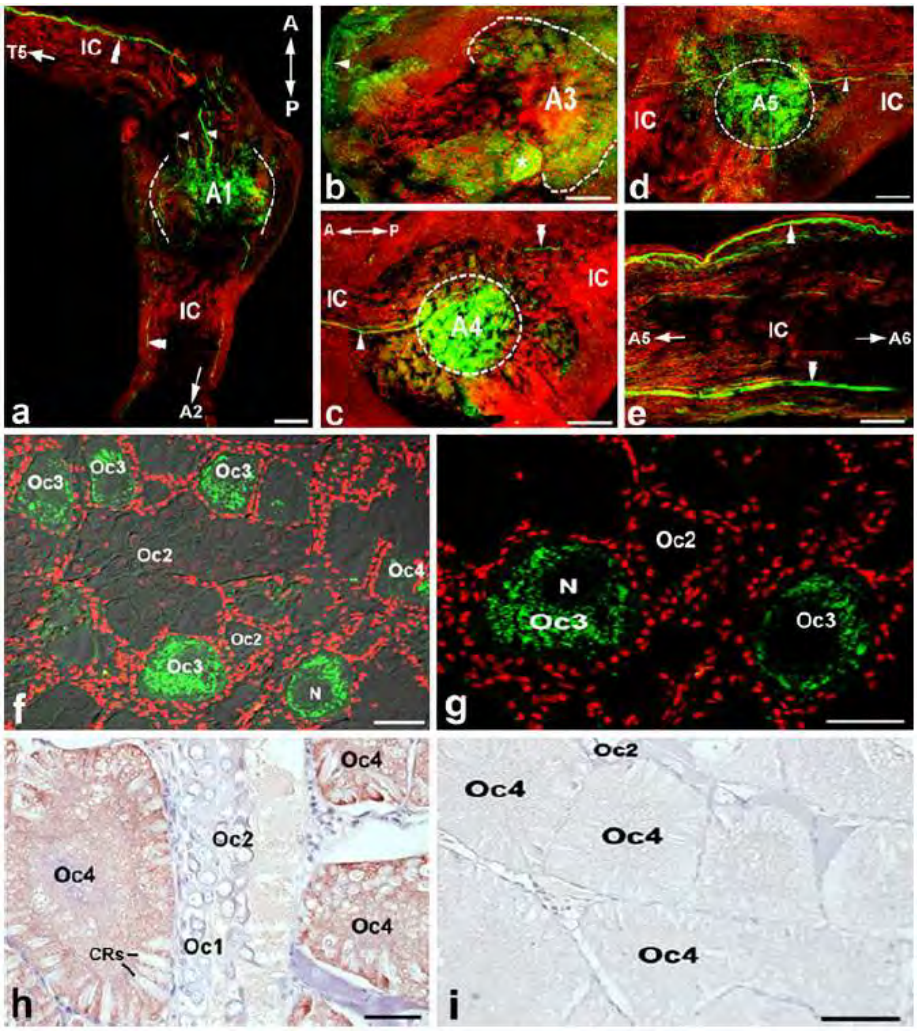

Fig. 5 Immunofluorescence detection of 5-HT-ir (green) in the abdominal ganglia (**a-e**) and ovaries (**f-i**). Cell nuclei are counterstained with ToPro-3 (red). The orientation of the abdominal ganglia is shown top right of **a** and top left of **c. a, b** 5-HT-ir neurons are located in the dorsolateral and ventrolateral cell clusters A1 and A3 (asterisks). Immunoreactive fibers are present in the LFB (double arrowheads). **c-e** The MFB (arrowheads) and LFB (double arrowheads) are detected in the IC of A1 to A6. Immunoreactive punctate fibers are also present in the neuropils of A1 to A6. **f-g** Moderate 5-HT-ir is present in the cytoplasm of vitellogenic oocytes (Oc3), but it is very weak in early previtellogenic oocytes (Oc2). **h** Immunoperoxidase detection showing intense 5-HT-ir in the mature oocytes (Oc4), whereas it is very pale in early oocytes (Oc1, Oc2). **i** No immunoperoxidase staining is observed in control sections of the ovary, or in immunofluorescence controls (data not shown) (*A* anterior, *A1 to A5* abdominal ganglia 1 and 5, *IC* intersegmental commissural fibers, *N* nucleus, *Oc1* early previtellogenic oocytes, *Oc2* late previtellogenic oocytes, *Oc3* early vitellogenic oocytes, *Oc4* mature oocytes, *P* posterior). *Bars* 400 μm (**a, f**), 100 μm (**b-e**), 50 μm (**g-i**)

3.5 Distribution of DA-ir in the CNS

In the optic lobe and lateral protocerebrum, DA-ir neurons were also present in clusters 4 (X-organ) and 5 (Fig. 6a, b). Some DA-ir fibers were present in the ME, MI, and medulla terminalis (MT) (Fig. 6a). In addition, immunoreactivity was very intense in fibers of the SG (Fig. 6a, b). In the median protocerebrum, many medium-sized DA-ir neurons were present in cluster 6 (Fig. 6c, d). Intense immunoreactive fibers were localized in the PB, AMPN, CB, and PMPN (Fig. 6c-e). In the deutocerebrum, mostly medium-sized DA-ir neurons were present in cluster 11 (Fig. 6c, inset), which was in close proximity to strongly labeled immunoreactive fibers in the ON, the olfactory globular neuropils (OGTN), AnN and TN (Fig. 6c). In the tritocerebrum, DA-ir was detected in medium- and large-sized neurons in cluster 17 (Fig. 6e). DA-ir was found in neurons of the CEG, and some were giant neurons with strongly labeled immunoreactive fibers projecting downwards via the CEC to the SEG (Figs. 6f, g, 7a), and joining a process of a nerve extending from the SEG (Figs. 6h, 7a, b).

In the SEG, DA-ir neurons were detected at the lateral margin of the MX-II to the MP-III (Fig. 7b). DA-ir fibers making up the MFB and LFB extended through the midline of this ganglion (Fig. 7b). Bilaterally paired DA-ir fibers projected outward from neurons in MP-III of the SEG (Fig. 7b). In the thoracic ganglia, DA-ir neurons were detected in most neuronal cell clusters, including the ventromedial cell clusters and dorsolateral cell clusters of T1 (Fig. 7c), T2 (Fig. 7e), T3 (Fig. 7g), and T5 (Fig. 7h). The MFB and LFB, passed from the SEG through T1 (Fig. 7c), and continued in the IC to T5 (Fig. 7d-h). The CFB was detected at the periphery of the MFB, and projected laterally to the T2 (Fig. 7d). The LFB extended branches laterally to T4 and T5, and also projected downward

to A1 (Fig. 7h). The T1 to T5 neuropils also contained intense DA-ir fibers (Fig. 7c-h).

In the abdominal ganglia, medium- and large-sized DA-ir neurons were detected in the dorso- and ventrolateral cell clusters, exemplified by DA-ir neurons in A1 (Fig. 8a), A3 (Fig. 8b), and A5 (Fig. 8c). The neuropils of A1 to A6 also contained intense immunoreactive fibers (Fig. 8a-c). The MFB and LFB were also present in the IC connecting between A1 to A6, as they were with 5-HT-ir (Fig. 8d-f). No positive fluorescence was observed in the control sections taken from different parts of the CNS. The distribution of DA-ir in the CNS is summarized in Fig. 9a, b, d, f and Table 1.

3.6 Distribution of DA-ir in the ovary

In the ovary, the intensity of DA-ir was highest in the cytoplasm of early oocytes, especially Oc1 and Oc2 (Fig. 8g, h), and by contrast, weak staining was detected in vitellogenic oocytes (Oc3 and Oc4). No DA-ir was observed in the oogonia and follicular cells. The control sections did not show any positive fluorescence (Fig. 8i). The distribution of DA-ir in different oocytes is summarized in Table 2.

The distribution patterns of DA-ir in the CNS at stage II were similar to the other stages, but the numbers and intensities of immunoreactive neurons and fibers in the latter were much lower (see Fig. 10b, d). This was confirmed in three replicated studies of each stage.

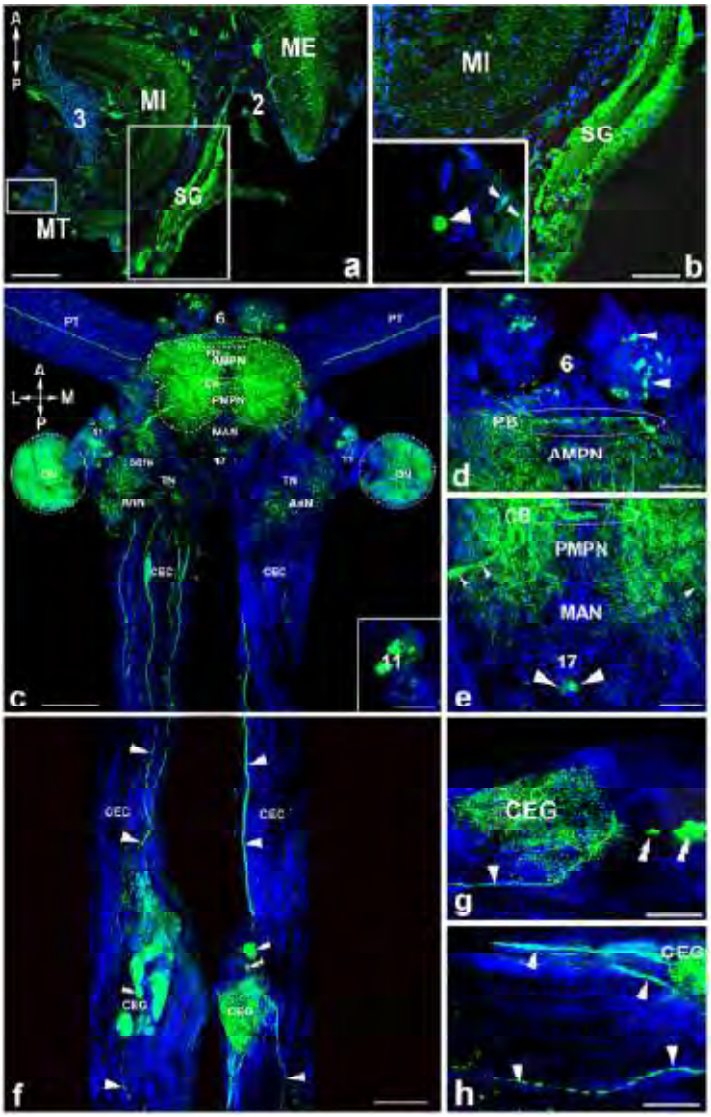

Fig. 6 Immunofluorescence detection of DA-ir (green) in the CNS, and cell nuclei are counterstained with ToPro-3 (blue). **a** In the eyestalk, intense DA-ir is present in the ME, MI, MT, SG (large boxed area), and a few neurons in cluster 4 (X-organ, small boxed area). **b** The two boxed areas from **a** are shown at higher magnifications: DA-ir is very intense in the SG and moderate in the ME, as well as DA-ir neurons are present in cluster 4 (**b, inset,** large arrowheads). DA-ir fibers are seen close to the XO (**b, inset,** small arrowheads). **c** Whole-mounts of the brain and CEG, orientation is given top left, showing DA-ir in neurons of clusters 6, 11, 17, PB, AMPN, CB, PMPN, AnN, TN neuropils, and nearby fibers. (**c, inset**) shows DA-ir neurons in cluster 11. **d, e** Many DA-ir neurons are present in clusters 6 (**d**, arrowheads), 17 (**e**, large arrowheads), and intense immunoreactive fibers are present in the PB, AMPN, and CB (dashed circles), as well as fibers close to cluster 11 (**e**, small arrowheads). **f** Many DA-ir neurons are present in the CEG (double arrowheads), and their immunoreactive fibers projecting through the CEC (arrowheads) to the SEG. **g, h** High-power micrographs showing the DA-ir neurons (double arrowheads) and the positive fibers (arrowheads) running into the SEG. Numbers indicate neuronal clusters (*AMPN* anterior medial protocerebral neuropil, *AnN* antenna II neuropil, *CEC* circumesophageal connective, *CB* central body, *CEG* circumesophageal ganglion, *L* lateral, *M* medial, *MAN* median antenna I neuropil, *ME* medulla externa, *MI* medulla interna, *MT* medulla terminalis, *OGTN* olfactory globular tract, *ON* olfactory neuropils, *PB* protocerebral bridge, *PMPN* posterior medial protocerebral neuropil, *PT* protocerebral tract, *SG* sinus gland, *TN* tegumentary neuropil). *Bars* 400 μm (**a, c, f**), 100 μm (**b, d, e**), 50 μm (inset in **c, g, h**)

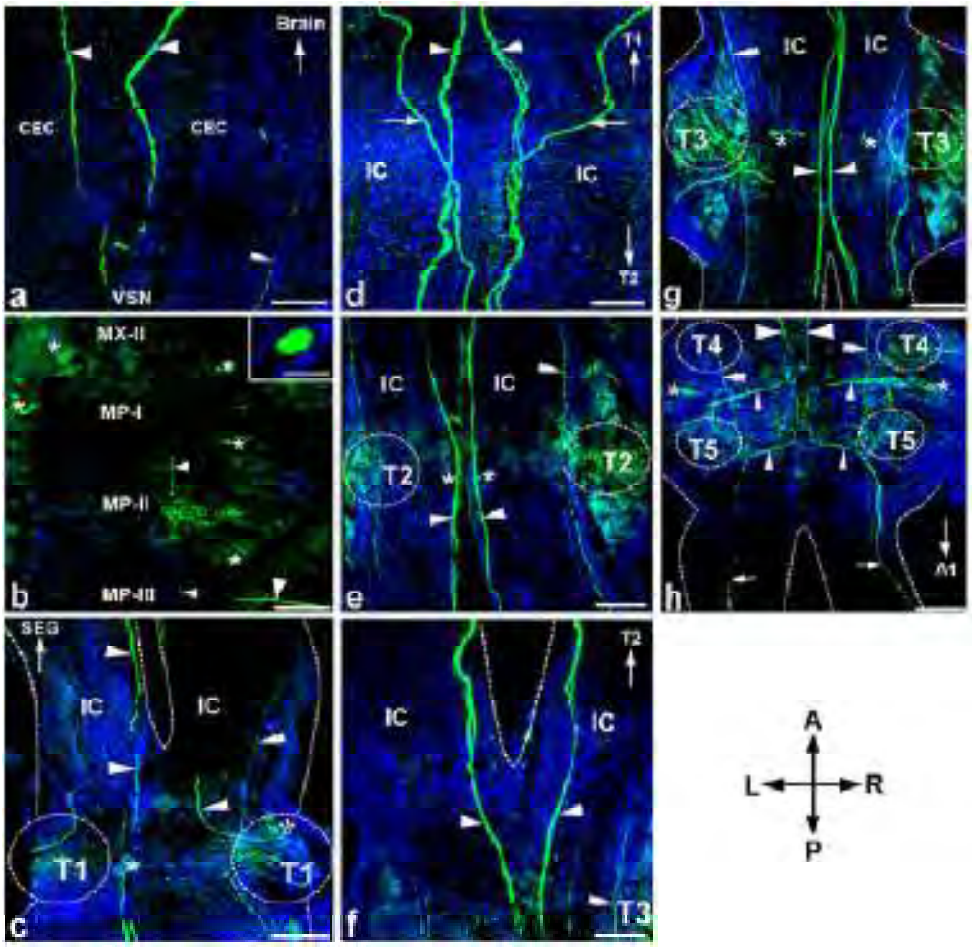

Fig. 7 Immunofluorescence detection of DA-ir (green) in the CNS, and cell nuclei are counterstained with ToPro-3 (blue). **a** DA-ir fibers, comprising the MFB (arrowheads) and LFB (double arrowheads) extend through the CEC to the SEG. **b** The SEG, with orientation given at the top right, showing DA-ir neurons which are located at the periphery of the MX-II to MP-III of the SEG (asterisks). DA-ir fibers are observed along the midline (small arrowheads). Bilaterally paired DA-ir fibers projected outward from neurons in MP-III of the SEG (large arrowhead). High-power micrograph showing medium-sized DA-ir neurons (**b, inset**). **c-g** DA-ir neurons are present in the dorsolateral and ventromedial clusters in T1 (**c**, asterisks), in the T2 (**e**, asterisks), and in the dorsomedial cluster in T3 (**g**, asterisks). Dashed lines in **c** and **f** indicate each side of the IC and area of the ganglion, respectively. The MFB (arrowheads) and LFB (double arrowheads) extend from the SEG to the T1 and T2 to T5 (**f**, **h** arrowheads). The CFB are just lateral to the MFB, and project to the T2 (**d**, arrows) and to the T3, T4 and T5. Very intense DA-ir fibers are present in the T1-T5 neuropils. **h** A pair of DA-ir neurons are located in the dorsolateral cell cluster in T5 (asterisks). The MFB (large arrowheads) and LFB (double arrowheads) connect between T4 and T5, and their branches extend laterally to T4 and T5 (small arrowheads), and project downward to A1 (arrows). Dotted circles surround the neuropils of each thoracic ganglion (*A* anterior, *A1* first abdominal ganglion, *CEC* circumesophageal connective, *IC* intersegmental commissural fibers, *L* left, *MP-I, MP-II and MP-III* first, second and third maxilipeds, *MX-I and MX-II* first and second maxillary neuropils, *P* posterior, *R* right, *T1 to T5* thoracic ganglia 1 and 5, *VSN* visceral sensory neuropil). *Bars* 100 μm (**a-h**), 50 μm (**b**, inset)

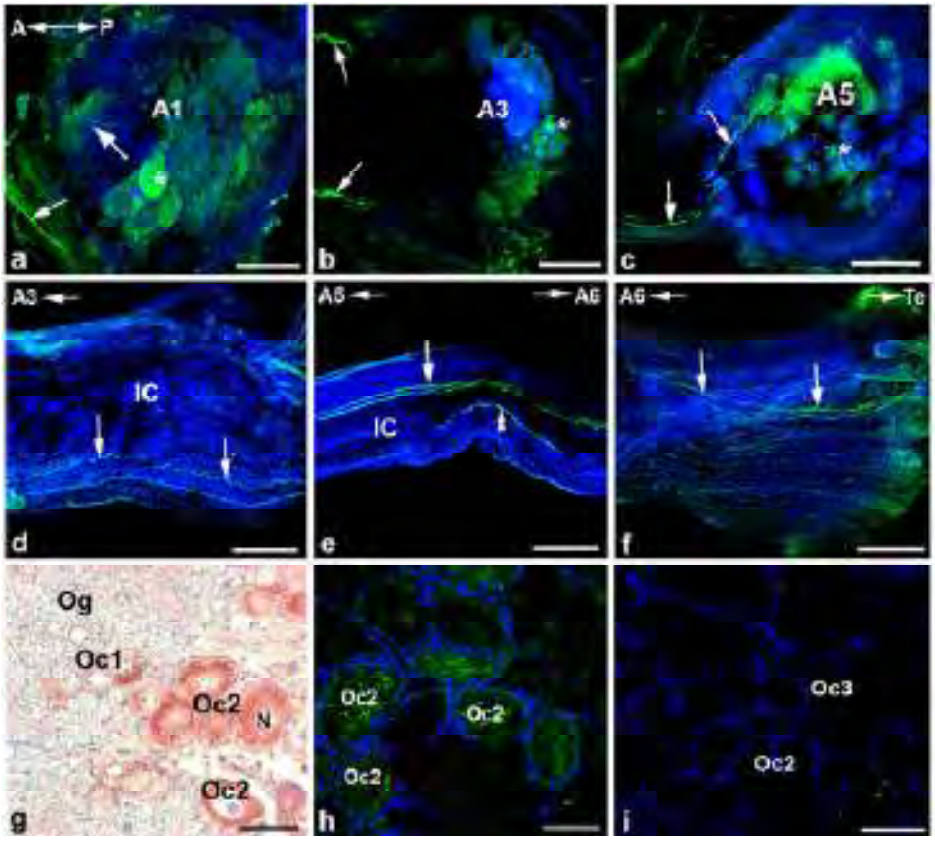

Fig. 8 Immunofluorescence detection of DA-ir (green) in the abdominal ganglia, whose orientation is shown at the top left of **a**, and ovaries, as well as cell nuclei counterstained with ToPro-3 (blue). **a-c** Large DA-ir neurons are present in the dorsolateral and ventrolateral cell clusters, and are exemplified in A1 (**a**, asterisk), A3 (**b**, asterisk), and A5 (**c**, asterisk). **d-f** DA-ir in the MFB (arrows) and LFB (double arrowheads) are shown within the IC of A1 to A6. Immunoreactive fibers are also present in the neuropils of A1 to A6. **g-h** DA-ir is moderate in early oocytes (Oc1), and more intense in Oc2, whereas the late oocytes (Oc3, Oc4) show very weak staining. **i** Control section of the ovary showing no staining (*A* anterior, *A1, A3, and A5* abdominal ganglia 1, 3, and 5, *IC* intersegmental commissural fibers, *LFB* lateral fiber bundle, *MFB* medial fiber bundle, *Oc1* early previtellogenic oocyte, *Oc2* late previtellogenic oocytes, *Oc3* early vitellogenic oocytes, *Og* oogonia, *P* posterior, *Te* telson). *Bars* 100 μm

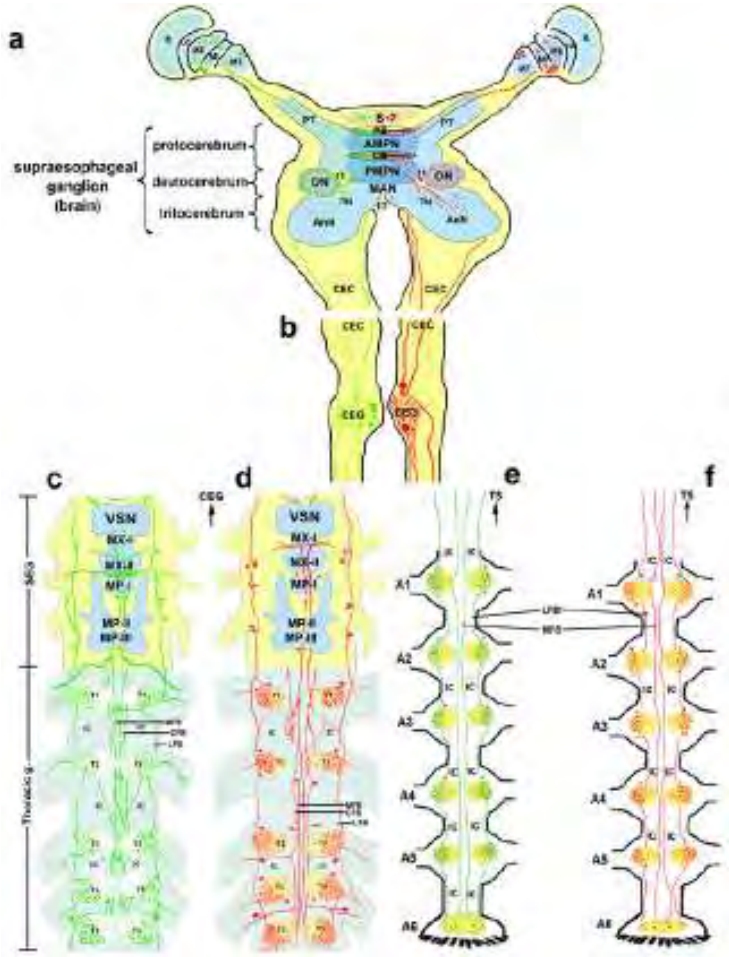

Fig. 9 Representations summarizing the distribution patterns of 5-HT-ir and DA-ir in the CNS of female *L. vannamei*. The presence of 5-HT-ir is represented by green color (**a-c, e**), and DA-ir by red color (**a, b, d, f**). The CNS is composed of: **a** the eyestalk and brain, **b** CEG, **c, d** SEG and five major thoracic ganglia (T1-T5), as well as **e, f** six abdominal ganglia (A1-A6). The brain is divided into a protocerebrum, deutocerebrum, and tritocerebrum; each comprising neuronal clusters (indicated by numbers), and corresponding neuropils. Major 5-HT-ir and DA-ir fiber bundles, including medial fiber bundles (MFB), central fiber bundles (CFB), and lateral fiber bundles (LFB) are detected within the ventral nerve cord. These fiber bundles are continuous from one ganglion to the next from the SEG to T5, and A1-A6, and they pass within each intersegmental commissural fiber (IC) of the ventral nerve cord. 5-HT-ir and DA-ir are also present throughout the T1-T5 neuropils. Immunoreactive neuropils are illustrated by stippling, whose density corresponds with intensity of the staining (immunoreactivity). The positive neurons in different clusters are illustrated by solid dots (*A* anterior, *A1-A6* abdominal ganglia 1-6, *AMPN* anterior medial protocerebral neuropil, *AnN* antenna II neuropil, *CB* central body, *CEC* circumesophageal connective, *CFB* central fiber bundle, *IC* intersegmental commissural fibers, *L* lateral, *LFB* lateral fiber bundle, *LG* lamina ganglionaris, *MAN* median antenna I neuropil, *ME* medulla externa, *MFB* medial fiber bundle, *MI* medulla interna, *MP-I, MP-II and MP-III* first, second and third maxilipeds, *MT* medulla terminalis, *MX-I and MX-II* first and second maxillary neuropils, *ON* olfactory neuropil, *P* posterior, *PB* protocerebral bridge, *PT* protocerebral tract, *PMPN* posterior medial protocerebral neuropil, *R* retina, *SEG* subesophageal ganglion, *T1-T6* thoracic ganglia 1-6, *TN* tegumentary neuropils, *VSN* visceral sensory neruropil).

3.7 Changes in the numbers and staining intensities of 5-HT-ir and DA-ir neurons and fibers in the CNS during ovarian maturation cycle

The numbers of 5-HT-ir and DA-ir neurons in the brain, CEG, SEG, thoracic ganglia, and abdominal ganglia, counted at different stages of ovarian maturation cycle, are given in Fig. 10a, b. The numbers of 5-HT-ir and DA-ir neurons were significantly higher in the brain, SEG, and thoracic ganglia, than in the CEG and abdominal ganglia (P<0.05) (Fig. 10a, b). At stage IV, the number of 5-HT-ir neurons was highest in the brain with 34 ± 3.4 neurons, then the SEG with 20 ± 2.5 neurons, the combined thoracic ganglia (T1-T5) with 22 ± 2.7 neurons, and the combined abdominal ganglia (A1-A6) with only 17 ± 1.8 neurons (P<0.05). The least number of 5-HT-ir neurons was 7 ± 0.6 in the CEG (Fig. 10a). The total number of 5-HT-ir neurons was about 4.5 times higher in the brain, and almost 3 times higher in the SEG and thoracic ganglia, at ovarian stage IV than at stage I (P<0.05) (Fig. 10a). In addition, the total number of 5-HT-ir neurons was about 2.5 times higher in all parts of the CNS at ovarian stage IV than at stage I (P<0.05). However, the number of 5-HT-ir neurons observed in the abdominal ganglia was not statistically different at any maturation stage (Fig. 10a). At stage IV, the intensities of 5-HT-ir neurons had also increased markedly in the brain, SEG, and thoracic ganglia, compared with stage I (P<0.05) (Fig. 10c).

The number of DA-ir neurons was higher in the brain, SEG, thoracic ganglia at stage II than at stage IV (P<0.05). Specifically, at stage II, the number of DA-ir neurons was higher in the brain (30 ± 4.5 neurons), the SEG (24 ± 2.1 neurons), and the combined thoracic ganglia (T1-T5) (26 ± 2.7 neurons), than in the CEG (least with 10 ± 0.8 neurons) and the combined abdominal ganglia (A1-A6) (16 ± 1.5 neurons) (P<0.05) (Fig. 10b). The numbers of DA-ir neurons in the

CEG and abdominal ganglia were not statistically different at any stage of ovarian maturation (Fig. 10b). The total number of DA-ir neurons was about 3 times higher in the brain, and about 3.2 times higher in the SEG and thoracic ganglia, at ovarian stage II than at stage IV (P<0.05) (Fig. 10b). When combining all parts of the CNS, the number of DA-ir neurons was about 2.4 times higher at ovarian stage II than at stage IV (P<0.05). In contrast, the number of DA-ir neurons in the abdominal ganglia was not statistically different at any stage of maturation (Fig. 10b). Furthermore, the intensities of DA-ir neurons were significantly greater in the brain, SEG and thoracic ganglia at stage II, compared with stage IV (P<0.05) (Fig. 10d). In contrast, the mean intensities of 5-HT-ir and DA-ir neurons and fibers in the abdominal ganglia appeared to be slightly higher at stages IV and II, than those at stage I and IV, but these were not statistically different (Fig. 10c, d).

Overall, the highest numbers of 5-HT-ir and DA-ir were detected in neurons of cluster 6 of the brain, whereas the lowest numbers were found in neurons of cluster 17 (P<0.05). In the thoracic ganglia, 5-HT-ir neurons in the midline clusters exhibited the highest numbers (Fig. 9c), whereas DA-ir neurons in dorsolateral clusters exhibited the highest numbers (Fig. 9d). In addition, 5-HT-ir and DA-ir fibers in the protocerebral- and deutocerebral areas of the brain showed the highest intensities, compared with other parts of the brain. In the thoracic and abdominal ganglia, the lateral margins of each neuropil exhibited the highest 5-HT-ir and DA-ir intensities, compared with other parts of the ganglia (Figs. 9c-f, 10c-d).

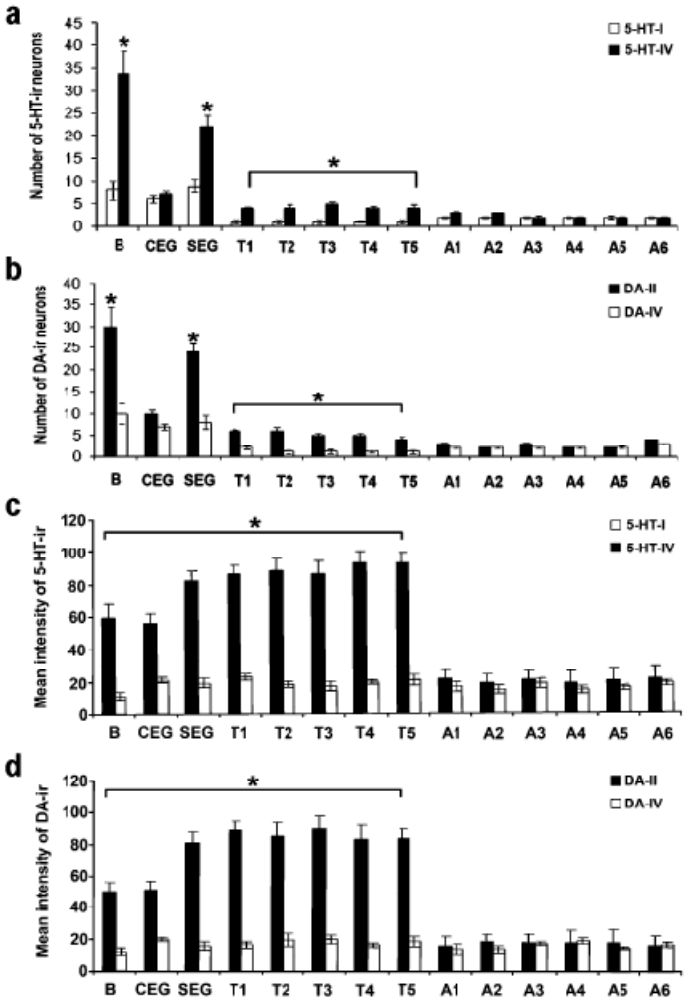

Fig. 10 Histograms showing the mean numbers of 5-HT-ir neurons at ovarian stages I and IV (**a**) and DA-ir neurons at ovarian stages II and IV (**b**) in various parts of the CNS of *L. vannamei*. There are significant differences of 5-HT-ir and DA-ir neuronal numbers in the brain, SEG, and thoracic ganglia (P<0.05). No significant differences of 5-HT-ir and DA-ir neuronal numbers are observed in the CEG and abdominal ganglia (P>0.05). **c, d** The mean intensities of 5-HT-ir (at ovarian stages I and IV), and DA-ir (at ovarian stages II and IV) neurons and fibers within different regions of the CNS. There are significant differences of 5-HT-ir and DA-ir neurons and fibers intensities in the brain, SEG, and thoracic ganglia (P<0.05), but not in the abdominal ganglia. For each data point, the means are calculated from whole mount preparations showing the staining intensities (immunoreactivities) of the two neurotransmitters. Values represent $\overline{X}$ ± SEM, and bars with asterisks are significantly different (P<0.05) (*B* brain, *CEG* circumesophageal ganglia, *SEG*, subesophageal ganglion, *T1 to T5* thoracic ganglia 1-5, *A1 to A6* abdominal ganglia 1-6).

Structures	Neuronal clusters/Neuropils	5-HT-ir		DA-ir	
		Neurons	Fibers	Neurons	Fibers
Eyestalk	C1–C2	–	–	–	–
	C4–C5	+ (S,M)	–	+ (S,M)	–
	SG	–	–	–	+
	Neuropils (T1–MT)	–	–	–	+
	Neuropils (MI, MT)	–	–	–	+
Protocerebrum	C6	+ (M)	–	+ (M)	–
	C7–C8	–	–	–	–
	Neuropils (PB, CB, AMPN, PMPN)	–	–	–	+
Deutocerebrum	C9, C10, C12, C13	–	–	–	–
	C11	+ (M)	–	+ (M)	–
	Neuropils (ON, OGTN, MAN)	–	–	–	+
Tritocerebrum	C14–C16	–	–	–	–
	C17	+ (S,M)	–	+ (M)	–
	Neuropils (AnN, TN)	–	–	–	+
Circumesophageal ganglia (CEG)	CEG	+ (M,L)	–	+ (M,L)	+
Subesophageal ganglia (SEG)	Mandibula (VSN)	–	–	–	+
	Maxillaries I–I	+ (S,M)	–	+ (S,M)	+
	Maxillipeds I–III	+ (S,M)	–	+ (M)	+
Thoracic ganglia	T1	+ (M)	–	+ (M)	+
	T2	+ (M)	–	+ (M)	+
	T3	+ (M)	–	+ (M)	+
	T4	+ (M,L)	–	+ (M,L)	+
	T5	+ (M,L)	–	+ (M,L)	+
Abdominal ganglia	A1	+ (M,L)	–	+ (M,L)	+
	A2	+ (M)	–	+ (M)	+
	A3	+ (M,L)	–	+ (M,L)	+
	A4	+ (M)	–	+ (M)	+
	A5	+ (M)	–	+ (M)	+
	A6	+ (M,L)	–	+ (M,L)	+

Table 1 Summary of the presence of 5-HT-ir and DA-ir in various parts of the CNS of *L. vannamei*. +, indicates the presence of immunoreactivity in neurons, fibers, and neuropils of the CNS parts; -, indicates no immunoreactivity in neurons, fibers, and neuropils of the CNS parts (*A1-A6* abdominal ganglia 1-6, *AnN* antenna II neuropil, *AMPN* anterior medial protocerebral neuropil, *C1-C17* neuronal clusters 1-17 in the brain, *CB* central body, *CEG* circumesophageal ganglion, *IC* intersegmental commissural fibers, *ir* immunoreactivity, *L* large-sized neuron, *LG* lamina ganglionaris, *M* medium-sized neuron, *ME* medulla externa, *MI* medulla interna, *MP-I, MP-II and MP-III* first, second and third maxiliped neuropils, *MT* medulla terminalis, *MX-I and MX-II* first and second maxillary neuropils, *MAN*, median antenna I neuropil, *OGTN* olfactory globular tract neuropil, *ON* olfactory neuropil, *PB* protocerebral bridge, *PMPN* posterior medial protocerebral neuropil, *S* small-sized neuron, *SG* sinus gland, *T1-T5* thoracic ganglia 1-5, *TN* tegumentary neuropils, *VSN* visceral sensory neruropil).

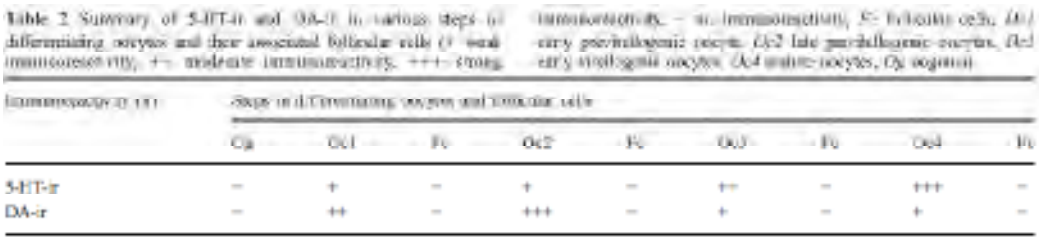

Table 2 Summary of 5-HT-ir and DA-ir in various steps of differentiating oocytes and their associated follicular cells (*-* weak immunoreactivity, *+-* moderate immunoreactivity, *+++* strong immunoreactivity, *-* no immunoreactivity, *Fc* follicular cells, *Oc1* early previtellogenic oocyte, *Oc2* late previtellogenic oocytes, *Oc3* early vitellogenic oocytes, *Oc4* mature oocytes, *Og* oogonia)

Immunoreactivity (-/+/++/+++)	Steps in differentiating oocytes and follicular cells								
	Og	Oc1	Fc	Oc2	Fc	Oc3	Fc	Oc4	Fc
5-HT-ir	-	+	-	+	-	++	-	+++	-
DA-ir	-	++	-	+++	-	+	-	+	-

Table 2 Summary of 5-HT-ir and DA-ir in various steps of differentiating oocytes and their associated follicular cells. +, weak immunoreactivity; ++, moderate immunoreactivity; +++, strong immunoreactivity; -, no immunoreactivity (*Fc* follicular cells, *Oc1* early previtellogenic oocyte, *Oc2* late previtellogenic oocytes, *Oc3* early vitellogenic oocytes, *Oc4* mature oocytes, *Og* oogonia).

4. Discussion

The present study demonstrated that there was a rise in 5-HT levels in the brain, thoracic ganglia, and ovaries as ovarian maturation progressed, while DA levels decreased. The highest levels of 5-HT were detected at stage IV in the brain, thoracic ganglia, and ovaries, whereas the highest levels of DA were detected at stage II in the same tissues. This implicates that the increased levels of these two neurotransmitters might be related to specific functions with regard to ovarian maturation. It is proposed that the increasing levels of 5-HT stimulate ovarian maturation, while DA acts in an opposing function.

Several studies have investigated the levels of 5-HT and DA in decapod crustaceans using HPLC analyses. In the spiny lobster, *Palinurus homarus*, 5-HT concentration was found to be higher in thoracic ganglia than in the brain at ovarian stage IV, suggesting that 5-HT is involved in regulating the ovarian maturation (Kirubagaran et al. 2005). In the crayfish, *P. clarkii,* levels of 5-HT were quantified in various regions of the brain, and it was found that the total concentration of 5-HT was higher in the brain (~ 0.6 μg/g) than in the eyestalks (~ 0.3 μg/g) (Cervantes et al. 1999). In the freshwater prawn, *M. rosenbergii*, 5-HT concentrations were highest in the brain and thoracic ganglia (~1.50 nmol/mg) at ovarian stage IV, and lowest at ovarian stage I (Tinikul et al. 2008). In contrast, they found that DA concentrations exhibited the highest level in the brain and thoracic ganglia at ovarian stage II (~1.30 nmol/mg), but the lowest (~ 0.06 nmol/mg) at ovarian stage IV. Our findings indicate that the changing patterns of 5-HT concentrations in the brain and thoracic ganglia of *L. vannamei* are similar with those reported in the three decapod crustaceans. We found that the concentration of 5-HT was about 3.5 times higher in the thoracic ganglia at stage

IV than in the brain at the same stage, whereas DA concentration was approximately 2.5 times higher in the thoracic ganglia at stage II, than in the brain at the same stage, thus indicating the strong influence of the thoracic ganglia. This is supported by a previous study in the freshwater prawn, *M. rosenbergii*, where the ovaries, following an injection with culture medium of 5-HT-primed thoracic ganglia, showed an increase in the oocyte numbers which developed into mature stages (Meeratana et al. 2006). They suggested that 5-HT and/or other hormonal factors from the thoracic ganglia could be major factors that stimulate ovarian maturation and oocyte development. Similarly, with mature *L. vannamei* females, the intraspecific implantation of thoracic ganglia also induced ovarian maturation (Yano et al. 1988). In the crab *Uca pugilator*, it was also shown that thoracic ganglion extracts from sexually active females induced precocious ovarian maturation in intact and eyestalk-ablated crabs (Eastman-Reks and Fingerman 1984). The combined data leads us to believe that the thoracic ganglia may act as a “primary center” in stimulating ovarian maturation in decapod crustaceans, including *L. vannamei*. However, the abdominal ganglia may not be involved in this process, as only basal levels of 5-HT and DA were detected there.

Several studies have reported the effects of 5-HT and DA on ovarian maturation in crustaceans. Specifically, 5-HT shortened the period of ovarian maturation in *P. monodon* (Wongprasert et al. 2006), and in *M. rosenbergii* (Tinikul et al. 2009a). As well, injecting 5-HT into *P. clarkii* caused increases in oocyte diameter and ovarian maturation (Kulkarni et al. 1992). In *L. stylirostris*, the combined injection of 5-HT and spiperone (a DA-antagonist) stimulated ovarian maturation to a greater extent than injection of 5-HT alone (Alfaro et al. 2004). 5-HT also induced ovarian maturation and spawning in *L. vannamei* (Vaca and Alfaro 2000). In contrast, injection of DA into *M. rosenbergii* delayed ovarian

maturation and embryonic development (Tinikul et al. 2009a), and DA injected in *P. clarkii* also lengthened gonadal maturation period (Sarojini et al. 1995b). There have been reports regarding the effects of 5-HT and DA on vitellogenesis. In *M. rosenbergii*, vitellogenin (Vg) concentrations of prawns treated with 5-HT were highest at ovarian stage IV, whereas treatment with DA produced lower Vg concentrations (Tinikul et al. 2008). These results indicated direct causal relationships, with 5-HT stimulating and DA inhibiting Vg synthesis. Moreover, after treating the Indian white shrimp, *F. indicus*, with 5-HT, the Vg concentration increased significantly from the early ovarian stages (stages I and II) to the mature stage (stage IV), indicating that the stimulatory role of 5-HT on the ovarian maturation with a correlated increase of Vg levels (Santhoshi et al. 2009). Taken together, these studies suggest a positive causal relationship between 5-HT and Vg, and a negative role for DA. As the level of Vg reflects ovarian maturation and oocyte development to the more mature stages (Tinikul et al. 2008; Santhoshi et al. 2009), we believe that 5-HT also exercises a positive control over the ovarian maturation process in *L. vannamei*. This is supported further by the finding that injection of 5-HT into *L. vannamei* stimulates ovarian maturation (Vaca and Alfaro 2000). In contrast, DA apparently exercises an opposite control, as demonstrated in other decapods species (Sarojini et al. 1995b; Tinikul et al. 2009a).

In an earlier report on *L. vannamei*, the presence of 5-HT-ir has been identified in the eyestalks and in the brain (Ye et al. 2004), but not in other parts of the CNS. Furthermore, the neuroanatomical pathways of 5-HT-ir and DA-ir neurons and fibers in the CNS, and their distribution patterns have not yet been reported. Ours is the first study to demonstrate the complete neural networks of 5-HT-ir and DA-ir neurons, fibers, and neuropils, which we found to be highly organized in the eyestalks, brain, and all ganglia of the ventral nerve cord of *L.*

vannamei. In general, the distributions of 5-HT-ir and DA-ir in the CNS overlapped extensively, indicating that the two systems share common pathways. There have been reports showing the presence of 5-HT in the eyestalk, particularly in the X-organ (XO) and in the SG of a few decapod crustaceans. In the crayfish, *P. leniusculus*, 5-HT-ir neurons and fibers were observed in various ganglia (MI and MT) in the eyestalks (Elofsson 1983). In the shrimp, *Metapenaeus ensis*, 5-HT-ir was found in XO-neurons and fibers of optic ganglia, implying that 5-HT may be involved in the synthesis and release of related neurohormones from this structure (Ye et al. 2006). In the Indian white shrimp, *F. indicus*, 5-HT-ir was found in the XO neurons and in the fibers of SG, suggesting this group of cells and fibers could be a primary source of 5-HT, and may regulate the release of other XO neurohormones, such as CHH (Santoshi et al. 2008). As well, distinct 5-HT-ir was observed in the MT and in the SG of the shrimp, *Palaemon serratus* (Bellon and Van Herp 1988), and *P. clarkii* (Escamilla-Chimal et al. 2001), implicating the role of 5-HT in the regulation of neurosecretory activity at these structures.

It has been shown that 5-HT induces the bursting of action potentials in the intact X-organ axons of *P. clarkii* (Sáenz et al. 1997), and to elicit electrical activity of X-organ cells in the crayfish, *Orconectes limosus,* and the crab, *Cardisoma carnifex* (Keller and Beyer 1968; Nagano and Cooke 1981). Injections of 5-HT into the crayfish hemolymph stimulated an increase in the number of CHH granules in the SG of *Astacus leptodactylus,* followed by a hyperglycemic response in the blood, suggesting a direct role of 5-HT in stimulating the release of CHH (Van Herp and Strolenberg 1980; Gorgels-Kallen 1985). In the present study, intense 5-HT-ir was detected within neurons of cluster 4 (XO neurons) and associated fibers, and was even more intense in the SG. Thus, we believe that 5-HT-ir is present in some XO neurons, and in the SG of *L. vannamei,* as reported

in other species. This suggests that 5-HT may also play a role in stimulating the synthesis of neuropeptides, such as CHH, from the XO neurons as reported in other decapod crustaceans, and possibly also causes the release of this hormone from the SG. As CHH belongs to the same family as GIH/MIH (gonad-inhibiting and molt inhibiting hormones) (Hsu et al. 2006), the same controlling mechanism may be applied to the synthesis and release of these hormones from the XO. This has yet to be demonstrated in *L. vannamei*. The 5-HT-ir neurons in the XO and their positive fibers in the SG may also be involved in controlling the X-organ neurosecretory neurons that synthesize the CHH family of hormones, as reported earlier in crabs and crayfish.

Ovarian maturation and vitellogenesis are regulated by GIH (Huberman 2000), which is a member of the neuropeptide family that is synthesized in neurons located in the X-organ and transported to the axon terminals that end at the SG, where it is secreted into the haemolymph (Skinner 1985; Chan et al. 2003; Treerattrakool et al. 2008). 5-HT and DA are thought to exercise their controls over the synthesis and release of a putative gonad-inhibiting hormone (GIH/VIH) or GIH-like peptides in the eyestalks of *P. monodon* (Treerattrakool et al. 2008), *M. ensis* (Gu et al. 2000), *L. vannamei* (Wang et al. 2000), and *Jasus lalandii* (Marco et al. 2002). 5-HT possibly acts by inhibiting the release of GIH from the XO and/or by stimulating putative GSH or gonadotropin-releasing hormone (GnRH-like peptide) from the brain and thoracic ganglia, as a GnRH-like gonad-stimulating neuropeptide has been reported to be present in these neural structures (Tinikul et al. 2011), whereas DA may play the opposite role (Sarojini et al. 1995b; Fingerman 1997). However, this hypothesis needs to be investigated further by studying the effects of these two neurotransmitters on the expression of the genes encoding the respective hormones. Furthermore, the presence and

distribution of 5-HT and DA receptors in the CNS and ovary should also be studied to identify the cellular targets of these two neurotransmitters.

In the lobster, *H. americanus*, about a hundred 5-HT-ir cells were detected in the central ganglia, thirty five 5-HT-ir neurons in the brain, one neuron in each of the paired circumesophageal ganglia, and at least two in each ganglion of the ventral nerve cord. 5-HT-ir fibers were also detected MFB, CFB, and LFB along the ventral nerve cord (Beltz and Kravitz 1983). In addition, a dense plexus of stained nerve endings were detected surrounding each of the thoracic second roots and the adjacent groups of peripheral neurosecretory neurons in this species, suggesting that the thoracic second roots may be neurohormonal organs (Beltz, 1999). These serotonergic nerve plexuses might be the source of 5-HT released into the hemolymph (Beltz and Kravitz 1983). In the thoracic ganglia of *L. vannamei* similar structures have not yet been identified. However, because of the relatively high level of 5-HT in the thoracic ganglia, it is possible that this organ may also be the major site that produces 5-HT and DA, which are then released via a similar nerve roots-associated neurohaemal sites, as reported in the lobster.

In the crayfishes, *P. leniusculus*, *P. clarkii*, and *C. destructor*, 5-HT-ir was present in clusters 6 and 11, nearby neuropils, as well as immunoreactive fibers in the ON (Elofsson 1983; Real and Czternasty 1990). In the squat lobster, *M. quadrispina*, one hundred and twenty 5-HT-ir neurons were detected in the CNS, of which sixty neurons were detected in the brain, two neurons in the CEG, and the rest in the ventral nerve cord (SEG, T1-T5, and A1-A6). Moreover, the MFB, CFB, and LFB were immunopositive within the series of thoracic ganglia. The MFB and LFB extended through the nerve cord from the SEG to A6, whereas the CFB was particularly distinct within the anterior thoracic ganglia (T1-T2), but could not be traced within the T4 and T5 (Antonsen and Paul 2001). In the freshwater

prawn, *M. rosenbergii*, about seventy 5-HT-ir neurons, numerous fibers, and neuropils, were detected within the brain and ventral nerve cord. Fibers with 5-HT-ir were also present in the MFB and LFB of this species (Vázquez-Acevedo et al. 2009). Our study showed that, in addition to the eyestalk and the brain, 5-HT-ir neurons were also present in the SEG, the thoracic ganglia, and their immunoreactivities were more intense than neurons in other parts of the CNS. We also detected intense immunoreactivity in the MFB, CFB, LFB in the SEG, and thoracic ganglia (T1-T5), but the pathway of the CFB in the abdominal ganglia was not clear. Furthermore, the positions of most 5-HT-ir neurons, neuropils, and the fiber tracts of *L. vannamei*, were found to be similar to those of other crustacean species, suggesting a highly conserved serotonergic pathway among decapod crustaceans.

The presence and distribution of DA has also been investigated in the eyestalk, brain, and the ventral nerve cord of many decapod crustaceans. DA-ir has been identified in neurons, fibers, and neuropils of the eyestalks (e.g., MT and the optic tracts of *C. sapidus* and *M. rosenbergii*), suggesting a role of DA in the regulation of neurosecretory activity of the eyestalk (Wood and Derby 1996; Tinikul et al. 2009b). In the crayfish, *P. clarkii*, DA has been shown to excite small neurons in the XO-SG, suggesting a direct role of DA in controlling the X-organ (Álvarez et al. 2005). Sarojini et al. (1995b) reported that DA stimulated the release of a putative GIH from the X-organ in *P. clarkii*, thereby inhibiting gonadal maturation. As well, DA has been reported to be a major influence on the release of other neurohormones from the XO-SG system. Injection of DA into the crayfish, *P. clarkii,* showed changes in blood glucose levels, presumably by affecting CHH release (Zhou et al. 2003). In the same species, DA reduced the rate of CHH release from the eyestalk, suggesting that DA acts to inhibit the release of CHH

(Sarojini et al. 1995b). Other studies have also demonstrated a direct effect of DA on the neurosecretory cells of the XO-SG system (Fingerman 1997; García and Aréchiga 1998). We found DA-ir neurons with strong staining intensity in some neurons in cluster 4 (XO) and in the SG, suggesting that DA may also play a role in controlling the synthesis and release of neuropeptides of the CHH family, as reported in the crayfish.

DA-ir has also been identified in neurons and fibers in various ON neuropils of the brain in *H. gammarus*, *C. sapidus, O. rusticus, P. argus*, and *M. rosenbergii* (Cournil et al. 1994; Wood and Derby 1996; Schmidt and Ache 1997; Tierney et al. 2003; Tinikul et al. 2009b). In *L. vannamei*, we found intense DA-ir in the ON as well as neurons of clusters 6, 11, and 17, and nearby fibers, suggesting that DA may also be involved in mediating olfaction in this species. In the CEG of *L. vannamei*, we detected large DA-ir neurons which could be homologous to “the L cell” described in the CEG of *H. gammarus* and *O. rusticus* (Cournil et al. 1994; Tierney et al. 2003). Furthermore, about 30 DA-ir neurons were detected in the SEG of *H. gammarus* (Cournil et al. 1994). In *L. vannamei*, about 25 DA-ir neurons were detected in the SEG and intense immunoreactive fibers were present throughout the SEG. Some of DA-ir fibers branched out from the MP-III of the SEG, and we believe that these DA-ir nerves may project from the MP-III of SEG to the well known neurohaemal organ, known as the pericardial organ, where DA is released into the blood to control heart rate (Tierney et al. 2003). DA-ir neurons were also detected in the thoracic ganglia (T1-T5), in which T1 contained six neurons (two pairs located laterally and one pair medially), and T2-T5 contained two pairs each (Cournil et al. 1994). In *O. rusticus,* 20-25 DA-ir neurons were observed in the lateral margin of the SEG, and about 40 DA-ir neurons were detected throughout the series of thoracic ganglia, with each

ganglion of T1-T3 containing three pairs of DA-ir (two pairs located laterally and one pair medially) (Tierney et al. 2003). As well, T4 contained two additional pairs of DA-ir neurons, and T5 contained one additional medial pair. In *C. sapidus*, at least one pair of DA-ir neurons was detected in the first SEG and all of the thoracic ganglia. The two pairs of DA-ir neurons were detected in the T3 and T5 (Wood and Derby 1996). In *L. vannamei*, we found that the distribution patterns of DA-ir neurons were similar to *H. gammarus* and *O. rusticus.* Moreover, we have provided the first evidence that DA-ir fibers are present in the MFB, CFB, and LFB, all of which extend through the SEG and thoracic ganglia.

In the three crayfishes, *O. limosus*, *O. rusticus, P. clarkii*, and in *H. gammarus*, and *M. rosenbergii,* there are DA-ir neurons in the abdominal ganglia (Cournil et al. 1994; Elekes et al. 1988; Mercier et al. 1991; Tierney et al. 2003; Tinikul et al. 2009b), which have been postulated to be neurons involved in regulating the movement of swimming legs. In *P. clarkii*, the anterior unpaired medial (AUM) neurons were found in A3 and A4, and their fibers project into the hindgut where they control its movement (Mercier et al. 1991). Similarly, the large DA-ir AUM-neurons detected in A3 of *L. vannamei* may also be motor neurons involved with hindgut movement. Since both our HPLC and immunolocalization data indicate that there is very little change of DA levels in these ganglia, it implies that the DA-ir neurons in these ganglia may be involved in the movement of swimming legs and hindgut, but not in the control of ovarian maturation.

In *L. vannamei*, both 5-HT and DA levels in ovaries showed the same patterns of change which occurred in the brain and SEG-thoracic ganglia. However, the levels of DA in the ovaries were higher than those of 5-HT at each stage of ovarian maturation cycle. Many studies have described different roles for 5-HT and DA in oocyte maturation in crustaceans. In *P. monodon*, 5-HT

concentrations in the ovary appeared higher in the late stages (III and IV), and that 5-HT-ir was more intense in mature oocytes (Oc4) (Wongprasert et al. 2006). As well, 5-HT1 receptors were also expressed in the oocyte membranes at these stages (Ongvarrasopone et al. 2006). These data indicated that 5-HT plays a direct role in regulating oocyte maturation. This is supported by the findings that 5-HT concentrations in the ovary of *M. rosenbergii* were higher in the late stages (III and IV) than in the early stages (I and II), whereas DA concentrations in the ovary were found to be much higher in early ovarian stages (I and II) than in the late stages (III and IV) (Tinikul et al. 2008). Furthermore, DA-ir was most intense in the cytoplasm of previtellogenic oocytes (Oc1, Oc2), but not in the oogonia and in follicular cells, suggesting that DA plays a key role in controlling early oocyte development (Tinikul et al. 2009b). In *L. vannamei*, we found 5-HT-ir was more intense in the ectoplasm of the late stage oocytes (Oc4), whereas DA-ir occurred in the early stage oocytes (Oc2). This implicates that 5-HT and DA may play a direct role in the oocyte development, but at different stages, i.e. 5-HT could be involved in the late oocyte stages, whereas DA could be involved in the early stages. These two neurotransmitters may be taken up in the oocytes from hemolymph, as there were no 5-HT-ir and DA-ir nerve fibers in the ovary. Alternatively, 5-HT and/or DA could be synthesized in the oocytes.

In addition to direct action on oocytes, 5-HT and DA could also exercise their controls over the synthesis and release of a putative gonad-inhibiting hormone (GIH) or GIH-like peptides in the eyestalk, as thought to occur in many decapods, including *P. monodon* (Treerattrakool et al. 2008), and *L. vannamei* (Wang et al. 2000). Apart from an inhibitory effect on GIH release, 5-HT could also stimulate a putative GSH, and/or gonadotropin-releasing hormone (GnRH)-like peptides, from the brain and thoracic ganglia, as these gonad-stimulating

neuropeptides are reported to be present in these neural structures (Tinikul et al. 2011). Conversely, DA could act in an opposite role. In salmonids, DA delayed ovarian development by inhibiting the release of GnRH and LH at the hypothalamus-pituitary level (Peter et al. 1986; Saligaut et al. 1999). As well, DA also exerts an inhibitory role during the early steps of oogenesis, by inhibiting the release of GnRH in many teleost species (Dufour et al. 2010). In tilapia, *Oreochromis aureus*, DA acting via the D2 receptor, inhibited GnRH activity and downregulated the GnRH receptor synthesis (Levavi-Sivan et al. 2004). The DA-mediated mechanism in the *L. vannamei* CNS may be similar to those occurring in salmonids and teleost fish as proposed earlier (Peter et al. 1986; Saligaut et al. 1999; Aizen et al. 2005; Dufour et al. 2010). However, this hypothesis needs to be investigated further by studying the effects of these two neurotransmitters on the expression of these genes. Furthermore, the presence and distribution of 5-HT and DA receptors in the CNS and ovary should also be studied to identify the cellular targets of these two neurotransmitters. In addition, further studies demonstrating the expressions of genes encoding the enzymes involved in the syntheses of 5-HT and DA by RT-PCR or *in situ* hybridization techniques would help to validate whether the two neurotransmitters are synthesized in or uptaken by the oocytes.

References

Aizen J, Meiri I, Tzchori I, Levavi-Sivan B, Rosenfeld H (2005) Enhancing spawning in the grey mullet (*Mugil cephalus*) by removal of dopaminergic inhibition. Gen Comp Endocrinol 142:212-221

Alfaro J, Zuniga G, Komen J (2004) Induction of ovarian maturation and spawning by combined treatment of serotonin and a dopamine antagonist, spiperone in *Litopenaeus stylirostris* and *Litopenaeus vannamei*. Aquaculture 236:511-522

Álvarez RA, Villalobos MGP, Rosete GC, Sosa LR, Aréchiga H (2005) Dopaminergic modulation of neurosecretory cells in the crayfish. Cell Mol Neurobiol 25:345-370

Antonsen BL, Paul DH (2001) Serotonergic and octopaminergic systems in the squat lobster *Munida quadrispina* (Anomura, Galatheidae). J Comp Neurol 439:450-468

Bell TA, Lightner DV (1988) A handbook of normal penaeid shrimp histology. World Aquaculture Society, Baton Rouge, LA, USA

Bellon-Humbert C, Van Herp F (1988) Localization of serotonin-like immunoreactivity in the eyestalk of the prawn, *Palaemon serratus*. J Morphol 196:307-320

Beltz BS (1999) Distribution and functional anatomy of amine-containing neurons in decapod crustaceans. Microsc Res Tech 44:105-120

Beltz BS, Kravitz EA (1983) Mapping of serotonin-like immunoreactivity in the lobster nervous system. J Neurosci 3:585-602

Boglino A, Darias MJ, Ortiz-Delgado JB, Özcan F, Estévez A, Andree KB, Hontoria F, Sarasquete C, Gisbert E (2012) Commercial products for Artemia enrichment affect growth performance, digestive system maturation,

ossification and incidence of skeletal deformities in Senegalese sole (*Solea senegalensis*) larvae. Aquaculture 324-325: 290-302

Bradford MM (1976) A rapid and sensitive method for the quantitation of microgram quantities of protein utilizing the principle of protein-dye binding. Anal Biochem 72:248-254

Cervantes OC, Battelle BA, Moles MLF (1999) Rhythmic changes in the serotonin content of the brain and eyestalk of crayfish during development. J Exp Biol 202:2823-2830

Chan SM, Gu PL, Chu KH, Tobe SS (2003) Crustacean neuropeptide genes of the CHH/MIH/GIH family: implications from molecular studies. Gen Comp Endocrinol 134:214-219

Chen YN, Fan HF, Hsieh SL, Kuo CM (2003) Physiological involvement of DA in ovarian development of the freshwater giant prawn, *Macrobrachium rosenbergii*. Aquaculture 228:383-395

Chen YN, Tseng DY, Ho PY, Kuo CM (1999) Site of vitellogenin synthesis determined from a cDNA encoding a vitellogenin fragment in the freshwater giant prawn, *Macrobrachium rosenbergii.* Molecular Reproduction and Development 54: 215-222

Cournil I, Helluy SM, Beltz BS (1994) Dopamine in the lobster *Homarus gammarus:*I Comparative analysis of dopamine and tyrosine hydroxylase immunoreactivities in the nervous system of the juvenile. J Comp Neurol 344:455-469

Dufour S, Sebert ME, Weltzien FA, Rousseau K, Pasqualini C (2010) Neuroendocrine control by dopamine of teleost reproduction. J Fish Biol 76:129-160.

Eastman-Reks S, Fingerman M (1984) Effects of neuroendocrine tissue and cyclic AMP on ovarian growth *in vivo* and *in vitro* in the fiddler crab, *Uca pugilator*. Comp Biochem Physiol A 79: 679-684

Elekes K, Florey E, Cahill MA, Hoeger U, Geffard M (1988) Morphology, synaptic connections and neurotransmitters of the efferent neurons of the crayfish hindgut. Symp Biol Hung 36:129-146

Elofsson R (1983) 5-HT-like immunoreactivity in the central nervous system of the crayfish, *Pacifastacus leniusculus*. Cell Tissue Res 232:231-236

Elofsson R, Laxmyr L, Rosengren E, Hansson C (1982) Identification and quantitative measurement of biogenic amines and DOPA in the central nervous system and hemolymph of the crayfish *Pacifastacus leniusculus* (Crustacea). Comp Biochem Physiol C 71:195-201

Escamilla-Chimal EG, Van Herp F, Fanjul-Moles ML (2001) Daily variations in crustacean hyperglycemic hormone and serotonin immunoreactivity during the development of crayfish. J Exp Biol 204:1073-1081

Fingerman M, Nagabhushanam R, Sarojini R, Reddy PS (1994) Biogenic amines in crustaceans: identification, localization, and roles. J Crustacean Biol 14:413-437

Fingerman M (1997) Roles of neurotransmitters in regulating the reproductive hormone release and gonadal maturation in decapod crustaceans. Invertebr Reprod Dev 31:47-54

García U, Arechiga H (1998) Regulation of crustacean neurosecretory cell activity. Cell Mol Neurobiol 18:81-99

Gorbman A, Sower SA (2003) Evolution of the role of GnRH in animal (Metazoan) biology. General and Comparative Endocrinology 134: 207-213

Gorgels-Kallen JL (1985) Appearance and innervation of CHH-producing cells in the eyestalk of the crayfish *Astacus leptodactylus* examined after tracing with Lucifer Yellow. Cell Tissue Res 240:385-391

Gu PL, Yu KL, Chan SM (2000) Molecular characterization of an additional shrimp hyperglycemic hormone: cDNA cloning, gene organization, expression and biological assay of recombinant proteins. FEBS Letters 472:122-128

Hsu YA, Messinger DI , Chung JS, Webster SG, de la Iglesia HO, Christie AE (2006) Members of the crustacean hyperglycemic hormone (CHH) peptide family are differentially distributed both between and within the neuroendocrine organs of *Cancer* crabs: implications for differential release and pleiotropic function. J Exp Biol 209:3241-3256

Huberman A (2000) Shrimp endocrinology. A review. Aquaculture 191:191-208

Keller R, Beyer J (1968) Zur hyperglykämischenWirkung von Serotonin und Augenstielextrakt beim Flusskrebs *Orconectes limosus*. Zeitschr vergl Physiol 59:78-85

Kirubagaran R, Peter DM, Dharani G, Vinithkumar NV, Sreeraj G, Ravindran M (2005) Changes in vertebrate-type steroids and 5-hydroxytryptamine during ovarian recrudescence in the Indian spiny lobster, *Panulirus homarus*. New Zeal J Mar Fresh 39:527-537

Kulkarni GK, Nagabhushanam R, Amaldoss G, Jaiswal RG, Fingerman M (1992) In vitro stimulation of ovarian development in the red swamp crayfish, *Procambarus clarkii* (Girard), by 5-hydroxytryptamine. Invertebr Reprod Dev 21:231-240

Levavi-Sivan B, Safarian H, Rosenfeld H, Elizur A, Avitan A (2004) Regulation of gonadotropin-releasing hormone (GnRH)-receptor gene expression in tilapia: effect of GnRH and dopamine. Biol Reprod 70:1545-1551

Lindemans M, Liu F, Janssen T, Husson SJ, Mertens I, Gäde G, Schoofs L (2009) Adipokinetic hormone signaling through the gonadotropin-releasing hormone receptor modulates egg-laying in *Caenorhabditis elegans.* Proceedings of the National Academy of Sciences United States of America 106: 1642-1647

Marco HG, Avarre JC, Lubzens E, Gäde G (2002) In search of a vitellogenesis-inhibiting hormone from the eyestalks of the South African spiny lobster, *Jasus lalandii.* Invertebr Reprod Dev 41:143-150

Meeratana P, Withyachumnarnkul B, Damrongphol P, Wongprasert K, Suseangtham A, Sobhon P (2006) Serotonin induces ovarian maturation in giant freshwater prawn broodstock, *Macrobrachium rosenbergii* de Man. Aquaculture 260:315-325

Mercier AJ, Orchard I, Schmoeckel A (1991) Catecholaminergic neurons supplying the hindgut of the crayfish *Procambarus clarkii*. Can J Zool 69: 2778-2785

Nagano M, Cooke IM (1981) Electrical activity in the crab X-organ sinus gland system: site of initiation, ionic bases and pharmacology. In: Neurosecretion, molecules, cells, systems (eds): 504–505. (Plenum Press, New York).

Ngernsoungnern P, Ngernsoungnern A, Kavanaugh S, Sobhon P, Sower SA, Sretarugsa P (2008a). The presence and distribution of gonadotropin-releasing hormone-liked factor in the central nervous system of the black tiger shrimp, *Penaeus monodon*. Gen Comp Endocrinol 155: 613-622

Ngernsoungnern P, Ngernsoungnern A, Kavanaugh S, Sobhon P, Sower SA, Sretarugsa P (2008b) The identification and distribution of gonadotropin-releasing hormone-like peptides in the central nervous system and ovary of the giant freshwater prawn, *Macrobrachium rosenbergii*. Invertebrate Neuroscience 8: 49-57

Ngernsoungnern P, Ngernsoungnern A, Sobhon P, Sretarugsa P (2009) Gonadotropin-releasing hormone (GnRH) and a GnRH analog induce ovarian maturation in the giant freshwater prawn, *Macrobrachium rosenbergii.* Invertebrate Reproduction and Development 53: 125-135

Ngernsoungnern A, Ngernsoungnern P, Weerachatyanukul W, Chavadej J, Sobhon P, Sretarugsa P (2008c) The existence of gonadotropin-releasing hormone (GnRH) immunoreactivity in the ovary and the effect of GnRHs on the ovarian maturation in the black tiger shrimp *Penaeus monodon*. Aquaculture 279: 197-203

Ongvarrasopone C, Roshorm Y, Somyong S, Pothiratana C, Petchdee S, Tangkhabuanbutra J, Sophasan S, Payim S (2006) Molecular cloning and functional expression of the *Penaeus monodon* 5-HT receptor. Biochem Biophys Acta 1759:328-339

Peter RE, Chang JP, Nahorniak CS, Omeljaniuk RJ, Sokolowska M, Shih SH, Billard R (1986) Interactions of catecholamines and GnRH in regulation of gonadotropin secretion in teleost fish. Recent Prog Horm Res 42: 513-548

Phoungpetchara I, Tinikul Y, Poljaroen J, Chotwiwatthanakun C, Vanichviriyakit R, Sroyraya M, Hanna PJ, Sobhon P (2011) Cells producing insulin-like androgenic gland hormone of the giant freshwater prawn, *Macrobrachium rosenbergii*, proliferate following bilateral eyestalk-ablation. Tissue Cell 43(3): 165-77

Poljaroen J, Tinikul Y, Phoungpetchara I, Kankoun W, Suwansa-ard S, Siangcham T, Meeratana P, Cummins SF, Hanna PJ, Sobhon P (2011) The effects of biogenic amines, gonadotropin-releasing hormones and corazonin on spermatogenesis in sexually mature small giant freshwater prawns, *Macrobrachium rosenbergii* (De Man, 1879) Aquaculture 321: 121-129.

Quackenbush LS (1989) Vitellogenesis in the shrimp, *Penaeus vannamei*: in vitro studies of the isolated hepatopancreas and ovary. Comp Biochem Physiol B 94:253-261

Real D, Czternasty G (1990) Mapping of serotonin-like immunoreactivity in the ventral nerve cord of crayfish. Brain Res 521:203-212

Ridchardson HGD, Decaraman M, Fingerman M (1991) The effect of biogenic amines on ovarian development in fiddler crab, *Uca pugilator*. Comp Biochem Physiol C 99:53-56

Sáenz F, Gárcia U, Aréchiga H (1997) Modulation of electrical activity by 5-hydroxytryptamine in crayfish neurosecretory cells. J Exp Biol 200:3079-3090

Saetan J, Senarai T, Tamtin M, Weerachatyanukul W, Chavadej J, Hanna PJ, Parhar I, Sobhon P, Sretarugsa P Histological organization of the CNS and distribution of a gonadotropin-releasing hormone-like peptide in the blue crab, *Portunus pelagicus.* Cell and Tissue Research. In press.

Sainath SB, Sreenivasula Reddy P (2010) Evidence for the involvement of selected biogenic amines (serotonin and melatonin) in the regulation of molting of the edible crab, *Oziotelphusa senex senex* Fabricius. Aquaculture 302: 261-264

Sainath SB, Sreenivasula Reddy P (2011) Effect of selected biogenic amines on reproduction in the fresh water edible crab, *Oziotelphusa senex senex*. Aquaculture 313: 144-148

Saligaut C, Linard B, Breton B, Anglade I, Bailhache T, Kah O, Jego P (1999) Brain aminergic systems in salmonids and other teleosts in relation to steroid feedback and gonadotropin release. Aquaculture 177: 13-20

Sandeman D, Sandeman R, Derby C, Schmidt M (1992) Morphology of the brain of crayfish, crabs, and spiny lobsters: A common nomenclature for homologous structures. Biol Bull 183:304-326

Sandeman DC, Sandeman RE, Aitken AR (1988) Atlas of serotonin containing neurons in the optic lobes and brain of the crayfish, *Cherax destructor*. J Comp Neurol 269:465-478

Santhoshi S, Sugumar V, Munuswamy N (2008) Histological and immunocytochemical localization of serotonin-like immunoreactivity in the brain and optic ganglia of the Indian white shrimp, *Fenneropenaeus indicus*. Microsc Res Tech 71:186-195

Santhoshi S, Sugumar V, Munuswamy N (2009) Serotonergic stimulation of ovarian maturation and hemolymph vitellogenin in the Indian white shrimp, *Fenneropenaeus indicus,* Aquaculture 291:192-199

Sarojini R, Nagabhushanam R, Fingerman M (1995a) Mode of action of the neurotransmitter 5-hydroxytryptamine in stimulating ovarian maturation in the red swamp crayfish, *Procambarus clarkii*: An in vivo and in vitro study. J Exp Zool 271:395-400

Sarojini R, Nagabhushanam R, Fingerman M (1995b) In vivo effects of DA and DArgic antagonists on testicular maturation in the red swamp crayfish, *Procambarus clarkii.* Biol Bull 189:340-346

Schmidt M, Ache BW (1994) Descending neurons with dopamine-like or with substance P/FMRFamide-like immunoreactivity target the somata of olfactory interneurons in the brain of the spiny lobster *Panulirus argus*. Cell Tissue Res 278:337-352

Schmidt M, Ache BW (1997) Immunocytochemical analysis of glomerular regionalization and neuronal diversity in the olfactory deutocerebrum of the spiny lobster. Cell Tissue Res 287: 541-563

Skinner DM (1985) Molting and regeneration. In the Biology of Crustacea, Integuments, Pigments and Hormonal Processes, vol. 9 (Bliss DE & Mantel LH eds), Academic Press, Orlando, FL. pp 43-146

Sower SA, Freamat M, Kavanaugh SI (2009) The origins of the vertebrate hypothalamic–pituitary–gonadal (HPG) and hypothalamic–pituitary–thyroid (HPT) endocrine systems: New insights from lampreys. General and Comparative Endocrinology 161: 20-29

Swayne TC, Lipkin TG, LA (2010) Live-Cell Imaging of the Cytoskeleton and Mitochondrial–Cytoskeletal Interactions in Budding Yeast. Cytoskeleton Methods and Protocols (Methods in Molecular Biology) 586:41-68

Terakado K (2001) Induction of gamete release by gonadotropin-releasing hormone in a protochordate, *Ciona intestinalis*. General and Comparative Endocrinology 124: 277-284

Tierney AJ, Godleski MS, Rattananont P (1999) Serotonin-like immunoreactivity in the stomatogastric nervous systems of crayfishes from four genera. Cell Tissue Res 295:537-551

Tierney AJ, Kim T, Abrams R (2003) Dopamine in crayfish and other crustaceans: distribution in the central nervous system and physiological functions. Microsc Res Techniq 60:325-335

Tinikul Y, Mercier AJ, Soonklang N, Sobhon P (2008) Changes in the levels of serotonin and dopamine in the central nervous system and ovary, and their possible roles in the ovarian development in the giant freshwater prawn, *Macrobrachium rosenbergii*. Gen Comp Endocrinol 158:250-258

Tinikul Y, Soonthornsumrith B, Phoungpetchara I, Meeratana P, Poljaroen J, Duangsuwan P, Soonklang N, Mercier AJ, Sobhon P (2009a) Effects of serotonin, dopamine, octopamine, and spiperone on ovarian maturation and embryonic development in the giant freshwater prawn, *Macrobrachium rosenbergii* (De Man, 1879). Crustaceana 82:1007-1022

Tinikul Y, Mercier AJ, Sobhon P (2009b) Distribution of dopamine and octopamine in the central nervous system and ovary during the ovarian maturation cycle of the giant freshwater prawn, *Macrobrachium rosenbergii*. Tissue Cell 41:430-442

Tinikul Y, Poljaroen J, Nuurai P, Anuracpreeda P, Chotwiwatthanakun C, Phoungpetchara I, Kornthong N, Poomtong T, Hanna PJ, Sobhon P (2011) Existence and distribution of gonadotropin-releasing hormone-like peptides in the central nervous system and ovary in the Pacific white shrimp, *Litopenaeus vannamei*. Cell Tissue Res 343:579-593

Tinikul Y, Poljaroen J, Kornthong N, Chotwiwatthanakun C, Anuracpreeda P, Poomtong T, Hanna PJ, Sobhon P (2011b) Distribution and changes of serotonin and dopamine levels in the central nervous system and ovary of the Pacific white shrimp, *Litopenaeus vannamei*, during ovarian maturation cycle. Cell and Tissue Research 345: 103-124

Treerattrakool S, Panyim S, Chan SM, Withyachumnarnkul B, Udomkit A (2008) Molecular characterization of gonad-inhibiting hormone of *Penaeus monodon* and elucidation of its inhibitory role in vitellogenin expression by RNA interference. FEBS J 275(5): 970-80.

Tropea C, López Greco, LS Effect of long-term injection of dopamine on the ovarian growth of *Cherax quadricarinatus* juvenile females (Parastacidae, Decapoda). Acta Zoologica (in press).

Tsai PS (2006) Gonadotropin-releasing hormone in invertebrates: structure, function, and evolution. Gen Comp Endocrinol 148: 48-53

Tsukimura B, Kamemoto FI (1991) In vitro stimulation of oocytes by presumptive mandibular organ secretions in the shrimp, *Penaeus vannamei*. Aquaculture 92: 59-66

Vaca AA, Alfaro J (2000) Ovarian maturation and spawning in the white shrimp, *Penaeus* v*annamei*, by serotonin injection. Aquaculture 182:373-385

Van Herp F, Strolenberg GECM (1980) Functional aspects of the neurosecretory system in the eyestalk of the crayfish *Astacus leptodactylus* with special reference to the hyperglycemic hormone. Gen Comp Endocrinol 40:364 (abstract)

Vázquez-Acevedo N, Reyes-Colón D, Ruíz-Rodríguez EA, Rivera NM, Rosenthal J, Kohn AB, Moroz LL, Sosa MA (2009) Cloning and immunoreactivity of the 5-HT 1Mac and 5-HT 2Mac receptors in the central nervous system of the freshwater prawn *Macrobrachium rosenbergii*. J Comp Neurol. 513:399-416

Wang YJ, Hayes TK, Holman GM, Chavez AR, Keeley LL (2000) Primary structure of CHH/MIH/GIH-like peptides in sinus gland extracts from *Penaeus vannamei*. Peptides 21(4):477-84

Wongprasert K, Asuvapongpatana S, Poltana P, Tiensuwan M, Withyachumnarnkul B (2006) Serotonin stimulates ovarian maturation and spawning in the black tiger shrimp *Penaeus monodon*. Aquaculture 261:1447-1454

Wood DE, Derby CD (1996) Distribution of dopamine-like immunoreactivity suggests a role for dopamine in the courtship display behavior of the blue crab C*allinectes sapidus*. Cell Tissue Res 285:321-330

Yang B, Ni J, Zeng Z, Shi B, You W, Ke C (2013) Cloning and characterization of the dopamine like receptor in the oyster *Crassostrea angulata*: Expression during the ovarian cycle. Comparative Biochemistry and Physiology B 164: 168-175

Yano I, Tsukimura B, Sweeney JN, Wyban JA (1988) Induced ovarian maturation of *Penaeus vannamei* by implantation of lobster ganglion. J World Aquac Soc 19:204-209

Ye HH, Wang GZ, Jin ZX, Huang HY, Li SJ (2004) Immunocytochemical studies on the optic ganglia and the brain of *Penaeus vannamei.* Oceanologia et Limnologia Sinica 35(1):78-83

Ye HH, Wang GZ, Jin ZX, Huang HY, Li SJ (2006) Immunocytochemical localization of neuropeptide Y, serotonin, substance P and 13-endorphin in optic ganglia and brain of *Metapenaeus ensis.* Oceanologia et Limnologia Sinica 24(4):384-389

Zhou HS, Juan CC, Chen SC, Wang HY, Lee CY (2003) Dopaminergic regulation of crustacean hyperglycaemic hormone and L-glucose levels in the hemolymph of the crayfish *Procambarus clarkii*. J Exp Zool A 298:44-52

Outputs

Outputs were supported by a Research Grant for New Scholar to Dr. Yotsawan Tinikul (grant no. MRG5480061, jointly funded by the Thailand Research Fund, the Commission on Higher Education, and Mahidol University) (please see appendix).

International publications:

1. **Tinikul Y,** Poljaroen J, Kornthong N, Chotwiwatthanakun C, Anuracpreeda P, Poomtong T, Hanna PJ, Sobhon P (2011) Distribution and changes of serotonin and dopamine levels in the central nervous system and ovary of the Pacific white shrimp, *Litopenaeus vannamei*, during ovarian maturation cycle. Cell and Tissue Research 345:103-124.
2. **Tinikul Y**, Poljaroen J, Tinikul R, Anuracpreeda P, Chotwiwatthanakun C, Senin N, Poomtong T, Hanna PJ, Sobhon P Effects of gonadotropin-releasing hormones and dopamine on ovarian maturation in the Pacific white shrimp, *Litopenaeus vannamei*, and their presence in the ovary during ovarian development (In revision)
3. Poljaroen J, **Tinikul Y**, Phoungpetchara I, Kankoun W, Suwansa-ard S, Siangcham T, Meeratana P, Cummins SF, Hanna PJ, Sobhon P (2011) The effects of biogenic amines, gonadotropin-releasing hormones and corazonin on spermatogenesis in sexually mature small giant freshwater prawns, *Macrobrachium rosenbergii* (De Man, 1879) Aquaculture 321 121-129.

Symposiums and Conferences

1. **Tinikul Y**, Poljaroen J, Tinikul R, Kornthong N, Chotwiwatthanakun C, Anuracpreeda P, Senin N, Poomtong T, Mercier AJ, Hanna PJ, Sobhon P. The presence and effects of serotonin, dopamine and gonadotropin-releasing hormone on ovarian maturation in the giant freshwater prawn, *Macrobrachium rosenbergii* and the Pacific white shrimp, *Litopenaeus vannamei*. Symposium on "Hormonal controls of the crustacean reproduction, and possible applications in aquaculture" 3 April 2013, Department of Anatomy, Faculty of Science, Bangkok, Thailand (Oral presentation).
2. **Tinikul Y,** Poljaroen J, Kornthong N, Chotwiwatthanakun C, Anuracpreeda P, Poomtong T, Hanna PJ, Sobhon P. The serotonergic and dopaminergic systems in the Pacific white shrimp, *Litopenaeus vannamei*: changes in the levels, existence and distribution in the central nervous system and ovary during ovarian maturation cycle. The 2nd International Anatomical Science and Cell Biology Conference (IASCBC2012) & 36th Annual Conferences of Anatomy Association of Thailand, 6th - 8th December, 2012, Chiang Mai, Thailand.

APPENDIX

Cell Tissue Res (2011) 345:103–124
DOI 10.1007/s00441-011-1176-8

REGULAR ARTICLE

Distribution and changes of serotonin and dopamine levels in the central nervous system and ovary of the Pacific white shrimp, *Litopenaeus vannamei*, during ovarian maturation cycle

Yotsawan Tinikul · Jaruwan Poljaroen · Napamanee Kornthong · Charoonroj Chotwiwatthanakun · Panat Anuracpreeda · Tanes Poomtong · Peter J. Hanna · Prasert Sobhon

Received: 1 March 2011 / Accepted: 13 April 2011 / Published online: 24 May 2011

Abstract We investigated changes in serotonin (5-HT) and dopamine (DA) levels and in their distribution patterns in the central nervous system (CNS) and ovary during the ovarian maturation cycle in the Pacific white shrimp, *Litopenaeus vannamei*. The concentrations of these two neurotransmitters were determined by using high performance liquid chromatography with electrochemical detection. The 5-HT concentration exhibited a gradual increase in the brain and thoracic ganglia during early ovarian stages I, II, and III, reaching a maximum at the mature ovarian stage IV, whereas DA showed its highest concentration at ovarian stage II in the brain and thoracic ganglia and then declined to its lowest concentration at ovarian stage IV. In the ovaries, 5-HT was lowest at ovarian stage I and gradually increased to a peak at ovarian stage IV. Conversely, the concentration of DA was highest at ovarian stages I and II and lowest at ovarian stage IV. In the brain, 5-HT immunoreactivity (−ir) from stage IV and DA-ir from stage II were distributed extensively in neurons of clusters 6, 11, and 17, in fibers, and in the anterior and posterior medial protocerebral, olfactory, antenna II, and tegumentary neuropils. In the circumesophageal, subesophageal, thoracic, and abdominal ganglia, both 5-HT-ir and DA-ir were detected in neuropils and surrounding neurons and fibers. 5-HT-ir and DA-ir were more intense in the thoracic ganglia than in other parts of the CNS. In the ovary, 5-HT-ir exhibited high intensity in late oocytes, whereas DA-ir was more intense in early oocytes. Thus, opposing changes occur in the levels of these two neurotransmitters and in their specific localizations in the CNS and ovary during ovarian maturation, indicating their important involvement in female reproduction.

Keywords Serotonin · Dopamine · Central nervous system · Ovary · Pacific white shrimp, *Litopenaeus vannamei* (Crustacea)

This research was supported by a Research Grant for New Scholar to Yotsawan Tinikul (MRG54), and a Distinguished Research Professor Grant to Prasert Sobhon (jointly funded by the Thailand Research Fund, the Commission on Higher Education, and Mahidol University).

Y. Tinikul · J. Poljaroen · N. Kornthong · C. Chotwiwatthanakun · P. Anuracpreeda · P. J. Hanna · P. Sobhon (✉)
Department of Anatomy, Faculty of Science, Mahidol University,
Rama VI Road, Ratchathewi,
Bangkok 10400, Thailand
e-mail: scpso@mahidol.ac.th

Y. Tinikul
e-mail: anatch2002@yahoo.com

Y. Tinikul · J. Poljaroen · C. Chotwiwatthanakun
Mahidol University, Nakhonsawan Campus,
Nakhonsawan 60000, Thailand

P. Anuracpreeda
Agricultural Science Division, Mahidol University,
Kanchanaburi Campus,
Saiyok,
Kanchanaburi 71150, Thailand

T. Poomtong
Coastal Fisheries Research and Development Center,
Banlaem,
Petchaburi 76100, Thailand

P. J. Hanna
Dean's Office, Faculty of Science and Technology,
Deakin University,
Geelong, VIC 3217, Australia

Introduction

The Pacific white shrimp, *Litopenaeus vannamei*, is one of the most important commercial species of decapod crustaceans that is widely cultured in Thailand and other Asian countries. Ovarian maturation of decapod crustaceans, including this species, is controlled by various neurohormones that are synthesized and released from the X-organ-sinus gland (XO-SG) complex located in the eyestalks (Quackenbush 1989; Chen et al. 2003). The biogenic amines, including serotonin (5-HT) and dopamine (DA) that have been detected in the central nervous system (CNS) of crustaceans, are believed to regulate the synthesis and release of the neurohormones of the XO-SG complex (Ridchardson et al. 1991; Fingerman et al. 1994; Tinikul et al. 2009a, b). In addition, these two neurotransmitters are involved in other physiological processes, including fighting behavior, escape, and tail-flipping behaviors (Antonsen and Paul 2001; Beltz 1999; Sarojini et al. 1995a). Several previous studies have reported the positive effects of 5-HT on gonadal maturation in many decapod crustaceans, including the red swamp crayfish, *Procambarus clarkii* (Kulkarni et al. 1992), the Pacific white shrimp, *L. vannamei* (Vaca and Alfaro 2000), the black tiger shrimp, *Penaeus monodon* (Wongprasert et al. 2006), the freshwater prawn, *Macrobrachium rosenbergii* (Meeratana et al. 2006; Tinikul et al. 2009a), and the Indian white shrimp, *Fenneropenaeus indicus* (Santhoshi et al. 2009). On the other hand, DA has been shown to inhibit testicular maturation in *P. clarkii* (Sarojini et al. 1995b), and ovarian maturation in *M. rosenbergii* (Tinikul et al. 2009a). Because of the important roles of 5-HT and DA in reproduction and in the control of ovarian maturation, the levels of 5-HT and DA have been determined by high performance liquid chromatography (HPLC) in relation to seasonality and reproductive stages in various regions of the eyestalks and intestinal nerves of *P. clarkii* (Alvarez et al. 2005; Mercier et al. 1991), the CNS of *Pacifastacus leniusculus* (Elofsson et al. 1982), and the CNS and ovary of *M. rosenbergii* (Tinikul et al. 2008). These studies have reported that the changes of 5-HT and DA levels occur in opposite directions during various stages of the ovarian cycle in these species.

In addition, 5-HT- and DA-immunoreactive cells, have been investigated in the CNS and gonads of decapod crustaceans by using immunohistochemistry. 5-HT-immunoreactive neurons and fibers have been reported to be distributed in the CNS of the squat lobster, *Munida quadrispina* (Antonsen and Paul 2001), the American lobster, *Homarus americanus* (Beltz and Kravitz 1983), the red swamp crayfish, *P. clarkii* (Real and Czternasty 1990; Tierney et al. 1999), and the yabby, *Cherax destructor* (Sandeman et al. 1988). Moreover, DA-immunoreactive neurons have been detected in several regions of the brain of the European lobster, *H. gammarus* (Cournil et al. 1994), the spiny lobster, *P. argus* (Schmidt and Ache 1994), several crayfish species (Tierney et al. 2003), the giant freshwater prawn, *M. rosenbergii* (Tinikul et al. 2009b), and the blue crab *Callinectes sapidus* (Wood and Derby 1996). Despite a few studies reporting the effects of 5-HT and DA on ovarian maturation of *L. vannamei*, the changing levels and distribution of 5-HT and DA in the CNS and ovary have not been investigated during ovarian maturation cycle of this species.

In this study, we have therefore determined the changes in the levels of 5-HT and DA in various regions of the CNS and ovaries during various phases of the ovarian maturation cycle of *L. vannamei* by HPLC. We also report the distribution patterns of 5-HT- and DA-immunoreactive structures in the CNS and ovary by using immunohistochemistry. The implications of the data with respect to the opposing roles of the two neurotransmitters are discussed.

Materials and methods

Experimental animals

Female broodstock of *L. vannamei* (86.44±7.21 g body weight) were obtained from a commercial farm, in Prachaubkirikhan, Thailand. The shrimps were kept in shaded concrete tanks filled with sea water at a temperature of approximately 28°C, with salinity between 30–32 ppt, and under constant aeration. The sea water was changed every day, and the shrimps were fed twice daily with fresh squids and polychaetes. The animals were acclimatized under a photoperiod of 12:12 h light-dark for 2 weeks before beginning the experiments.

Histological observations of CNS anatomy and stages of ovary

The anatomical nomenclature of the various parts of the supraesophageal ganglion (brain) was based on that described previously by Sandeman et al. (1992), whereas other parts of the CNS were named as described by Tinikul et al. (2011). The ovarian stages during the maturation cycle were observed directly and classified on the basis of criteria described previously by Bell and Lightner (1988) and Tinikul et al. (2011).

Chemicals and sample preparations

All chemicals used in the HPLC experiments, including 5-HT and DA, were obtained from Sigma-Aldrich (St. Louis, Mo., USA). Standards of 5-HT and DA were dissolved in

ice-cold 0.1 M perchloric acid on the day of analysis. They were then filtered through a 0.45-μm filter and stored on ice between injections into the HPLC system. The brain, subesophageal ganglion (SEG), five thoracic ganglia (combined), the six abdominal ganglia (combined), and the ovaries, were collected at mid-day from ten animals at each ovarian stage. Each organ was carefully dissected out, and its wet weight was determined before being prepared for analysis (see below).

Procedures for quantification of 5-HT and DA concentrations

The detection and quantification of 5-HT and DA in the CNS and ovaries were performed by using HPLC with electrochemical detection (HPLC-ECD). The average concentrations of 5-HT and DA were estimated in three replicates. The quantifications of 5-HT and DA concentrations were based on the methods described previously by Mercier et al. (1991) and Tinikul et al. (2008). After being dissected out and weighed, each tissue of the CNS and ovary was placed in 50 μl 0.1 M perchloric acid and homogenized at 4°C. The concentrations of 5-HT and DA were detected electrochemically by using a completely isocratic mode. A glassy carbon electrode, serving as the working electrode, was set with an Ag/AgCl reference electrode. The potential of the detector was set at a range between +0.7 to +0.8 V. The sensitivity of the detector was maintained at 100 nA with full-scale deflection. The composition of the mobile phase was 75 mM NaH_2PO_4, 50 μM EDTA, 0.3 mM sodium octylsulfate, 4% methanol, and 2.5% acetonitrile. The pH was adjusted to 2.75 with orthophosphoric acid. The flow rate was kept constant at 0.7 ml/min. The mixture was sonicated and centrifuged at 14,000*g* at 4°C. The supernatants were collected and then filtered through a 0.22-μm Spin-x centrifugal filter tube (Corning, Mass., USA) before injection. Samples were then injected into a 20-μl injection loop and passed onto a Brownlee C_{18}-Aquapore OD-300 HPLC column (250×4.6 mm i.d.; Perkin-Elmer, Conn., USA). The electrochemical signals were recorded and integrated by using data analysis software (Millennium, Waters). The concentrations of 5-HT and DA were quantified by an external standard method in which peaks corresponding to the two neurotransmitters were detected in the extracts at the same elution times as their corresponding standards. Furthermore, the identities of the peaks were verified by spiking the tissue extracts with appropriate amounts of 5-HT and DA standards in repeated separations. The Bio-Rad Protein Assay System (Mississauga, Canada) was employed for protein determination in the extracts, following the method described by Bradford (1976).

Processing of tissues for immunohistochemistry

Immunofluorescence and immunoperoxidase techniques were used for the detection of 5-HT immunoreactivity (5-HT-ir) and DA immunoreactivity (DA-ir) in neurons, fibers, and neuropils, in various parts of the CNS and ovaries, during various stages of the ovarian cycle. The methods used were as described previously (Mercier et al. 1991; Tinikul et al. 2009b, 2011). For observations of immunoreactivity in whole-mounts, the brain, circumesophageal ganglia (CEG), SEG, thoracic ganglia, abdominal ganglia, and ovaries were obtained from 20 female shrimps at four stages of the ovarian cycle (n=5 animals per stage). Prior to dissection of the organs, the shrimps were anesthetized on ice for 15 min. The CNS and ovaries were fixed with 4% paraformaldehyde in 0.1 M phosphate-buffered saline (PBS) at 4°C for 12 h, for 5-HT detection, whereas the CNS was fixed with 4% paraformaldehyde in Millonig's buffer (containing 120 mM NaH_2PO_4, 1% D-glucose, 0.005% $CaCl_2$, buffered with NaOH to pH 7.4) and 1% sodium meta-bisulfite in PBS at 4°C for 12 h, for DA detection. For observation of the immunoreactivity in sections, another 20 female shrimps (n=5 animals per stage) were used, and organs were dissected out, fixed, and processed by the same protocols as described above. After fixation and paraffin-embedding, the tissue sections were cut at a thickness of 6 μm, mounted on slides coated with 3-aminopropyl triethoxy-silane solution (Sigma-Aldrich), and then processed for immunoperoxidase and immunofluorescence detection.

Immunoperoxidase detection

Sections of the CNS and ovaries were deparaffinized with xylene and rehydrated through a graded series of ethyl alcohol (100%, 95%, 90%, 80%, and 70%), for 5 min each. The sections were then immersed in 1% lithium carbonate in 70% ethanol for 15 min. Subsequently, endogenous peroxidase and free aldehyde groups were removed by immersing the sections in 3% H_2O_2 in methanol for 45 min, followed by 1% glycine in 0.1 M PBS for 15 min. The sections were then washed three times with 0.4% Triton X-100 with 1% sodium meta-bisulfite in 0.1 M PBS (PBST). Non-specific binding of proteins was blocked by incubating the sections in blocking solution (10% normal goat serum [NGS], 0.4% Triton X-100, 1% sodium meta-bisulfite in PBS), at room temperature for 2 h. The sections were subsequently incubated overnight in the primary antibodies, namely rabbit anti-5-HT (Chemicon International, USA), diluted 1:100 in blocking solution, or rabbit anti-DA (Gemacbio, St. Jean d'Illac, France), diluted 1:500 in blocking solution, at room temperature. After being washed three times, the sections were incubated for 2 h in

secondary antibody, namely horseradish-peroxidase-conjugated goat anti-rabbit IgG (SouthernBiotech, Birmingham, Ala., USA), diluted 1:200 in blocking solution, and then washed three times. The color reactions were developed by adding NovaRed (Vector, Burlingame, Calif., USA) for 1–5 min, until a red color was observed. Subsequently, the sections were washed with tap water for 15 min, counterstained with Mayer's hematoxylin, dehydrated, and mounted with Permount (Bio-Optica, Milan, Italy). Finally, the sections were examined under a Nikon ECLIPSE E600 light microscope, and images were obtained by using a Nikon digital DXM1200 camera.

Immunofluorescence detection

After fixation, whole-mounts of the CNS were washed with 0.1 M PBS for 6 h, by changing the washing solution every 30 min. Each CNS was desheathed by using microforceps and pre-incubated with 4% Triton X-100-PBS (10% NGS, 4% Triton X-100, 1% sodium meta-bisulfite in PBS) at 4°C for 24 h. The tissues were then washed three times with 0.1 M PBS, by changing the washing solution every 15 min, subsequently permeabilized with Dent's solution (80% ethanol, 20% dimethylsufoxide) at −20°C for 8 h, and washed five times with 0.1 M PBS, by changing the washing solution every 15 min. The CNS whole-mounts were incubated in the primary antibodies (rabbit anti-5-HT diluted 1:100 or rabbit anti-DA diluted 1:500), in 2% NGS, 0.4% Triton X-100, 1% sodium meta-bisulfite in PBS, at 4°C for 6–7 days with gentle shaking, washed five times with PBST by changing the washing solution every 20 min, followed by two washes with 0.1 M PBS by changing the washing solution every 15 min, and incubated in the second antibody, namely Alexa-488-conjugated goat anti-rabbit IgG (Molecular Probes, Eugene, Ore., USA) diluted 1:500 in 5% NGS, 0.4% Triton X-100, 1% sodium meta-bisulfite in 0.1 M PBS, at 4°C for 72 h, with gentle shaking. In addition, the nuclei of cells in the CNS and ovaries were counterstained with ToPro-3 (Molecular Probes), diluted 1:2000 in blocking solution (ToPro-3 is shown in either red or blue). The whole-mounts were then washed with PBST for 2 h with six changes and subsequently with PBS for 1 h with three changes. They were subsequently dehydrated through increasing concentrations of ethanol (50%, 70%, 80%, 90%, 95%, 3×100%) and cleared in methyl salicylate for 30–45 min.

The detection of immunofluorescence in tissue sections was based on the protocol of Tinikul et al. (2011). In brief, the sections were deparaffinized, rehydrated through a graded ethanol series, and incubated with 1% glycine in PBS for 10 min. Non-specific binding of proteins was blocked by immersing the sections in blocking solution (10% NGS and 1% sodium meta-bisulfite in PBST), at room temperature for 2 h. The sections were subsequently incubated overnight in the primary antibodies (rabbit anti-5-HT diluted 1:100 or rabbit anti-DA diluted 1:500) in blocking solution at room temperature and then incubated in the secondary antibody, namely Alexa-488-conjugated goat anti-rabbit IgG (Molecular Probes) diluted at 1:500 in blocking solution, at room temperature for 2 h. In addition, the nuclei of cells were counterstained with ToPro-3 (Molecular Probes) diluted at 1:2000 in blocking solution. Finally, the sections were mounted in Vectashield (Vector Laboratory, Burlingame, Calif., USA).

Confocal laser scanning microscopy and image analysis

The whole-mounts and sections of the CNS and the ovarian sections prepared for immunofluorescence detection were viewed and photographed with an Olympus Fluoview 1000 laser-scanning confocal microscope (Olympus America, Center Valley, Pa., USA). The tissues were scanned sequentially for each fluorophore to obtain separate images for each label and an overlay image of all three channels for each optical section. These projected images were produced by using subsets of the z-stacks. Furthermore, the digital images were exported and converted from the Olympus confocal system as .tiff images and then transferred into Photoshop CS software (Adobe Systems, San Jose, Calif., USA) to adjust the contrast and brightness in order to obtain optimal clarity. In addition, negative controls for each fluorochrome were scanned by using the same parameter settings.

Estimating numbers and staining intensities of 5-HT- and DA-immunoreactive neurons and fibers

The numbers of 5-HT- and DA-immunoreactive neurons in four whole-mounts of various regions of the brain (protocerebrum, deutocerebrum, and tritocerebrum), CEG, SEG (visceral sensory neuropil [VSN], first maxillary neuropil [MX-I], second maxillary neuropil [MX-II], first maxiliped [MP-I], second maxiliped [MP-II], third maxiliped neuropils [MP-III]), thoracic ganglia 1–5, and abdominal ganglia 1–6, at each ovarian stage were determined. The methods used as were described previously (Phoungpetchara et al. 2011). The digital images of tissues at magnifications of 20× and 40× were photographed. The images obtained were 512×512 or 1024×1024 pixels. Each image had a resolution of at least 300 dpi. The numbers of 5-HT- and DA-immunoreactive neurons were counted per visual field (mm^2 area) by using the Cell Counter function in ImageJ software (version 1.43, NIH, Bethesda, Md., USA; available on the internet: http://rsb.info.nih.gov/ij/). At least ten areas in each section (15 random sections per organ) from

both positive and negative areas were counted to compare the numbers of 5-HT- and DA-immunoreactive neurons during various stages of the ovarian maturation cycle. Counting was performed in triplicate.

The intensities of 5-HT-ir and DA-ir in neurons and fibers in various CNS areas and at each ovarian stage were quantified by using ImageJ computer image analysis software (http://rsb.info.nih.gov/ij/) as described previously (Ngernsoungnern et al. 2008; Swayne et al. 2010). In brief, digital images of the whole-mounts and sections at magnifications of 20× and 40× from five randomized sections of each area to be analyzed were obtained. The resolutions and pixels of images were defined as mentioned above, and images were then converted to a grayscale (*Image/Type/8-bit*). A box of 100 × 100 pixels was further generated and placed over the areas of neurons and fibers in order to ensure equivalent areas for all analyzed images. A densitometric analysis of staining intensities was conducted by using NIH ImageJ software. In addition, the "subtract background" function (*Process/Subtract Background*) in the ImageJ software was used to minimize background signals. The viewers did not know the identities of the sections in order to minimize bias in the analysis. Data are expressed as means±SEM.

Specificities of antibodies and controls

The specificities of the polyclonal antibodies against 5-HT and DA were tested by the manufacturer by using standard immunohistochemical methods. The manufacturer also demonstrated that the anti-5-HT and anti-DA antibodies did not cross-react with other biogenic amines. In the controls, the specificities of the anti-5-HT and anti-DA antibodies were ascertained by omitting the primary antibodies from the staining procedure or by pre-absorption of the primary antibodies with 100 μg/ml of synthetic 5-HT or DA (Sigma-Aldrich) at 4°C for 16–18 h, before staining (Tierney et al. 1999). In these controls, no immunostaining was observed.

Statistical analyses

Experimental data were analyzed with the SPSS program for Windows software (version 12.0, SPSS, Chicago, Ill., USA) by using a one-way analysis of variance (ANOVA) and Tukey's post hoc test. A probability value less than 0.05 ($P<0.05$) indicated statistical significance. Data were presented as $\overline{X}$ ± SEM.

Results

Stages of ovarian maturation cycle were identified on the basis of the appearance and size of ovaries that could be seen through the carapace in live females (Fig. 1a, c, e, g); these were verified by histological examination of the ovaries (Fig. 1b, d, f, h). The four major ovarian stages included: stage I containing mainly Oc1 (Fig. 1a, b), stage II containing previtellogenic oocytes (Oc1 and Oc2) (Fig. 1c, d), stage III comprising mostly pre-mature Oc3 (Fig. 1e, f), and stage IV containing mainly mature oocytes Oc4 (Fig. 1g, h). The mature Oc4 of stage IV were characterized by the presence of cortical rods (CRs) around the periphery (Fig. 1h).

Changes of 5-HT and DA concentrations in CNS and ovary

In the HPLC-ECD analyses, the standard peaks of DA and 5-HT showed elution times of about 10 and 25 min, respectively (Fig. 2a). The peaks of 5-HT and DA, in extracts of various parts of the CNS and in ovaries at various reproductive stages exhibited the same elution times as their corresponding standards (Fig. 2b). Moreover, when 5-HT and DA were added to each sample (repeated three times), higher spiked peaks appeared at the same positions as the standards (data not shown), thereby confirming that the peaks were 5-HT and DA in each of the organ extracts.

The concentrations of 5-HT in the brain and thoracic ganglia showed a gradual increase from ovarian stage I and reached the highest concentration at stage IV (Fig. 2c). The concentration of 5-HT at stage I in the brain was 0.15±0.05 nmol/mg and then gradually increased through ovarian stage II (0.22±0.06 nmol/mg) and ovarian stage III (0.45±0.05 nmol/mg) to reach a maximum level (0.62±0.08 nmol/mg) at stage IV. The 5-HT concentration in the brain at stage IV exhibited approximately a four-fold increase over stage I. The pattern was similar in the thoracic ganglia in which the 5-HT concentration was 0.21±0.07 nmol/mg at ovarian stage I, 0.59±0.12 nmol/mg at stage II, 1.37±0.09 nmol/mg at stage III, reaching the highest level of 1.95±0.12 nmol/mg at stage IV and exhibiting approximately a 9.5-fold increase. In the abdominal ganglia, little change occurred in 5-HT concentrations from ovarian stage I to stage II (0.1±0.02 to 0.17±0.03 nmol/mg, respectively), with a small decrease at ovarian stage III (0.09±0.03 nmol/mg) and stage IV (0.11±0.02 nmol/mg). Interestingly, when various parts of the CNS were compared, the concentration of 5-HT was about three to four times higher in the brain at ovarian stages III and IV ($P<0.05$), respectively, than in the brain at ovarian stage I (Fig. 2c). The concentration of 5-HT was about 2.5, 7, and 9.5 times higher in the thoracic ganglia at ovarian stages II, III, and IV ($P<0.05$), respectively, than at stage I. The concentration of 5-HT in the thoracic ganglia at any ovarian stage was about three times higher than that in the

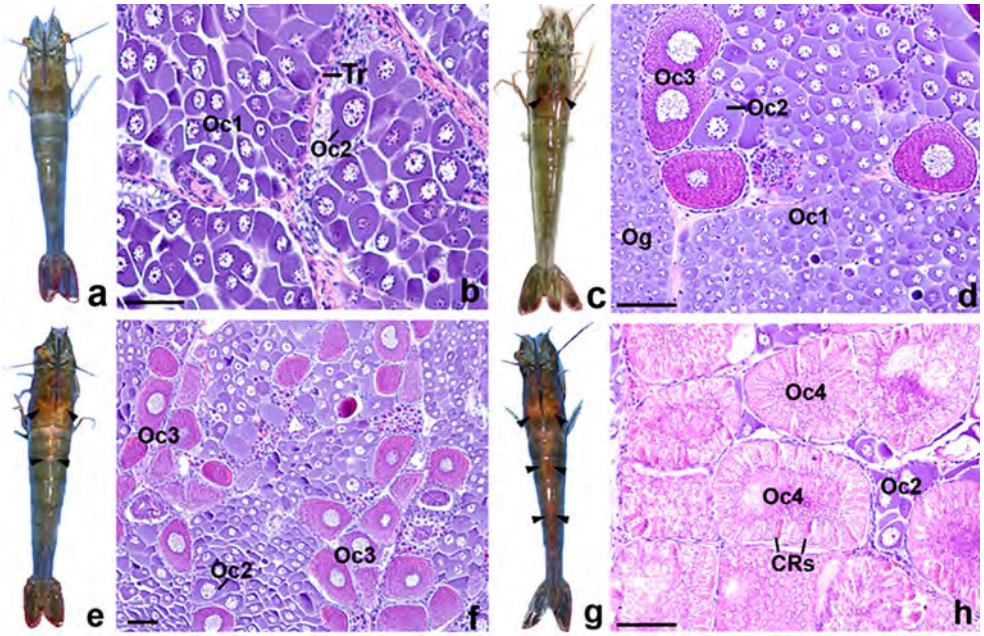

Fig. 1 **a**, **c**, **e**, **g** Dorsal views of female *L. vannamei* showing the locations of ovaries (*black arrowheads*) at four stages of the ovarian maturation: stage I, stage II, stage III, and stage IV, respectively. **b**, **d**, **f**, **h** Light micrographs of sections of ovarian stages I–IV stained by hematoxylin and eosin and demonstrating the histology of oocyte development (*CRs* cortical rods, *Og* oogonia, *Oc1* early previtellogenic oocyte, *Oc2* late previtellogenic oocytes, *Oc3* early vitellogenic oocytes, *Oc4* late vitellogenic or mature oocytes, *Tr* trabeculae). *Bars* 50 μm (**b**, **d**, **f**, **h**)

brain and about 20 times higher than that in the abdominal ganglia. These results were statistically significant ($P<0.05$). Significant increases occurred in 5-HT concentrations in the brain and thoracic ganglia at stages III and IV compared with stages I and II ($P<0.05$; Fig. 2c). In the ovaries, the 5-HT concentration increased from ovarian stage I (0.42±0.12 nmol/mg) to reach a maximum (2.28±0.15 nmol/mg) at ovarian stage IV ($P<0.05$) exhibiting approximately a 5.5-fold increase (Fig. 2c).

The concentration of DA in the brain (Fig. 2d) increased slightly from ovarian stage I (0.35±0.08 nmol/mg) to stage II (0.71±0.06 nmol/mg), then declined by ovarian stage III (0.21±0.07 nmol/mg), and was at a minimum by stage IV (0.11±0.03 nmol/mg). Moreover, the concentration of DA in the thoracic ganglia increased slightly from ovarian stage I to stage II (1.15±0.06 nmol/mg to 1.88±0.07 nmol/mg) and then declined during ovarian stages III and IV, (0.91±0.07 and 0.60±0.06 nmol/mg, respectively; Fig. 2d). The pattern in the abdominal ganglia varied only slightly, similar to that of 5-HT. The DA concentration was highest (0.16±0.04 nmol/mg) at ovarian stage I and then decreased during ovarian stages II, III, and IV (0.11±0.03, 0.12±0.02, 0.07±0.02 nmol/mg, respectively). However, the minor variations in DA levels in the abdominal ganglia were not statistically significant. At ovarian stages I to IV, the concentrations of DA in the thoracic ganglia were about 3-, 2.5-, 4.5-, and 5.5-fold higher than that in the brain ($P<0.05$). In addition, the DA concentrations in the thoracic ganglia were higher by 12-fold, 8.5-fold, 7-fold, and 10-fold at stages I, II, III, and IV, respectively, compared with those in the abdominal ganglia ($P<0.05$). In comparisons within a tissue, the concentrations of DA were about 2, 3.5, and 7 times higher in the brain at ovarian stage II than in the brain at ovarian stages I, III, and IV. The DA concentration was about 1.6, 2, and 3 times higher in the thoracic ganglia at ovarian stage II ($P<0.05$) than in the thoracic ganglia at ovarian stages I, III, and IV, respectively. The lowest and the highest concentrations of DA, in each part of the CNS at each ovarian stage, were the converse of those for 5-HT (Fig. 2d).

The concentration of DA in the ovaries (Fig. 2d) was high at ovarian stage I (17.92±1.42 nmol/mg), then increased further to a maximum level at ovarian stage II (20.31±1.94 nmol/mg), and subsequently decreased at ovarian stage III (11.03±1.04 nmol/mg), reaching a minimum (9.71±0.78 nmol/mg) at ovarian stage IV. The concentrations of DA at stages I and II were significantly higher by about 2–2.5 times than at stages III and IV ($P<0.05$). The concentration of DA in the ovary at ovarian stage II was about 10 times higher than that of 5-HT, but at stage IV, was 5 times higher ($P<0.05$).

Distribution of 5-HT-ir and DA-ir in CNS and ovary

The distribution patterns of both neurotransmitters were similar in all stages of the ovarian cycle; however, the intensity of 5-HT-ir was highest at ovarian stage IV and of DA-ir at stage II. These results thus support the HPLC results. The descriptions of the distribution patterns of 5-HT- and DA-immunoreactive neurons in the brain, CEG, SEG, thoracic ganglia, and abdominal ganglia illustrated here are from whole-mounts taken at stage IV for 5-HT and from stage II for DA. However, the micrographs of 5-HT-ir and DA-ir in the eyestalks and ovaries have been obtained

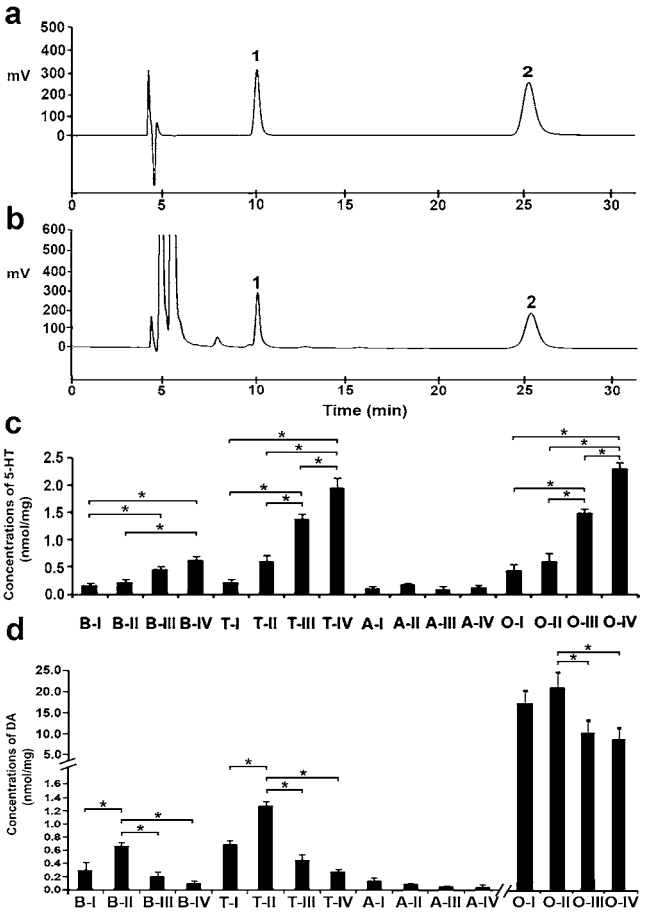

Fig. 2 **a** HPLC chromatograms of DA (*1*) and 5-HT (*2*) standards. The biphasic deflection just before 5 min indicates the application of the standards. The standard peaks of DA and 5-HT show elution times of about 10 and 25 min, respectively. **b** HPLC chromatogram of brain extract showing DA (*1*) and 5-HT (*2*). **c**, **d** Concentrations of 5-HT and DA in the brain, thoracic ganglia, abdominal ganglia, and ovary, at stages I–IV of ovarian maturation cycle. Concentrations are expressed as nanomoles/milligram protein in the organ extracts and are presented as means±SEM (*B* brain, *T* thoracic ganglia, *A* abdominal ganglia, *O* ovaries); significant differences at $*P<0.05$

from sections. In addition, the distribution patterns of 5-HT-ir and DA-ir in whole-mounts have also been compared with 5-HT- and DA-ir in the sections (Figs. 3, 4, 5, 6, 7, 8, 9).

Distribution of 5-HT-ir in CNS

We have previously classified neurons of *P. monodon* into three types, based on their distinct sizes (Ngernsoungnern et al. 2008). In *L. vannamei*, we also found three types of neurons with distinct sizes; the diameters of the small-, medium-, and large-sized neurons were 9±2.5 μm, 28±5.1 μm, and 68±8.2 μm, respectively (mean±SD of 30 cells). In the eyestalks, 5-HT-ir was detected in neurons of cluster 4 (X-organ [XO]) and in fibers in the medulla externa (ME) and medulla interna (MI; Fig. 3a, b). Intensely immunoreactive fibers were numerous in the sinus gland (SG; Fig. 3a, b). In the median protocerebrum of the brain, strong 5-HT-ir was detected in many medium-sized neurons within cluster 6 (Fig. 3c, d). In addition, intense immunoreactive fibers were observed in the protocerebral bridge (PB), anterior medial protocerebral neuropil (AMPN), central body (CB), and posterior medial protocerebral neuropil (PMPN; Fig. 3c, d). In the deutocerebrum, 5-HT-ir was detected in medium-sized neurons in cluster 11 and in the fibers of the olfactory neuropil (ON; Fig. 3c). In the tritocerebrum, 5-HT-ir was detected in medium-sized neurons in cluster 17, fibers in the median antenna I neuropil (MAN), antenna II neuropil (AnN), and in the tegumentary neuropil (TN). Intense 5-HT-immunoreactive medium- and large-sized neurons, and fibers were detected in the CEG (Fig. 3e).

In the SEG (Fig. 4a, b), intense 5-HT-immunoreactive neurons were distributed at the periphery of the MP-I to the MP-III segments of the ganglion. At the anterior end of the SEG, highly intense 5-HT-immunoreactive fibers projected from the CEC to the SEG (Fig. 4a). These fibers extended along the midline and branched at the MX-I to MP-III toward the lateral margin of each ganglion. Paired 5-HT-immunoreactive fibers branched bilaterally from the MP-III to the SEG nerve roots (Fig. 4b). In the thoracic ganglia, most of 5-HT-immunoreactive neurons were localized in ventromedial cell clusters of the ganglia (Fig. 4c–f). Each of the thoracic ganglia contained intense 5-HT-immunoreactive neurons and fibers that were more numerous and intensely stained compared with those in other parts of the CNS. In the chain of thoracic ganglia, we could detect three major 5-HT-immunoreactive fiber bundles, namely, medial fiber bundles (MFB), central fiber bundles (CFB), and lateral fiber bundles (LFB). These fiber bundles were continuous from one ganglion to the next, passing within each intersegmental commissural fiber (IC) of the ventral nerve cord. The MFB and LFB were distinct in T1 to T3 (Fig. 4c–f). Moreover, the CFB was located between the MFB and LFB (Fig. 4d), which both then passed between T3 to T4 and T5 (Fig. 4g, h). In addition, a pair of 5-HT-immunoreactive neurons was detected at the dorsolateral cell cluster in T5 (Fig. 4i), and intense 5-HT-ir was also present throughout the T1–T5 neuropils (Fig. 4c–i).

In the abdominal ganglia, medium- and large-sized 5-HT-immunoreactive neurons were present in the dorso- and ventrolateral cell clusters, exemplified by 5-HT-immunoreactive neurons in A1 (Fig. 5a) and in A3 (Fig. 5b). The MFB and LFB also passed through the IC of all abdominal ganglia (Fig. 5c–e). Intensely immunoreactive punctate fibers were also detected in the neuropils of A1–A6 (Fig. 5a, c, d). No 5-HT-ir was detected in control sections of any part of the CNS. The distribution of 5-HT-ir in the CNS is summarized in Fig. 9a, b, c, e, Table 1.

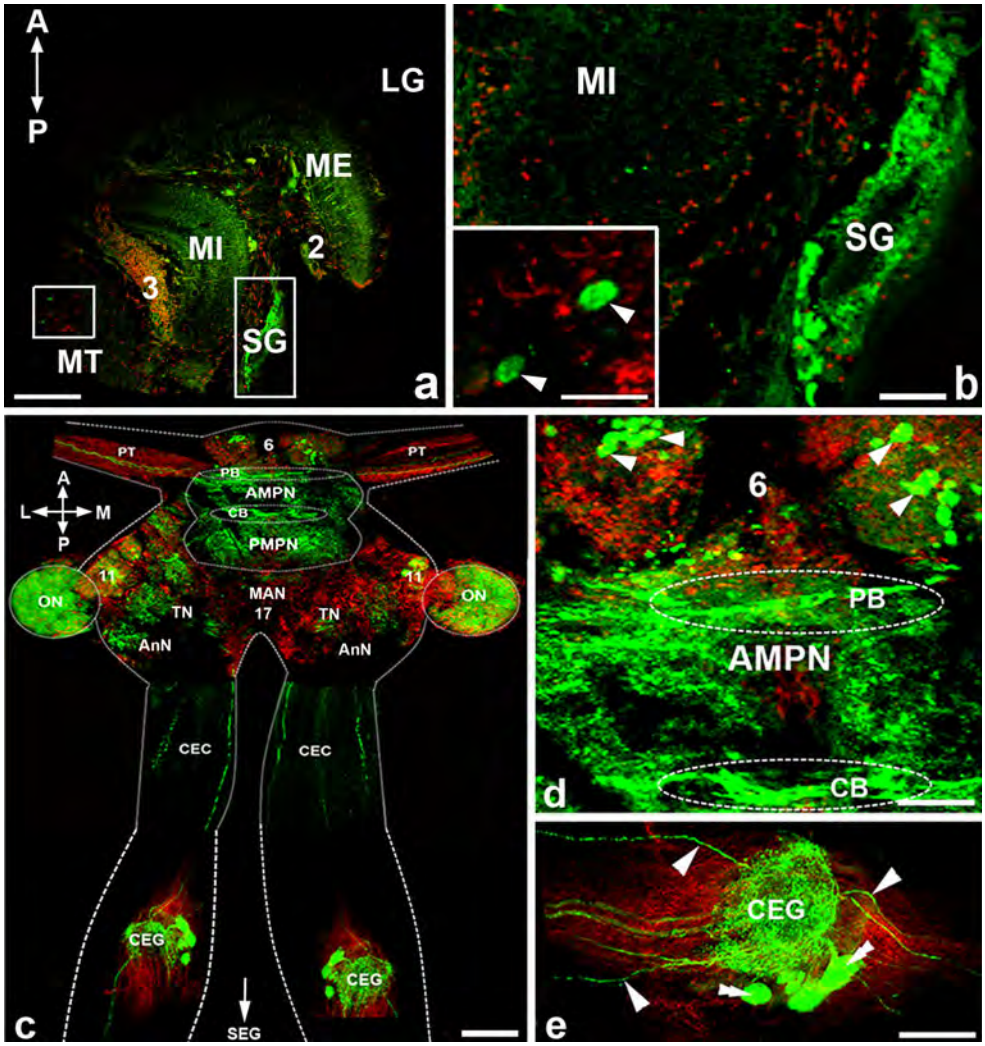

Fig. 3 Immunofluorescence detection of 5-HT-immunoreactivity (ir; *green*) in the central nervous system (CNS) with nuclei counterstained with ToPro-3 (*red*). **a** The eyestalk (orientation given *top left*; *A* anterior, *P* posterior) shows 5-HT-ir in the medulla externa (*ME*), medulla interna (*MI*), medulla terminalis (*MT*), and the sinus gland (*SG*, *large boxed area*). Some neurons in cluster 4 (*small boxed area*) exhibit strong immunofluorescence (*2*, *3* clusters 2 and 3, *LG* lamina ganglionalis). **b** High-power magnification of *boxed areas* in **a** showing the location of 5-HT-immunoreactive neurons in cluster 4 (*inset* X-organ neurons indicated by *arrowheads*) and highly intense 5-HT-immunoreactive fibers in the SG. **c** Whole-mounts of the brain and circumesophageal ganglia (*CEG*; orientation given *top left*; *A* anterior, *P* posterior, *L* lateral, *M* medial) exhibiting 5-HT-ir in neurons of clusters 6, 11, and 17 (*6*, *11*, *17*, respectively), protocerebral bridge (*PB*), anterior medial protocerebral neuropil (*AMPN*), central body (*CB*), posterior medial protocerebral neuropil (*PMPN*), antenna II neuropil (*AnN*), tegumentary neuropil (*TN*), and nearby fibers (*CEC* circumesophageal connective, *MAN* median antenna I neuropil, *ON* olfactory neuropils, *PT* protocerebral tract). **d** Numerous 5-HT-immunoreactive neurons in cluster 6 (*6*, *arrowheads*) and distinctive 5-HT-ir in the PB (*upper dashed oval*), AMPN, and CB (*lower dashed oval*). **e** Highly intense 5-HT-ir in a neuropil of the CEG, in neurons (*double arrowheads*), and in fibers (*arrowheads*) connecting the CEG with the brain. *Bars* 400 μm (**a**, **c**), 100 μm (**b**), 50 μm (**d**, **e**), 25 μm (*inset* in **b**)

Distribution of 5-HT-ir in ovary

In the ovary, 5-HT-ir was intense in the cytoplasm of the late vitellogenic oocytes (Oc3, Oc4; Fig. 5f–h) and appeared much weaker in early oocytes (Oc1, Oc2; Fig. 5h). The oogonia were not immunoreactive (data not shown). No staining was observed in the control sections of the ovary (Fig. 5i). Other control sections by using anti-5-HT pre-absorbed with synthetic 5-HT also showed no immunoreactivity. A summary of the distribution of 5-HT-ir during the various steps of oocyte development is shown in Table 2.

The distribution patterns of 5-HT-ir in the CNS at stage IV were similar to those of the other stages, but

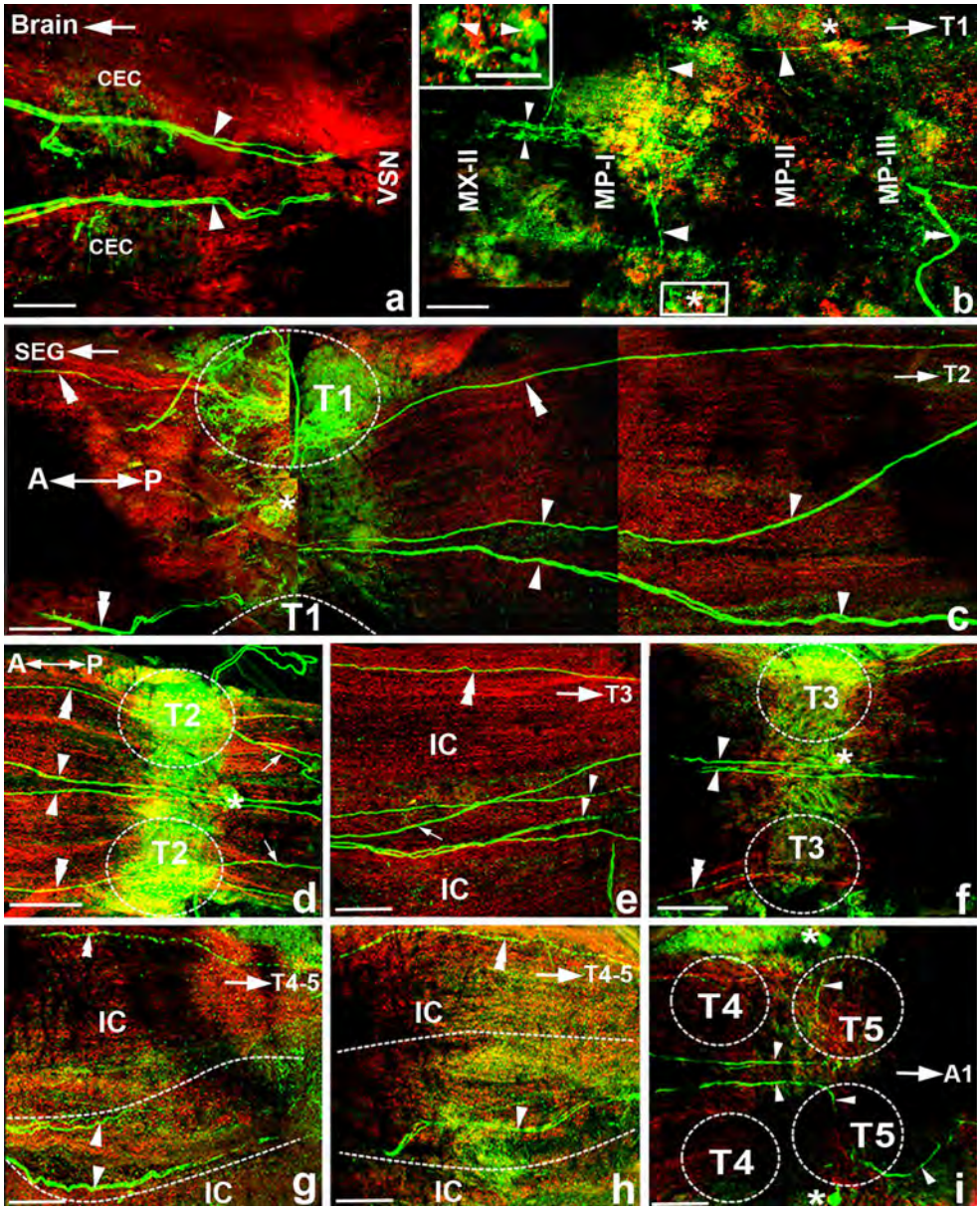

Fig. 4 Immunofluorescence detection of 5-HT-ir (*green*) in the CNS with cell nuclei counterstained with ToPro-3 (*red*). **a** Intense 5-HT-immunoreactive fibers (*arrowheads*) run through the circumesophageal connective (*CEC*) to connect with the subesophageal ganglion (SEG; *VSN* visceral sensory neuropil). **b** 5-HT-immunoreactive neurons of the SEG are located at the periphery of first to third maxilipeds (*MP-I* to *MP-III*, *asterisks*). In addition, 5-HT-immunoreactive fibers run along the midline from MX-II to MP-III (*small arrowheads*) and, at MP-I (*large arrowheads*), they branch off laterally (*large arrowheads*). Furthermore, the paired 5-HT-immunoreactive fibers branch out bilaterally at MP-III of the SEG nerve root (*double arrowheads*). *Inset* High-power micrograph showing intense 5-HT-ir within neurons (*arrowheads*) in the lateral clusters of MP-I to MP-II. **c–f** Thoracic ganglia (orientation shown *top left*; *A* anterior, *P* posterior) with distinctive 5-HT-immunoreactive fiber bundles in the medial fiber bundle (MFB, *arrowheads*) and lateral fiber bundle (LFB, *double arrowheads*) running from thoracic ganglia 1 to 3 (*T1–T3*), with the central fiber bundle (*arrows*) lying lateral to the MFB and locating medial to the LFB. 5-HT-immunoreactive neurons in T2 are located at the ventromedial cell cluster in T1–T3 (**c**, **d**, **f**, *asterisks*). Immunoreactive fibers are distinct in T1–T5 neuropils. **g**, **h** MFB (*arrowheads*) and LFB (*double arrowheads*) extend from T3 to T5. **i** Pair of 5-HT-immunoreactive neurons located at the dorsolateral cluster in T5 (*asterisks*). The areas of the neuropils of each thoracic ganglion are delineated by *dotted lines*. Each side of the intersegmental commissural fibers (*IC*) is indicated by *dashed lines*. *Bars* 100 μm (**a–i**), 50 μm (*inset* in **b**)

the numbers and intensities of immunoreactive neurons and fibers in the latter were much lower (see Fig. 10a, c). This was confirmed in three replicated studies of each stage.

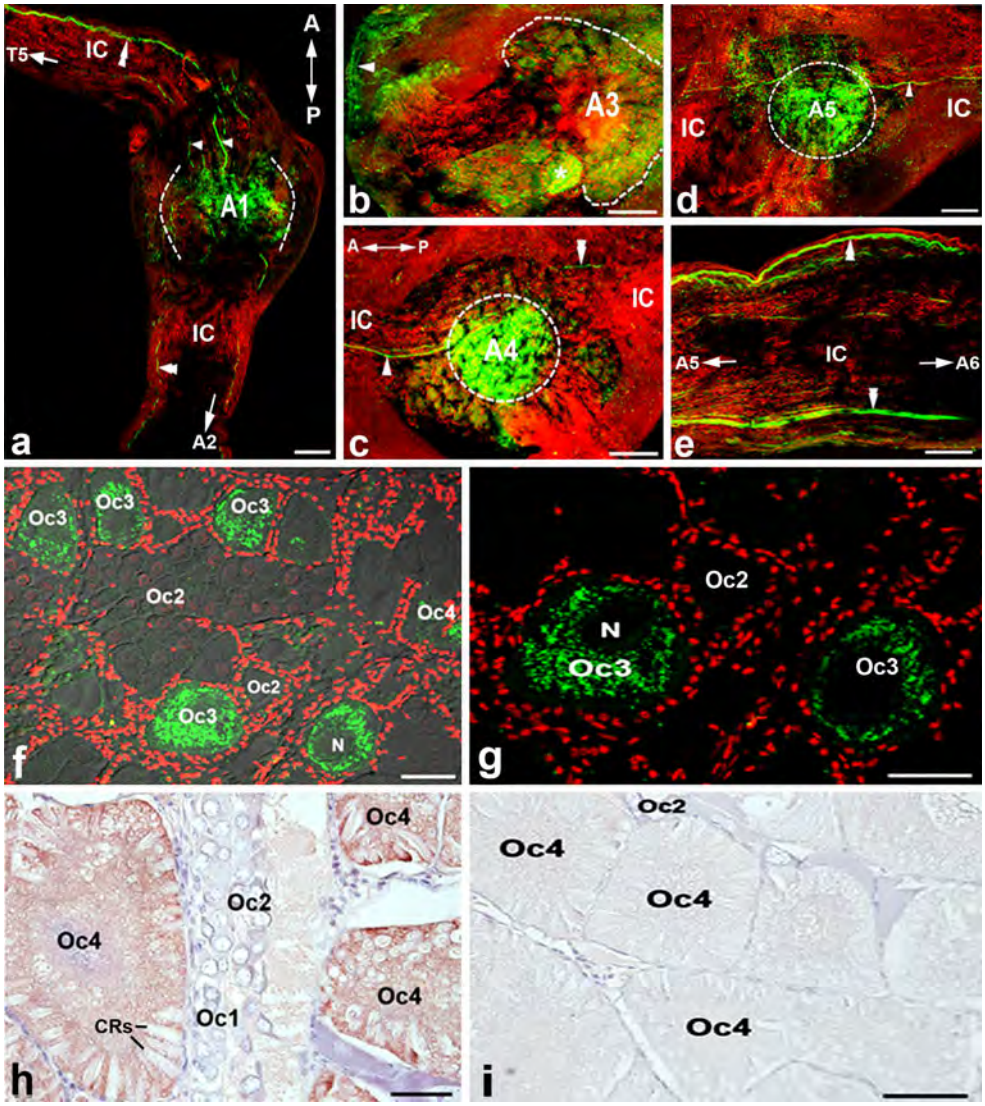

Fig. 5 Immunofluorescence detection of 5-HT-ir (*green*) in the abdominal ganglia (**a–e**) and ovaries (**f–i**). Cell nuclei are counterstained with ToPro-3 (*red*). The orientation of the abdominal ganglia is shown *top right* in **a** and *top left* in **c** (*A* anterior, *P* posterior). **a**, **b** 5-HT-immunoreactive neurons are located in the dorsolateral and ventrolateral cell clusters of abdominal ganglia 1 and 3 (*A1*, *A3*; *asterisk*). Immunoreactive fibers are present in LFB (*double arrowheads*) and MFB (*arrowheads*). **c–e** MFB (*arrowheads*) and LFB (*double arrowheads*) are detected in the intersegmental commissural fibers (*IC*) of A1–A6. Immunoreactive punctate fibers are also present in the neuropils of A1–A6. **f**, **g** Moderate 5-HT-ir is present in the cytoplasm of early vitellogenic oocytes (*Oc3*) but is very weak in previtellogenic oocytes (*Oc1*, *Oc2*; *N* nucleus). **h** Immunoperoxidase detection showing intense 5-HT-ir in the mature oocytes (*Oc4*) but pale immunoperoxidase in early (*Oc1*) and late (*Oc2*) previtellogenic oocytes (*CRs* cortical rods). **i** No immunoperoxidase staining is observed in control sections of the ovary or in immunofluorescence controls. *Bars* 400 μm (**a**, **f**), 100 μm (**b–e**), 50 μm (**g–i**)

Distribution of DA-ir in CNS

In the optic lobe and lateral protocerebrum, DA-immunoreactive neurons were also present in clusters 4 (XO) and 5 (Fig. 6a, b). Some DA-immunoreactive fibers were present in the ME, MI, and medulla terminalis (MT; Fig. 6a). In addition, immunoreactivity was highly intense in fibers of the SG (Fig. 6a, b). In the median protocerebrum, many medium-sized DA-immunoreactive neurons were present in cluster 6 (Fig. 6c, d). Intense immunoreactive fibers were localized in the PB, AMPN, CB, and PMPN (Fig. 6c–e). In the deutocerebrum, mostly medium-sized DA-immunoreactive neurons were present in cluster 11 (Fig. 6c, inset), which was in close proximity to strongly labeled immunoreactive fibers in the ON, the olfactory globular neuropils (OGTN), AnN, and TN (Fig. 6c). In the

tritocerebrum, DA-ir was detected in medium-sized and large neurons in cluster 17 (Fig. 6e). DA-ir was found in neurons of the CEG; some of these neurons were giant neurons with strongly labeled immunoreactive fibers projecting downward via the CEC to the SEG (Figs. 6f, g, 7a) and joining a process of a nerve extending from the SEG (Figs. 6h, 7a, b).

In the SEG, DA-immunoreactive neurons were detected at the lateral margin of the MX-II to the MP-III (Fig. 7b). The DA-immunoreactive fibers making up the MFB and LFB extended through the midline of this ganglion (Fig. 7b). Bilaterally paired DA-immunoreactive fibers projected outward from neurons in MP-III of the SEG (Fig. 7b). In the thoracic ganglia, DA-immunoreactive neurons were detected in most neuronal cell clusters, including the ventromedial cell clusters and dorsolateral cell clusters of T1 (Fig. 7c), T2 (Fig. 7e), T3 (Fig. 7g), and T5 (Fig. 7h). The MFB and LFB passed from the SEG through T1 (Fig. 7c) and continued in the IC to T5 (Fig. 7d–h). The CFB was detected at the periphery of the MFB and projected laterally to the T2 (Fig. 7d). The LFB extended branches laterally to T4 and T5 and also projected downward to A1 (Fig. 7h). The T1–T5 neuropils also contained intense DA-immunoreactive fibers (Fig. 7c–h).

In the abdominal ganglia, medium- and large-sized DA-immunoreactive neurons were detected in the dorso- and ventrolateral cell clusters, exemplified by the DA-immunoreactive neurons in A1 (Fig. 8a), A3 (Fig. 8b), and A5 (Fig. 8c). The neuropils of A1–A6 also contained intense immunoreactive fibers (Fig. 8a–c). The MFB and LFB were also present in the IC connecting between A1 to A6, as for 5-HT-ir (Fig. 8d–f). No positive fluorescence was observed in the control sections taken from various parts of the CNS. The distribution of DA-ir in the CNS is summarized in Fig. 9a, b, d, f, Table 1.

Distribution of DA-ir in ovary

In the ovary, the intensity of DA-ir was highest in the cytoplasm of early oocytes, especially Oc1 and Oc2 (Fig. 8g, h), and in contrast, weak staining was detected in vitellogenic oocytes (Oc3 and Oc4). No DA-ir was observed in the oogonia and follicular cells. The control sections showed no positive fluorescence (Fig. 8i). The distribution of DA-ir in the various oocyte stages is summarized in Table 2.

The distribution patterns of DA-ir in the CNS at ovarian stage II were similar to those of the other stages, but the numbers and intensities of immunoreactive neurons and fibers in the latter were much lower (see Fig. 10b, d). This was confirmed in three replicated studies of each stage.

Changes in numbers and staining intensities of 5-HT- and DA-immunoreactive neurons and fibers in CNS during ovarian maturation cycle

The numbers of 5-HT- and DA-immunoreactive neurons in the brain, CEG, SEG, thoracic ganglia, and abdominal ganglia, counted at various stages of the ovarian maturation cycle, are given in Fig. 10a, b. The numbers of 5-HT- and DA-immunoreactive neurons were significantly higher in the brain, SEG, and thoracic ganglia, than in the CEG and abdominal ganglia ($P<0.05$; Fig. 10a, b). At stage IV, the number of 5-HT-immunoreactive neurons was highest in the brain with 34±3.4 neurons, then in the SEG with 20±2.5 neurons, the combined thoracic ganglia (T1–T5) with 22±2.7 neurons, and the combined abdominal ganglia (A1–A6) with only 17±1.8 neurons ($P<0.05$). The lowest number of 5-HT-immunoreactive neurons was 7±0.6 in the CEG (Fig. 10a). The total number of 5-HT-immunoreactive neurons was about 4.5 times higher in the brain and almost 3 times higher in the SEG and thoracic ganglia at ovarian stage IV than at stage I ($P<0.05$; Fig. 10a). In addition, the total number of 5-HT-immunoreactive neurons was about 2.5 times higher in all parts of the CNS at ovarian stage IV than at stage I ($P<0.05$). However, the number of 5-HT-immunoreactive neurons observed in the abdominal ganglia was not statistically different at any maturation stage (Fig. 10a). At stage IV, the intensities of 5-HT-immunoreactive neurons had also increased markedly in the brain, SEG, and thoracic ganglia compared with stage I ($P<0.05$; Fig. 10c).

The number of DA-immunoreactive neurons was higher in the brain, SEG, thoracic ganglia at stage II than at stage IV ($P<0.05$). Specifically, at stage II, the number of DA-immunoreactive neurons was higher in the brain (30±4.5 neurons), the SEG (24±2.1 neurons), and the combined thoracic ganglia (T1–T5; 26±2.7 neurons) than in the CEG (lowest with 10±0.8 neurons) and the combined abdominal ganglia (A1–A6; 16±1.5 neurons; $P<0.05$; Fig. 10b). The numbers of DA-immunoreactive neurons in the CEG and abdominal ganglia were not statistically different at any stage of ovarian maturation (Fig. 10b). The total number of DA-immunoreactive neurons was about three times higher in the brain and about 3.2 times higher in the SEG and thoracic ganglia at ovarian stage II than at stage IV ($P<0.05$; Fig. 10b). When combining all parts of the CNS, the number of DA-immunoreactive neurons was about 2.4 times higher at ovarian stage II than at stage IV ($P<0.05$). In contrast, the number of DA-immunoreactive neurons in the abdominal ganglia was not statistically different at any stage of maturation (Fig. 10b). Furthermore, the intensities of DA-immunoreactive neurons were significantly greater in the brain, SEG, and thoracic ganglia at stage II compared

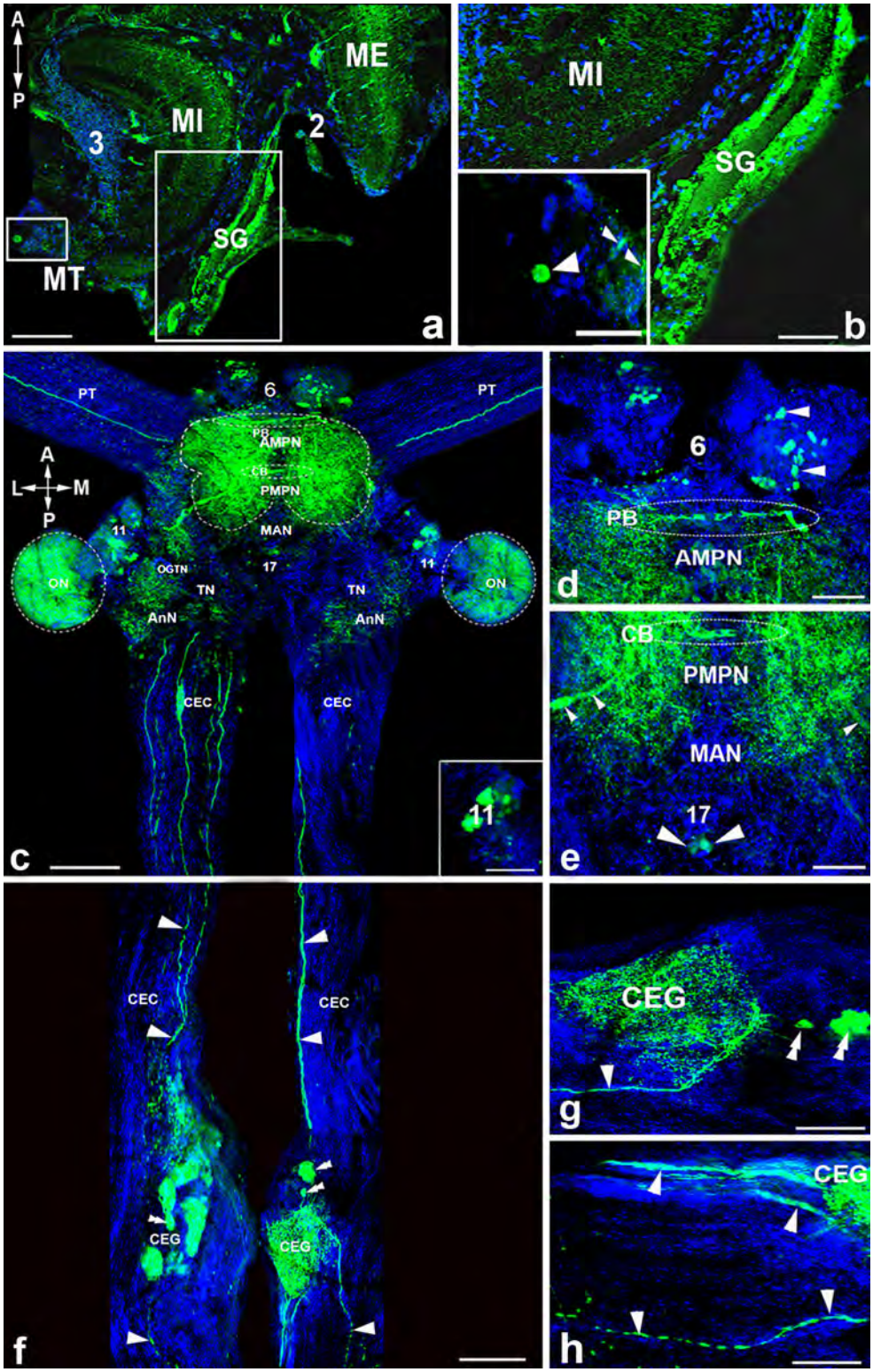

with stage IV ($P<0.05$; Fig. 10d). In contrast, the mean intensities of 5-HT- and DA-immunoreactive neurons and fibers in the abdominal ganglia appeared to be slightly higher at stages IV and II than those at stages I and IV, but these were not statistically different (Fig. 10c, d).

Overall, the highest numbers of 5-HT-ir and DA-ir were detected in neurons of cluster 6 of the brain, whereas the lowest numbers were found in neurons of cluster 17 ($P<0.05$). In the thoracic ganglia, 5-HT-immunoreactive neurons in the midline clusters exhibited the highest numbers

◀ **Fig. 6** Immunofluorescence detection of DA-ir (*green*) in the CNS; cell nuclei are counterstained with ToPro-3 (*blue*). **a** In the eyestalk (orientation is given *top left*; *A* anterior, *P* posterior), intense DA-ir is present in the medulla externa (*ME*), medulla interna (*MI*), medulla terminalis (*MT*), sinus gland (*SG*, *large boxed area*), and a few neurons in cluster 4 (*small boxed area* X-organ [XO]; *2*, *3* clusters 2 and 3, respectively). **b** The two *boxed areas* from **a** are shown at higher magnifications: DA-ir is highly intense in the SG and moderate in the ME; DA-immunoreactive neurons are also present in cluster 4 (*inset*, *large arrowheads*). DA-immunoreactive fibers are seen close to the XO (*inset*, *small arrowheads*). **c** Whole-mounts of the brain and circumesophageal ganglia (orientation is given *top left*; *A* anterior, *P* posterior, *L* lateral, *M* medial) showing DA-ir in neurons of clusters 6, 11, 17 (*6*, *11*, *17*, respectivley), protocerebral bridge (*PB*), anterior medial protocerebral neuropil (*AMPN*), central body (*CB*), posterior medial protocerebral neuropil (*PMPN*), antenna II neuropil (*AnN*), tegumentary neuropil (*TN*), and nearby fibers (*CEC* circumesophageal connective, *MAN* median antenna I neuropil, *OGTN* olfactory globular tract, *ON* olfactory neuropils, *PT* protocerebral tract). *Inset* DA-immunoreactive neurons in cluster 11 (*11*). **d**, **e** Many DA-immunoreactive neurons are present in clusters 6 (**d**, *arrowheads*) and 17 (**e**, *large arrowheads*) and intense immunoreactive fibers are present in the PB, AMPN, and CB (*dashed ovals*) and fibers close to cluster 11 (**e**, *small arrowheads*). **f** Many DA-immunoreactive neurons are present in the circumesophageal ganglia (*CEG*, *double arrowheads*) and in their immunoreactive fibers projecting through the CEC (*arrowheads*) to the SEG. **g**, h High-power micrographs showing the DA-immunoreactive neurons (*double arrowheads*) and positive fibers (*arrowheads*) running into the SEG. *Bars* 400 μm (**a**, **c**, **f**), 100 μm (**b**, **d**, **e**), 50 μm (*insets*)

(Fig. 9c), whereas the numbers of DA-immunoreactive neurons in the dorsolateral clusters were the highest (Fig. 9d). In addition, 5-HT- and DA-immunoreactive fibers in the protocerebral- and deutocerebral areas of the brain showed the highest intensities compared with other parts of the brain. In the thoracic and abdominal ganglia, the lateral margins of each neuropil revealed the highest 5-HT- and DA-immunoreactive intensities compared with other parts of the ganglia (Figs. 9c–f, 10c–d).

Discussion

The present study demonstrated a rise in 5-HT levels in the brain, thoracic ganglia, and ovaries as ovarian maturation progressed, and a decrease in DA levels. The highest levels of 5-HT were detected at stage IV in the brain, thoracic ganglia, and ovaries, whereas the highest levels of DA were detected at stage II in the same tissues. This implies that the increased levels of these two neurotransmitters might be related to specific functions with regard to ovarian maturation. We propose that the increasing levels of 5-HT stimulate ovarian maturation, while DA acts in an opposing function.

Several studies have investigated the levels of 5-HT and DA in decapod crustaceans by using HPLC analyses. In the spiny lobster, *Palinurus homarus*, the 5-HT concentration has been found to be higher in thoracic ganglia than in the brain at ovarian stage IV, suggesting that 5-HT is involved in regulating ovarian maturation (Kirubagaran et al. 2005). In the crayfish, *P. clarkii*, the levels of 5-HT have been quantified in various regions of the brain, with the total concentration of 5-HT being found to be higher in the brain (~0.6 μg/g) than in the eyestalks (~0.3 μg/g; Cervantes et al. 1999). In the freshwater prawn, *M. rosenbergii*, 5-HT concentrations are highest in the brain and thoracic ganglia (~1.50 nmol/mg) at ovarian stage IV and lowest at ovarian stage I (Tinikul et al. 2008); in contrast, DA concentrations exhibit the highest level in the brain and thoracic ganglia at ovarian stage II (~1.30 nmol/mg), but the lowest (~ 0.06 nmol/mg) at ovarian stage IV. Our findings indicate that the changing patterns of 5-HT concentrations in the brain and thoracic ganglia of *L. vannamei* are similar to those reported in the three decapod crustaceans. We have found that the concentration of 5-HT is about 3.5 times higher in the thoracic ganglia at stage IV than in the brain at the same stage, whereas the DA concentration is approximately 2.5 times higher in the thoracic ganglia at stage II than in the brain at the same stage, thus indicating the strong influence of the thoracic ganglia. This is supported by a previous study in the freshwater prawn, *M. rosenbergii*, in which the ovaries, following an injection with culture medium of 5-HT-primed thoracic ganglia, show an increase in the oocyte numbers developing into mature stages (Meeratana et al. 2006). This suggests that 5-HT and/or other hormonal factors from the thoracic ganglia are major factors that stimulate ovarian maturation and oocyte development. Similarly, in mature *L. vannamei* females, the intraspecific implantation of thoracic ganglia also induces ovarian maturation (Yano et al. 1988). In the crab *Uca pugilator*, thoracic ganglion extracts from sexually active females have been shown to induce precocious ovarian maturation in intact and eyestalk-ablated crabs (Eastman-Reks and Fingerman 1984). The combined data lead us to believe that the thoracic ganglia acts as a "primary center" in stimulating ovarian maturation in decapod crustaceans, including *L. vannamei*. However, the abdominal ganglia might not be involved in this process, as only basal levels of 5-HT and DA have been detected there.

Several studies have reported the effects of 5-HT and DA on ovarian maturation in crustaceans. Specifically, 5-HT shortens the period of ovarian maturation in *P. monodon* (Wongprasert et al. 2006) and in *M. rosenbergii* (Tinikul et al. 2009a). Furthermore, the injection of 5-HT into *P. clarkii* causes increases in oocyte diameter and ovarian maturation (Kulkarni et al. 1992). In *L. stylirostris*, the combined injection of 5-HT and spiperone (a DA-antagonist) stimulates ovarian maturation to a greater extent than the injection of 5-HT alone (Alfaro et al. 2004). 5-HT also induces ovarian maturation and spawning in *L. vannamei* (Vaca and Alfaro 2000). In contrast, the injection of DA

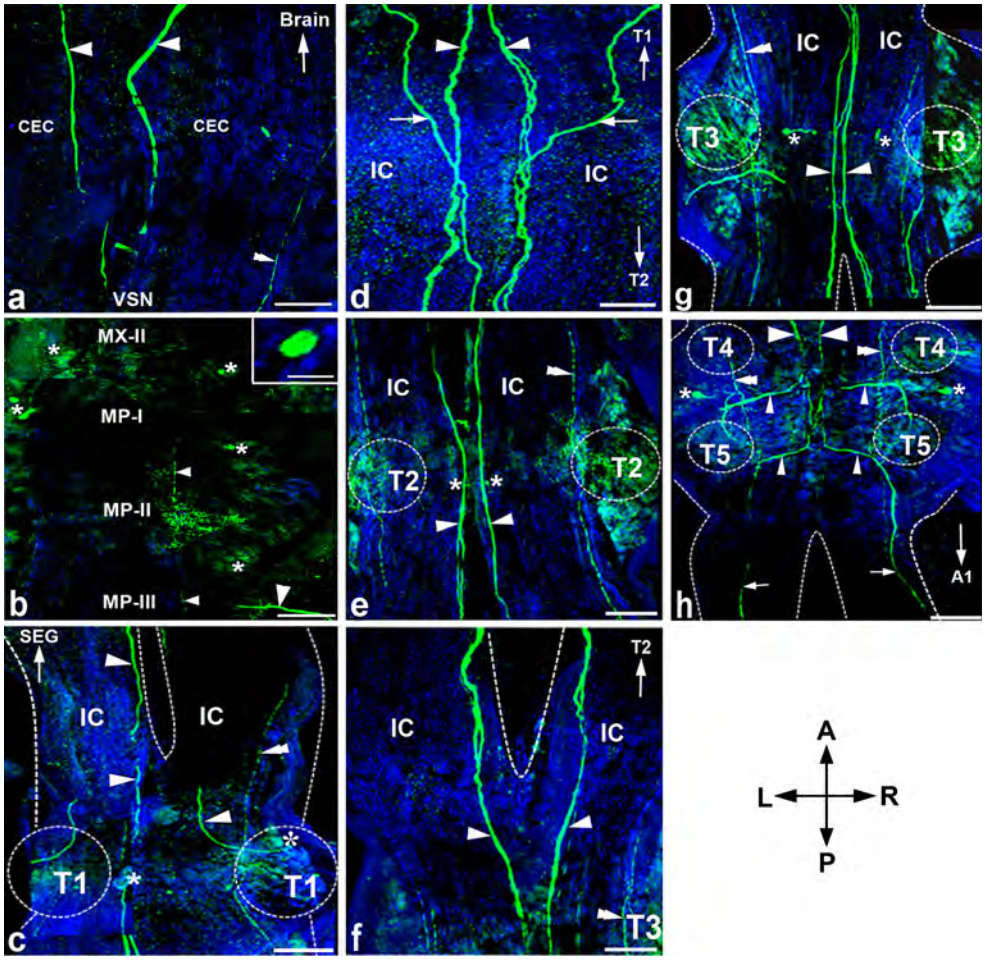

Fig. 7 Immunofluorescence detection of DA-ir (*green*) in the CNS; cell nuclei are counterstained with ToPro-3 (*blue*). **a** DA-immunoreactive fibers, comprising the MFB (*arrowheads*) and LFB (*double arrowheads*) extend through the circumesophageal connective (*CEC*) to the SEG (*VSN* visceral sensory neuropil). **b** SEG showing DA-immunoreactive neurons located at the periphery of the second to third maxilipeds (*MX-II*, *MP-III*) of the SEG (*asterisks*). DA-immunoreactive fibers are observed along the midline (*small arrowheads*). Bilaterally paired DA-immunoreactive fibers project outward from neurons in MP-III of the SEG (*large arrowhead*; *MP-I* first maxiliped). *Inset* High-power micrograph showing medium-sized DA-immunoreactive neurons. **c–g** DA-immunoreactive neurons are present in the dorsolateral and ventromedial clusters in T1 (**c**, *asterisks*), in T2 (**e**, *asterisks*), and in the dorsomedial cluster in T3 (**g**, *asterisks*). *Dashed lines* in **c**, **f** indicate each side of the intersegmental commissural fibers (*IC*) and the area of the ganglion, respectively. MFB (*arrowheads*) and LFB (*double arrowheads*) extend from the SEG to T5 (**f**, **h**, *arrowheads*). The CFB are just lateral to the MFB and project to the T2 (**d**, *arrows*) and to the T3, T4, and T5. Highly intense DA-immunoreactive fibers are present in the T1–T5 neuropils. **h** A pair of DA-immunoreactive neurons are located in the dorsolateral cell cluster in T5 (*asterisks*). MFB (*large arrowheads*) and LFB (*double arrowheads*) connect between T4 and T5, and their branches extend laterally to T4 and T5 (*small arrowheads*), and project downward to first abdominal ganglion (*A1*, *arrows*). *Dotted circles* surround the neuropils of each thoracic ganglion (*A* anterior, *L* left, *P* posterior, *R* right). *Bars* 100 μm (**a–h**), 50 μm (*inset* in **b**)

into *M. rosenbergii* delays ovarian maturation and embryonic development (Tinikul et al. 2009a), and DA injected into *P. clarkii* also lengthens the gonadal maturation period (Sarojini et al. 1995b). Reports regarding the effects of 5-HT and DA on vitellogenesis have been presented. In *M. rosenbergii*, vitellogenin (Vg) concentrations of prawns treated with 5-HT are highest at ovarian stage IV, whereas treatment with DA produces lower Vg concentrations (Tinikul et al. 2008). These results indicate direct causal relationships, with 5-HT stimulating and DA inhibiting Vg synthesis. Moreover, after treating the Indian white shrimp, *F. indicus*, with 5-HT, the Vg concentration increases significantly from the early ovarian stages (stages I and II) to the mature stage (stage IV), indicating the stimulatory role of 5-HT on ovarian maturation with a correlated increase of Vg levels (Santhoshi et al. 2009). Taken together, these studies suggest a positive causal relationship between 5-HT and Vg, and a negative role for DA. As the level of Vg reflects ovarian maturation and oocyte development to the more mature stages (Tinikul et al. 2008; Santhoshi et al. 2009), we believe that 5-HT also exercises a positive control over the ovarian maturation

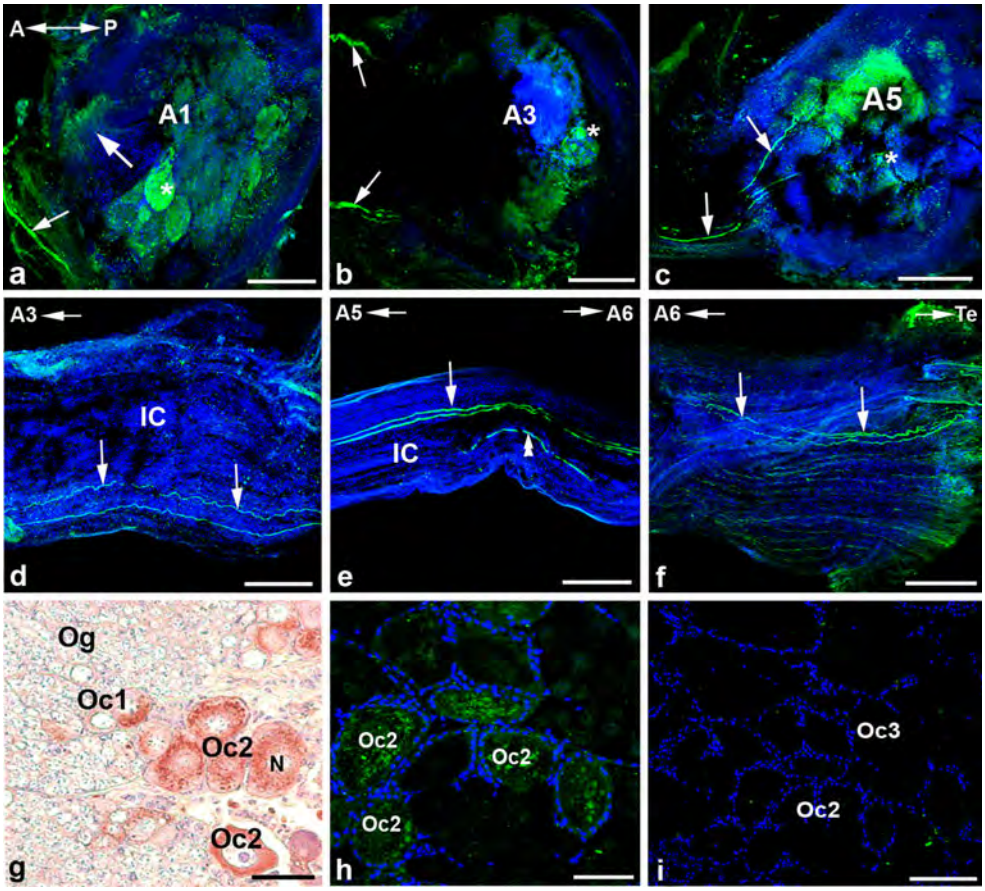

Fig. 8 Immunofluorescence detection of DA-ir (*green*) in the abdominal ganglia (*A1*, *A3*, *A5*) whose orientation is shown *top left* in **a** (*A* anterior, *P* posterior), and ovaries; cell nuclei are counterstained with ToPro-3 (*blue*). **a–c** Large DA-immunoreactive neurons are present in the dorsolateral and ventrolateral cell clusters and are exemplified in A1 (**a**, *asterisk*), A3 (**b**, *asterisk*), and A5 (**c**, *asterisk*). **d–f** DA-ir in MFB (*arrows*) and LFB (*double arrowheads*) are shown within the intersegmental commissural fibers (*IC*) of A1–A6. Immunoreactive fibers are also present in the neuropils of A1–A6 (*Te* telson). **g–h** DA-ir is moderate in early previtellogenic oocytes (*Oc1*) and more intense in late previtellogenic oocytes (*Oc2*), whereas the late oocytes (*Oc3*, *Oc4*) show weak staining (*Og* oogonia, *N* nucleus). **i** Control section of the ovary showing no staining. *Bars* 100 μm

process in *L. vannamei*. This is supported further by the finding that injection of 5-HT into *L. vannamei* stimulates ovarian maturation (Vaca and Alfaro 2000). In contrast, DA apparently exercises an opposite control, as demonstrated in other decapods species (Sarojini et al. 1995b; Tinikul et al. 2009a).

In an earlier report on *L. vannamei*, the presence of 5-HT-ir has been identified in the eyestalks and in the brain (Ye et al. 2004), but not in other parts of the CNS. Furthermore, no reports as yet exist with regard to the neuroanatomical pathways of 5-HT- and DA-immunoreactive neurons and fibers in the CNS and their distribution patterns. Ours is the first study to demonstrate the complete neural networks of 5-HT- and DA-immunoreactive neurons, fibers, and neuropils, which we have found to be highly organized in the eyestalks, brain, and all ganglia of the ventral nerve cord of *L. vannamei*. In general, the distributions of 5-HT-ir and DA-ir in the CNS overlap extensively, indicating that the two systems share common pathways. Some reports have shown the presence of 5-HT in the eyestalk, particularly in the XO and in the SG of a few decapod crustaceans. In the crayfish, *P. leniusculus*, 5-HT-immunoreactive neurons and fibers have been observed in various ganglia (MI and MT) in the eyestalks (Elofsson 1983). In the shrimp, *Metapenaeus ensis*, 5-HT-ir has been found in XO neurons and fibers of the optic ganglia, implying that 5-HT is involved in the synthesis and release of related neurohormones from this structure (Ye et al. 2006). In the Indian white shrimp, *F. indicus*, 5-HT-ir has been found in XO neurons and in the fibers of SG, suggesting that this group of cells and fibers are a primary source of 5-HT and regulate the release of other XO neurohormones, such as crustacean hyperglycemic hormone (CHH; Santhoshi et al. 2008). Moreover, distinct 5-HT-ir has been observed in the MT and in the SG of the shrimp, *Palaemon serratus* (Bellon-Humbert and Van Herp 1988), and *P. clarkii* (Escamilla-Chimal et al. 2001), implicating 5-HT in the regulation of neurosecretory activity at these structures.

5-HT has been shown to induce the bursting of action potentials in the intact XO axons of *P. clarkii* (Saenz et al. 1997) and to elicit electrical activity of XO cells in the crayfish, *Orconectes limosus*, and the crab, *Cardisoma carnifex* (Keller and Beyer 1968; Nagano and Cooke 1981). Injections of 5-HT into the crayfish hemolymph stimulate an increase in the number of CHH granules in the SG of *Astacus leptodactylus*, followed by a hyperglycemic response in the blood, suggesting a direct role of 5-HT in stimulating the release of CHH (Van Herp and Strolenberg 1980; Gorgels-Kallen 1985). In the present study, intense 5-HT-ir has been detected within neurons of cluster 4 (XO

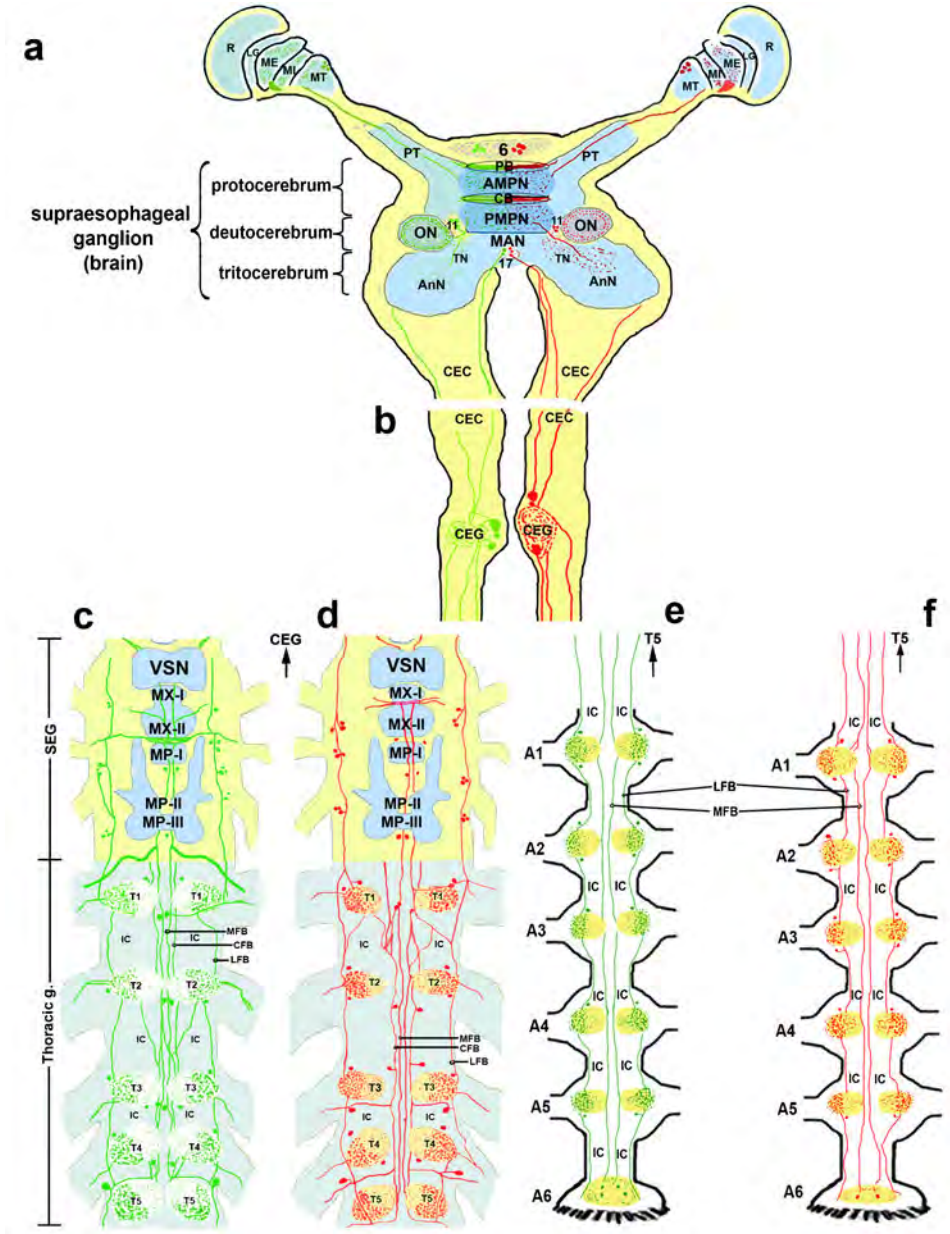

Fig. 9 Representations summarizing the distribution patterns of 5-HT-ir and DA-ir in the CNS of female *L. vannamei* (*green* presence of 5-HT-ir in **a**–**c**, **e**, *red* presence of DA-ir in **a**, **b**, **d**, **f**). The CNS is composed of: (**a**) the eyestalk and brain, (**b**) circumesophageal ganglia (*CEG*), (**c**, **d**) subesophageal ganglion (*SEG*) and five major thoracic ganglia (*T1–T5*), and (**e**, **f**) six abdominal ganglia (*A1–A6*). The brain is divided into a protocerebrum, deutocerebrum, and tritocerebrum, each comprising neuronal clusters (*numbers*) and corresponding neuropils. Major 5-HT- and DA-immunoreactive fiber bundles, including medial fiber bundles (*MFB*), central fiber bundles (*CFB*), and lateral fiber bundles (*LFB*) are detected within the ventral nerve cord. These fiber bundles are continuous from one ganglion to the next from the SEG to T5 and A1-A6, and pass within each intersegmental commissural fiber (*IC*) of the ventral nerve cord. 5-HT-ir and DA-ir are also present throughout the T1–T5 neuropils. Immunoreactive neuropils are illustrated by *stippling* whose density corresponds to the intensity of the staining (immunoreactivity). The positive neurons in the different clusters are illustrated by *solid dots* (*A* anterior, *AMPN* anterior medial protocerebral neuropil, *AnN* antenna II neuropil, *CB* central body, *CEC* circumesophageal connective, *L* lateral, *LG* lamina ganglionaris, *MAN* median antenna I neuropil, *ME* medulla externa, *MI* medulla interna, *MP-I*, *MP-II*, *MP-III* first, second, and third maxilipeds, respectively, *MT* medulla terminalis, *MX-I*, *MX-II* first and second maxillary neuropils, respectively, *ON* olfactory neuropil, *P* posterior, *PB* protocerebral bridge, *PT* protocerebral tract, *PMPN* posterior medial protocerebral neuropil, *R* retina, *TN* tegumentary neuropils, *VSN* visceral sensory neruropil)

neurons) and associated fibers and is even more marked in the SG. Thus, we believe that 5-HT-ir is present in some XO neurons and in the SG of *L. vannamei*, as reported in other species. This suggests that 5-HT also plays a role in

Table 1 Summary of the presence of 5-HT-immunoreactivity (*ir*) and DA-ir in various parts of the central nervous system (CNS) of *L. vannamei* (+ presence of immunoreactivity in neurons, fibers, and neuropils of the CNS regions, − no immunoreactivity in neurons, fibers, and neuropils of the CNS regions, *A1–A6* abdominal ganglia 1–6, *AnN* antenna II neuropil, *AMPN* anterior medial protocerebral neuropil, *C1–C17* neuronal clusters 1–17 in the brain, *CB* central body, *CEG* circumesophageal ganglia, *IC* intersegmental commissural fibers, *L* large-sized neuron, *LG* lamina ganglionaris, *M* medium-sized neuron, *ME* medulla externa, *MI* medulla interna, *MP-I, MP-II and MP-III* first, second and third maxiliped neuropils, *MT* medulla terminalis, *MX-I and MX-II* first and second maxillary neuropils, *MAN*, median antenna I neuropil, *OGTN* olfactory globular tract neuropil, *ON* olfactory neuropil, *PB* protocerebral bridge, *PMPN* posterior medial protocerebral neuropil, *S* small-sized neuron, *SG* sinus gland, *T1–T5* thoracic ganglia 1–5, *TN* tegumentary neuropils, *VSN* visceral sensory neruropil)

Stuctures	Neuronal clusters/Neuropils	5-HT-ir		DA-ir	
		Neurons	Fibers	Neurons	Fibers
Eyestalk	C1–C3	−	−	−	−
	C4–C5	+ (S,M)	−	+ (S,M)	−
	SG	−	+	−	+
	Neuropils (LG, ME)	−	+	−	+
	Neuropils (MI, MT)	−	+	−	+
Protocerebrum	C6	+ (M)	−	+ (M)	−
	C7–C8	−	−	−	−
	Neuropils (PB, CB, AMPN, PMPN)	−	+	−	+
Deutocerebrum	C9, C10, C12, C13	−	−	−	−
	C11	+ (M)	−	+ (M)	−
	Neuropils (ON, OGTN, MAN)	−	+	−	+
Tritocerebrum	C14-C16	−	−	−	−
	C17	+ (S,M)	−	+ (M)	−
	Neuropils (AnN, TN)	−	+	−	+
Circumesophageal ganglia (CEG)	CEG	+ (M,L)	+	+ (M,L)	+
Subesophageal ganglion (SEG)	Mandibular (VSN)	−	+	−	+
	Maxilliaries I–II	+ (S,M)	+	+ (S,M)	+
	Maxilipeds I–III	+ (S,M)	+	+ (M)	+
Thoracic ganglia	T1	+ (M)	+	+ (M)	+
	T2	+ (M)	+	+ (M)	+
	T3	+ (M)	+	+ (M)	+
	T4	+ (M,L)	+	+ (M,L)	+
	T5	+ (M,L)	+	+ (M,L)	+
Abdominal ganglia	A1	+ (M,L)	+	+ (M,L)	+
	A2	+ (M)	+	+ (M)	+
	A3	+ (M,L)	+	+ (M,L)	+
	A4	+ (M)	+	+ (M)	+
	A5	+ (M)	+	+ (M)	+
	A6	+ (M,L)	+	+ (M,L)	+

Table 2 Summary of 5-HT-ir and DA-ir in various steps of differentiating oocytes and their associated follicular cells (+ weak immunoreactivity, ++ moderate immunoreactivity, +++ strong immunoreactivity, − no immunoreactivity, *Fc* follicular cells, *Oc1* early previtellogenic oocyte, *Oc2* late previtellogenic oocytes, *Oc3* early vitellogenic oocytes, *Oc4* mature oocytes, *Og* oogonia)

Immunoreactivity (ir)	Steps in differentiating oocytes and follicular cells								
	Og	Oc1	Fc	Oc2	Fc	Oc3	Fc	Oc4	Fc
5-HT-ir	−	+	−	+	−	++	−	+++	−
DA-ir	−	++	−	+++	−	+	−	+	−

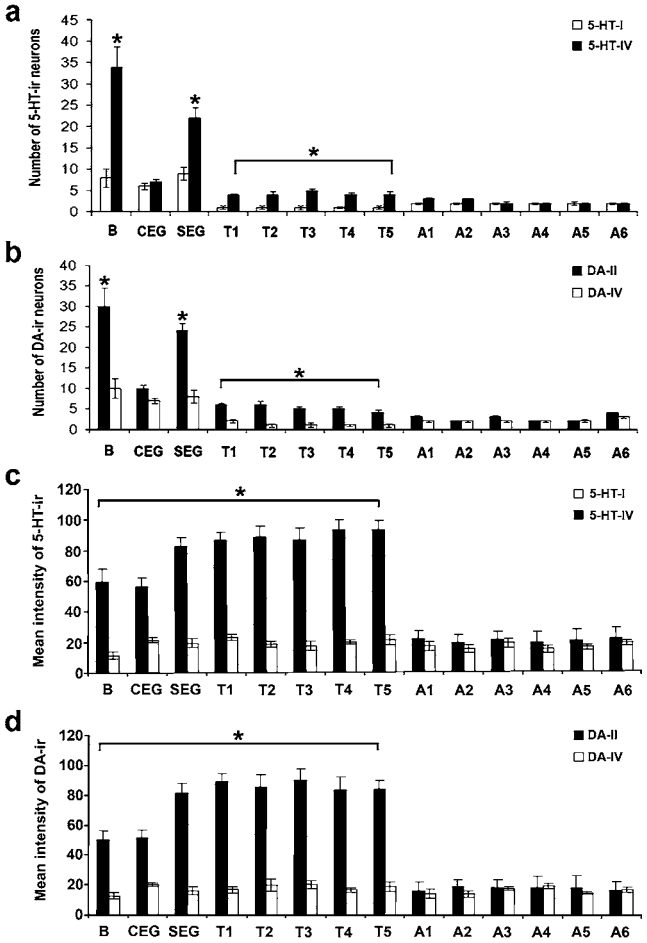

Fig. 10 Histograms showing the mean numbers of 5-HT-immunoreactive neurons at ovarian stages I and IV (**a**) and DA-immunoreactive neurons at ovarian stages II and IV (**b**) in various parts of the CNS of *L. vannamei*. Significant differences of 5-HT- and DA-immunoreactive neuronal numbers were found in the brain, SEG, and thoracic ganglia ($P<0.05$). No significant differences in 5-HT- and DA-immunoreactive neuronal numbers were observed in the CEG and abdominal ganglia ($P>0.05$). **c**, **d** Mean intensities of 5-HT-immunoreactive (at ovarian stages I and IV) and DA-immunoreactive (at ovarian stages II and IV) neurons and fibers within various regions of the CNS. Significant differences were seen between the intensities of 5-HT- and DA-immunoreactive neurons and fibers in the brain, SEG, and thoracic ganglia ($P<0.05$) but not in the abdominal ganglia. For each data point, the means are calculated from whole-mount preparations showing the staining intensities (immunoreactivities) of the two neurotransmitters. Values represent $\overline{X}$ ± SEM; significantly different at $^*P<0.05$ (*B* brain, *CEG* circumesophageal ganglia, *SEG*, subesophageal ganglion, *T1–T5* thoracic ganglia 1–5, *A1–A6* abdominal ganglia 1–6)

stimulating the synthesis of neuropeptides, such as CHH, from the XO neurons, as reported in other decapod crustaceans, and possibly also causes the release of this hormone from the SG. As CHH belongs to the same family as GIH/MIH (gonad-inhibiting and molt inhibiting hormones; Hsu et al. 2006), the same controlling mechanism might apply to the synthesis and release of these hormones from the XO. This has yet to be demonstrated in *L. vannamei*. The 5-HT-immunoreactive neurons in the XO and their positive fibers in the SG might also be involved in controlling the XO neurosecretory neurons that synthesize the CHH family of hormones, as reported earlier in crabs and crayfish.

Ovarian maturation and vitellogenesis are regulated by GIH (Huberman 2000), which is a member of the neuropeptide family that is synthesized in neurons located in the XO and transported to the axon terminals that end at the SG from which it is secreted into the hemolymph (Skinner 1985; Chan et al. 2003; Treerattrakool et al. 2008). 5-HT and DA are thought to exercise their controls over the synthesis and release of a putative gonad-inhibiting hormone (GIH/VIH) or GIH-like peptides in the eyestalks of *P. monodon* (Treerattrakool et al. 2008), *M. ensis* (Gu et al. 2000), *L. vannamei* (Wang et al. 2000), and *Jasus lalandii* (Marco et al. 2002). 5-HT possibly acts by inhibiting the release of GIH from the XO and/or by stimulating putative gonad-stimulating hormone or gonadotropin-releasing hormone (GnRH-like peptide) from the brain and thoracic ganglia, as a GnRH-like gonad-stimulating neuropeptide has been reported to be present in these neural structures (Tinikul et al. 2011), whereas DA might play the opposite role (Sarojini et al. 1995b; Fingerman 1997). However, this hypothesis needs to be investigated further by studying the effects of these two neurotransmitters on the expression of the genes encoding the respective hormones. Furthermore, the presence and distribution of 5-HT and DA receptors in the CNS and ovary should also be studied to identify the cellular targets of these two neurotransmitters.

In the lobster, *H. americanus*, about one hundred 5-HT-immunoreactive cells have been detected in the central ganglia, thirty five 5-HT-immunoreactive neurons in the brain, one neuron in each of the paired circumesophageal ganglia, and at least two in each ganglion of the ventral nerve cord. 5-HT-immunoreactive fibers have also been detected in the MFB, CFB, and LFB along the ventral nerve cord (Beltz and Kravitz 1983). In addition, a dense plexus of stained nerve endings have been observed surrounding each of the thoracic second roots and the adjacent groups of peripheral neurosecretory neurons in this species, suggesting that the thoracic second roots might be neurohormonal organs (Beltz 1999). These serotonergic nerve plexuses might be the source of 5-HT released into the hemolymph (Beltz and Kravitz 1983). In the thoracic ganglia of *L. vannamei*, similar structures have not as yet been identified. However, because of the relatively high level of 5-HT in the thoracic ganglia, this organ might also be the major site that produces 5-HT and DA, which are then released via a similar nerve-root-associated neurohemal site, as reported in the lobster.

In the crayfishes, *P. leniusculus*, *P. clarkii*, and *C. destructor*, 5-HT-ir is present in clusters 6 and 11, nearby neuropils, and immunoreactive fibers in the ON (Elofsson 1983; Real and Czternasty 1990). In the squat lobster, *M. quadrispina*, one hundred and twenty 5-HT-immunoreactive neurons have been detected in the CNS, of which sixty neurons have been found in the brain, two neurons in the CEG, and the rest in the ventral nerve cord (SEG, T1–T5, and A1–A6). Moreover, the MFB, CFB, and LFB are immunopositive within the series of thoracic ganglia. The MFB and LFB extend through the nerve cord from the SEG to A6, whereas the CFB is particularly distinct within the anterior thoracic ganglia (T1–T2) but cannot be traced within the T4 and T5 (Antonsen and Paul 2001). In the freshwater prawn, *M. rosenbergii*, about seventy 5-HT-immunoreactive neurons, numerous fibers, and neuropils have been detected within the brain and ventral nerve cord. Fibers with 5-HT-ir are also present in the MFB and LFB of this species (Vázquez-Acevedo et al. 2009). Our study has shown that, in addition to occurring in the eyestalk and the brain, 5-HT-immunoreactive neurons are also present in the SEG and the thoracic ganglia and that their immunoreactivities are more intense than neurons in other parts of the CNS. We have also detected intense immunoreactivity in the MFB, CFB, and LFB in the SEG and in thoracic ganglia (T1–T5), but the pathway of the CFB in the abdominal ganglia is not clear. Furthermore, the positions of most 5-HT-immunoreactive neurons, neuropils, and the fiber tracts of *L. vannamei* have been found to be similar to those of other crustacean species, suggesting a highly conserved serotonergic pathway among decapod crustaceans.

The presence and distribution of DA has also been investigated in the eyestalk, brain, and the ventral nerve cord of many decapod crustaceans. DA-ir has been identified in neurons, fibers, and neuropils of the eyestalks (e.g., MT and the optic tracts of *C. sapidus* and *M. rosenbergii*), suggesting a role of DA in the regulation of neurosecretory activity of the eyestalk (Wood and Derby 1996; Tinikul et al. 2009b). In the crayfish, *P. clarkii*, DA has been shown to excite small neurons in the XO-SG, suggesting a direct role of DA in controlling the XO (Alvarez et al. 2005). Sarojini et al. (1995b) have reported that DA stimulates the release of a putative GIH from the XO in *P. clarkii*, thereby inhibiting gonadal maturation. Furthermore, DA has been reported to be a major influence on the release of other neurohormones from the XO-SG system. Injection of DA into the crayfish, *P. clarkii*, results in changes in blood glucose levels, presumably by affecting CHH release (Zhou et al. 2003). In the same species, DA reduces the rate of CHH release from the eyestalk, suggesting that DA acts to inhibit the release of CHH (Sarojini et al. 1995b). Other studies have also demonstrated a direct effect of DA on the neurosecretory cells of the XO-SG system (Fingerman 1997; Garcia and Arechiga 1998). We have found DA-immunoreactive neurons with strong staining intensity in some neurons in cluster 4 (XO) and in the SG, suggesting that DA also plays a role in controlling the synthesis and release of neuropeptides of the CHH family, as reported in the crayfish.

DA-ir has also been identified in neurons and fibers in various ON neuropils of the brain in *H. gammarus*, *C. sapidus*, *O. rusticus*, *P. argus*, and *M. rosenbergii* (Cournil et al. 1994; Wood and Derby 1996; Schmidt and Ache 1997; Tierney et al. 2003; Tinikul et al. 2009b). In *L. vannamei*, we have found intense DA-ir in the ON and in neurons of clusters 6, 11, and 17 and nearby fibers, suggesting that DA is also involved in mediating olfaction in this species. In the CEG of *L. vannamei*, we have detected large DA-immunoreactive neurons that might be homologous to "the L cell" described in the CEG of *H. gammarus* and *O. rusticus* (Cournil et al. 1994; Tierney et al. 2003). Furthermore, about 30 DA-immunoreactive neurons have been detected in the SEG of *H. gammarus* (Cournil et al. 1994). In *L. vannamei*, about 25 DA-immunoreactive neurons have been identified in the SEG, and intense immunoreactive fibers are present throughout this ganglion. Some of DA-immunoreactive fibers branch out from the MP-III of the SEG, and we believe that these DA-immunoreactive nerves project from the MP-III of SEG to the well-known neurohemal organ, known as the pericardial organ, in which DA is released into the blood to control heart rate (Tierney et al. 2003). DA-immunoreactive neurons have also been detected in the thoracic ganglia (T1–T5), in which T1 contains six neurons (two pairs located laterally and one pair medially), and T2–T5 contain two pairs each (Cournil et al. 1994). In *O. rusticus*, 20–25 DA-immunoreactive neurons have been observed in the lateral margin of the SEG, and about 40 DA-immunoreactive neurons have been detected throughout the series of thoracic ganglia, with each ganglion of T1–T3 containing three pairs with DA-ir (two pairs located laterally and one pair medially; Tierney et al. 2003). In addition, T4 contains two additional pairs of DA-immunoreactive neurons, and T5 contains one additional medial pair. In *C. sapidus*, at least one pair of DA-immunoreactive neurons has been detected in the first SEG and all of the thoracic ganglia. Two pairs of DA-immunoreactive neurons have been observed in the T3 and T5 (Wood and Derby 1996). In *L. vannamei*, we have found that the distribution patterns of DA-immunoreactive neurons are similar to thsoe of *H. gammarus* and *O. rusticus*. Moreover, we have provided the first evidence that DA-immunoreactive fibers are present in the MFB, CFB, and LFB, all of which extend through the SEG and thoracic ganglia.

In the three crayfishes, *O. limosus*, *O. rusticus*, and *P. clarkii* and in *H. gammarus* and *M. rosenbergii*, DA-immunoreactive neurons have been reported in the abdominal ganglia (Cournil et al. 1994; Elekes et al. 1988; Mercier et al. 1991; Tierney et al. 2003; Tinikul et al. 2009b) and are postulated to be neurons involved in regulating the movement of the swimming legs. In *P. clarkii*, the anterior unpaired medial (AUM) neurons have been found in A3 and A4, and their fibers project into the hindgut where they control its movement (Mercier et al. 1991). Similarly, the large DA-immunoreactive AUM-neurons detected in A3 of *L. vannamei* might also be motor neurons involved in hindgut movement. Both our HPLC and immunolocalization data indicate little change of DA levels in these ganglia, implying that the DA-immunoreactive neurons in these ganglia are involved in the movement of the swimming legs and hindgut, but not in the control of ovarian maturation.

In *L. vannamei*, both 5-HT and DA levels in the ovaries show the same patterns of change that occur in the brain and SEG-thoracic ganglia. However, the levels of DA in the ovaries are higher than those of 5-HT at each stage of the ovarian maturation cycle. Many studies have described various roles for 5-HT and DA in oocyte maturation in crustaceans. In *P. monodon*, 5-HT concentrations in the ovary appear to be higher in the late stages (III and IV), and 5-HT-ir is more intense in mature oocytes (Oc4; Wongprasert et al. 2006). Additionally, 5-HT1 receptors are also expressed in the oocyte membranes at these stages (Ongvarrasopone et al. 2006). These data indicate that 5-HT plays a direct role in regulating oocyte maturation. This is supported by the findings that 5-HT concentrations in the ovary of *M. rosenbergii* are higher in the later stages (III and IV) than in the early stages (I and II), whereas DA concentrations in the ovary have been found to be much higher in the early ovarian stages (I and II) than in the late stages (III and IV) (Tinikul et al. 2008). Furthermore, DA-ir is most intense in the cytoplasm of previtellogenic oocytes (Oc1, Oc2), but not in oogonia or follicular cells, suggesting that DA plays a key role in controlling early oocyte development (Tinikul et al. 2009b). In *L. vannamei*, we have found that 5-HT-ir is more intense in the ectoplasm of the late stage oocytes (Oc4), whereas DA-ir occurs in the early stage oocytes (Oc2). This implies that 5-HT and DA play a direct role in oocyte development, but at different stages, i.e., 5-HT might be involved in the late oocyte stages, whereas DA might be involved in the early stages. These two neurotransmitters might be taken up into the oocytes from hemolymph, as no 5-HT- and DA-immunoreactive nerve fibers have been found in the ovary. Alternatively, 5-HT and/or DA might be synthesized in the oocytes themselves. Further studies demonstrating the expression of genes encoding the enzymes involved in the syntheses of 5-HT and DA by reverse transcription with the polymerase chain reaction or in situ hybridization techniques should help to validate whether the two neurotransmitters are synthesized in or taken up by the oocytes. These two neurotransmitters might be present in the oocytes in order to exercise direct control over these oocytes and subsequent embryonic development, but further studies are now required to determine their actions.

Acknowledgements We are grateful to Assoc. Prof. Chaitip Wanichanon, Dr. Ittipon Phoungpetchara, Mrs. Ruchanok Tinikul, Mr. Jenrit Thongkampadung, and Mr. Anurak Prabyai for useful suggestions and technical assistance.

References

Alfaro J, Zuniga G, Komen J (2004) Induction of ovarian maturation and spawning by combined treatment of serotonin and a dopamine antagonist, spiperone in *Litopenaeus stylirostris* and *Litopenaeus vannamei*. Aquaculture 236:511–522

Alvarez RA, Villalobos MGP, Rosete GC, Sosa LR, Arechiga H (2005) Dopaminergic modulation of neurosecretory cells in the crayfish. Cell Mol Neurobiol 25:345–370

Antonsen BL, Paul DH (2001) Serotonergic and octopaminergic systems in the squat lobster *Munida quadrispina* (Anomura, Galatheidae). J Comp Neurol 439:450–468

Bell TA, Lightner DV (1988) A handbook of normal penaeid shrimp histology. World Aquaculture Society, Baton Rouge

Bellon-Humbert C, Van Herp F (1988) Localization of serotonin-like immunoreactivity in the eyestalk of the prawn, *Palaemon serratus*. J Morphol 196:307–320

Beltz BS (1999) Distribution and functional anatomy of amine-containing neurons in decapod crustaceans. Microsc Res Tech 44:105–120

Beltz BS, Kravitz EA (1983) Mapping of serotonin-like immunoreactivity in the lobster nervous system. J Neurosci 3:585–602

Bradford MM (1976) A rapid and sensitive method for the quantitation of microgram quantities of protein utilizing the principle of protein-dye binding. Anal Biochem 72:248–254

Cervantes OC, Battelle BA, Moles MLF (1999) Rhythmic changes in the serotonin content of the brain and eyestalk of crayfish during development. J Exp Biol 202:2823–2830

Chan SM, Gu PL, Chu KH, Tobe SS (2003) Crustacean neuropeptide genes of the CHH/MIH/GIH family: implications from molecular studies. Gen Comp Endocrinol 134:214–219

Chen YN, Fan HF, Hsieh SL, Kuo CM (2003) Physiological involvement of DA in ovarian development of the freshwater giant prawn, *Macrobrachium rosenbergii*. Aquaculture 228:383–395

Cournil I, Helluy SM, Beltz BS (1994) Dopamine in the lobster *Homarus gammarus*. I. Comparative analysis of dopamine and tyrosine hydroxylase immunoreactivities in the nervous system of the juvenile. J Comp Neurol 344:455–469

Eastman-Reks S, Fingerman M (1984) Effects of neuroendocrine tissue and cyclic AMP on ovarian growth in vivo and in vitro in the fiddler crab, *Uca pugilator*. Comp Biochem Physiol A 79:679–684

Elekes K, Florey E, Cahill MA, Hoeger U, Geffard M (1988) Morphology, synaptic connections and neurotransmitters of the

efferent neurons of the crayfish hindgut. Symp Biol Hung 36:129–146
Elofsson R (1983) 5-HT-like immunoreactivity in the central nervous system of the crayfish, *Pacifastacus leniusculus*. Cell Tissue Res 232:231–236
Elofsson R, Laxmyr L, Rosengren E, Hansson C (1982) Identification and quantitative measurement of biogenic amines and DOPA in the central nervous system and hemolymph of the crayfish *Pacifastacus leniusculus* (Crustacea). Comp Biochem Physiol [C] 71:195–201
Escamilla-Chimal EG, Van Herp F, Fanjul-Moles ML (2001) Daily variations in crustacean hyperglycemic hormone and serotonin immunoreactivity during the development of crayfish. J Exp Biol 204:1073–1081
Fingerman M, Nagabhushanam R, Sarojini R, Reddy PS (1994) Biogenic amines in crustaceans: identification, localization, and roles. J Crustacean Biol 14:413–437
Fingerman M (1997) Roles of neurotransmitters in regulating the reproductive hormone release and gonadal maturation in decapod crustaceans. Invertebr Reprod Dev 31:47–54
Garcia U, Arechiga H (1998) Regulation of crustacean neurosecretory cell activity. Cell Mol Neurobiol 18:81–99
Gorgels-Kallen JL (1985) Appearance and innervation of CHH-producing cells in the eyestalk of the crayfish *Astacus leptodactylus* examined after tracing with Lucifer Yellow. Cell Tissue Res 240:385–391
Gu PL, Yu KL, Chan SM (2000) Molecular characterization of an additional shrimp hyperglycemic hormone: cDNA cloning, gene organization, expression and biological assay of recombinant proteins. FEBS Lett 472:122–128
Hsu YA, Messinger DI, Chung JS, Webster SG, Iglesia HO de la, Christie AE (2006) Members of the crustacean hyperglycemic hormone (CHH) peptide family are differentially distributed both between and within the neuroendocrine organs of *Cancer* crabs: implications for differential release and pleiotropic function. J Exp Biol 209:3241–3256
Huberman A (2000) Shrimp endocrinology. A review. Aquaculture 191:191–208
Keller R, Beyer J (1968) Zur hyperglykämischen Wirkung von Serotonin und Augenstielextrakt beim Flusskrebs *Orconectes limosus*. Zeitschr Vergl Physiol 59:78–85
Kirubagaran R, Peter DM, Dharani G, Vinithkumar NV, Sreeraj G, Ravindran M (2005) Changes in vertebrate-type steroids and 5-hydroxytryptamine during ovarian recrudescence in the Indian spiny lobster, *Panulirus homarus*. N Z J Mar Freshwater Res 39:527–537
Kulkarni GK, Nagabhushanam R, Amaldoss G, Jaiswal RG, Fingerman M (1992) In vitro stimulation of ovarian development in the red swamp crayfish, *Procambarus clarkii* (Girard), by 5-hydroxytryptamine. Invertebr Reprod Dev 21:231–240
Marco HG, Avarre JC, Lubzens E, Gäde G (2002) In search of a vitellogenesis-inhibiting hormone from the eyestalks of the South African spiny lobster, *Jasus lalandii*. Invertebr Reprod Dev 41:143–150
Meeratana P, Withyachumnarnkul B, Damrongphol P, Wongprasert K, Suseangtham A, Sobhon P (2006) Serotonin induces ovarian maturation in giant freshwater prawn broodstock, *Macrobrachium rosenbergii* de Man. Aquaculture 260:315–325
Mercier AJ, Orchard I, Schmoeckel A (1991) Catecholaminergic neurons supplying the hindgut of the crayfish *Procambarus clarkii*. Can J Zool 69:2778–2785
Nagano M, Cooke IM (1981) Electrical activity in the crab X-organ sinus gland system: site of initiation, ionic bases and pharmacology. In: Farner DS, Lederis K (eds) Neurosecretion: molecules, cells, systems. Plenum, New York, pp 504–505
Ngernsoungnern P, Ngernsoungnern A, Kavanaugh S, Sobhon P, Sower SA, Sretarugsa P (2008) The presence and distribution of gonadotropin-releasing hormone-liked factor in the central nervous system of the black tiger shrimp, *Penaeus monodon*. Gen Comp Endocrinol 155:613–622
Ongvarrasopone C, Roshorm Y, Somyong S, Pothiratana C, Petchdee S, Tangkhabuanbutra J, Sophasan S, Payim S (2006) Molecular cloning and functional expression of the *Penaeus monodon* 5-HT receptor. Biochem Biophys Acta 1759:328–339
Phoungpetchara I, Tinikul Y, Poljaroen J, Chotwiwatthanakun C, Vanichviriyakit R, Sroyraya M, Hanna PJ, Sobhon P (2011) Cells producing insulin-like androgenic gland hormone of the giant freshwater prawn, *Macrobrachium rosenbergii*, proliferate following bilateral eyestalk-ablation. Tissue Cell 43:165–177
Quackenbush LS (1989) Vitellogenesis in the shrimp, *Penaeus vannamei*: in vitro studies of the isolated hepatopancreas and ovary. Comp Biochem Physiol [B] 94:253–261
Real D, Czternasty G (1990) Mapping of serotonin-like immunoreactivity in the ventral nerve cord of crayfish. Brain Res 521:203–212
Ridchardson HGD, Decaraman M, Fingerman M (1991) The effect of biogenic amines on ovarian development in fiddler crab, *Uca pugilator*. Comp Biochem Physiol [C] 99:53–56
Saenz F, Garcia U, Arechiga H (1997) Modulation of electrical activity by 5-hydroxytryptamine in crayfish neurosecretory cells. J Exp Biol 200:3079–3090
Sandeman DC, Sandeman RE, Aitken AR (1988) Atlas of serotonin containing neurons in the optic lobes and brain of the crayfish, *Cherax destructor*. J Comp Neurol 269:465–478
Sandeman D, Sandeman R, Derby C, Schmidt M (1992) Morphology of the brain of crayfish, crabs, and spiny lobsters: a common nomenclature for homologous structures. Biol Bull 183:304–326
Santhoshi S, Sugumar V, Munuswamy N (2008) Histological and immunocytochemical localization of serotonin-like immunoreactivity in the brain and optic ganglia of the Indian white shrimp, *Fenneropenaeus indicus*. Microsc Res Tech 71:186–195
Santhoshi S, Sugumar V, Munuswamy N (2009) Serotonergic stimulation of ovarian maturation and hemolymph vitellogenin in the Indian white shrimp. *Fenneropenaeus Indicus* Aquac 291:192–199
Sarojini R, Nagabhushanam R, Fingerman M (1995a) Mode of action of the neurotransmitter 5-hydroxytryptamine in stimulating ovarian maturation in the red swamp crayfish, *Procambarus clarkii*: an in vivo and in vitro study. J Exp Zool 271:395–400
Sarojini R, Nagabhushanam R, Fingerman M (1995b) In vivo effects of DA and DArgic antagonists on testicular maturation in the red swamp crayfish, *Procambarus clarkii*. Biol Bull 189:340–346
Schmidt M, Ache BW (1994) Descending neurons with dopamine-like or with substance P/FMRFamide-like immunoreactivity target the somata of olfactory interneurons in the brain of the spiny lobster *Panulirus argus*. Cell Tissue Res 278:337–352
Schmidt M, Ache BW (1997) Immunocytochemical analysis of glomerular regionalization and neuronal diversity in the olfactory deutocerebrum of the spiny lobster. Cell Tissue Res 287:541–563
Skinner DM (1985) Molting and regeneration. In: Bliss DE, Mantel LH (eds) The biology of crustacea, integuments, pigments and hormonal processes, vol 9. Academic Press, Orlando, pp 43–146
Swayne TC, Lipkin TG, Pon LA (2010) Live-cell imaging of the cytoskeleton and mitochondrial–cytoskeletal interactions in budding yeast. Cytoskeleton Meth Protoc Meth Mol Biol 586:41–68

Tierney AJ, Godleski MS, Rattananont P (1999) Serotonin-like immunoreactivity in the stomatogastric nervous systems of crayfishes from four genera. Cell Tissue Res 295:537–551

Tierney AJ, Kim T, Abrams R (2003) Dopamine in crayfish and other crustaceans: distribution in the central nervous system and physiological functions. Microsc Res Tech 60:325–335

Tinikul Y, Mercier AJ, Soonklang N, Sobhon P (2008) Changes in the levels of serotonin and dopamine in the central nervous system and ovary, and their possible roles in the ovarian development in the giant freshwater prawn, *Macrobrachium rosenbergii*. Gen Comp Endocrinol 158:250–258

Tinikul Y, Soonthornsumrith B, Phoungpetchara I, Meeratana P, Poljaroen J, Duangsuwan P, Soonklang N, Mercier AJ, Sobhon P (2009a) Effects of serotonin, dopamine, octopamine, and spiperone on ovarian maturation and embryonic development in the giant freshwater prawn, *Macrobrachium rosenbergii* (De Man, 1879). Crustaceana 82:1007–1022

Tinikul Y, Mercier AJ, Sobhon P (2009b) Distribution of dopamine and octopamine in the central nervous system and ovary during the ovarian maturation cycle of the giant freshwater prawn, *Macrobrachium rosenbergii*. Tissue Cell 41:430–442

Tinikul Y, Poljaroen J, Nuurai P, Anuracpreeda P, Chotwiwatthanakun C, Phoungpetchara I, Kornthong N, Poomtong T, Hanna PJ, Sobhon P (2011) Existence and distribution of gonadotropin-releasing hormone-like peptides in the central nervous system and ovary in the Pacific white shrimp, *Litopenaeus vannamei*. Cell Tissue Res 343:579–593

Treerattrakool S, Panyim S, Chan SM, Withyachumnarnkul B, Udomkit A (2008) Molecular characterization of gonad-inhibiting hormone of *Penaeus monodon* and elucidation of its inhibitory role in vitellogenin expression by RNA interference. FEBS J 275:970–980

Vaca AA, Alfaro J (2000) Ovarian maturation and spawning in the white shrimp, *Penaeus vannamei*, by serotonin injection. Aquaculture 182:373–385

Van Herp F, Strolenberg GECM (1980) Functional aspects of the neurosecretory system in the eyestalk of the crayfish *Astacus leptodactylus* with special reference to the hyperglycemic hormone (abstract). Gen Comp Endocrinol 40:364

Vázquez-Acevedo N, Reyes-Colón D, Ruíz-Rodríguez EA, Rivera NM, Rosenthal J, Kohn AB, Moroz LL, Sosa MA (2009) Cloning and immunoreactivity of the 5-HT 1Mac and 5-HT 2Mac receptors in the central nervous system of the freshwater prawn *Macrobrachium rosenbergii*. J Comp Neurol 513:399–416

Wang YJ, Hayes TK, Holman GM, Chavez AR, Keeley LL (2000) Primary structure of CHH/MIH/GIH-like peptides in sinus gland extracts from *Penaeus vannamei*. Peptides 21:477–484

Wongprasert K, Asuvapongpatana S, Poltana P, Tiensuwan M, Withyachumnarnkul B (2006) Serotonin stimulates ovarian maturation and spawning in the black tiger shrimp *Penaeus monodon*. Aquaculture 261:1447–1454

Wood DE, Derby CD (1996) Distribution of dopamine-like immunoreactivity suggests a role for dopamine in the courtship display behavior of the blue crab *Callinectes sapidus*. Cell Tissue Res 285:321–330

Yano I, Tsukimura B, Sweeney JN, Wyban JA (1988) Induced ovarian maturation of *Penaeus vannamei* by implantation of lobster ganglion. J World Aquac Soc 19:204–209

Ye HH, Wang GZ, Jin ZX, Huang HY, Li SJ (2004) Immunocytochemical studies on the optic ganglia and the brain of *Penaeus vannamei*. Oceanol Limnol Sin 35:78–83

Ye HH, Wang GZ, Jin ZX, Huang HY, Li SJ (2006) Immunocytochemical localization of neuropeptide Y, serotonin, substance P and 13-endorphin in optic ganglia and brain of *Metapenaeus ensis*. Oceanol Limnol Sin 37:384–389

Zhou HS, Juan CC, Chen SC, Wang HY, Lee CY (2003) Dopaminergic regulation of crustacean hyperglycaemic hormone and L-glucose levels in the hemolymph of the crayfish *Procambarus clarkii*. J Exp Zool A 298:44–52

Aquaculture 321 (2011) 121–129

Contents lists available at SciVerse ScienceDirect

Aquaculture

journal homepage: www.elsevier.com/locate/aqua-online

The effects of biogenic amines, gonadotropin-releasing hormones and corazonin on spermatogenesis in sexually mature small giant freshwater prawns, *Macrobrachium rosenbergii* (De Man, 1879)

Jaruwan Poljaroen [a,b], Yotsawan Tinikul [a,b], Ittipon Phoungpetchara [a], Wilairat Kankoun [a], Saowaros Suwansa-ard [a], Tanapan Siangcham [a], Prasert Meeratana [c], Scott F. Cummins [d], Prapee Sretarugsa [a], Peter J. Hanna [a,e], Prasert Sobhon [a,*]

[a] Department of Anatomy, Faculty of Science, Mahidol University, Rama VI Road, Ratchathewi, Bangkok 10400, Thailand
[b] Mahidol University, Nakhonsawan Campus, Nakhonsawan 60000, Thailand
[c] Faculty of Allied Health Sciences, Burapha University, 169 Long-Hard Bangsaen Road, Chonburi 20131, Thailand
[d] Faculty of Science, Health and Education, University of the Sunshine Coast, Locked Bag 4, Maroochydore, Queensland 4558, Australia
[e] Dean's Office, Faculty of Science and Technology, Deakin University, Locked Bag 20000, Geelong, Victoria 3220, Australia

ARTICLE INFO

Article history:
Received 31 May 2011
Received in revised form 10 August 2011
Accepted 20 August 2011
Available online 2 September 2011

Keywords:
Macrobrachium rosenbergii
Spermatogenesis
Serotonin
Dopamine
GnRH
Corazonin

ABSTRACT

Neurotransmitters such as the serotonin (5-HT) and dopamine (DA), as well as the neurohormones gonadotropin-releasing hormones (GnRHs) and corazonin (Crz), are known to have various effects on decapod crustaceans, including ovarian maturation and spermatogenesis. The effects of these neurotransmitters and neurohormones on spermatogenesis in the small male freshwater prawns, *Macrobrachium rosenbergii*, have not been reported. So, we undertook histological and histochemical observations, as well as germ cell proliferation assays to examine the effects of 5-HT, DA, two exogenous GnRH isoforms (l-GnRH-III and oct-GnRH) and Crz. Ten experimental groups were injected with 5-HT and DA at 2.5×10^{-7} and 2.5×10^{-6} mol/prawn, and l-GnRH-III, oct-GnRH and Crz at 50 and 500 ng/gBW, at 4-day intervals from days 0 to 16. We found that prawns treated with 5-HT and GnRH isoforms exhibited significant increases in their testis-somatic index (TSI), seminiferous tubules at early maturation, i.e., stages I and III, with increased diameter of the tubules (DST), and germ cell proliferation, by days 4, 12 and 16, compared with saline control groups. In contrast, prawns treated with DA and Crz showed mostly seminiferous tubules at late maturation stages VIII and IX, and decreases of TSI, DST, and cell proliferation, by day 12, compared with saline control groups. By day 16 the Crz-treated prawns had died. These data indicate that 5-HT and GnRHs can stimulate spermatogenesis, while DA and Crz inhibit spermatogenesis. Consequently, hormonal treatment of male broodstocks in aquaculture with 5-HT and GnRHs could provide valuable tools to enhance reproduction by accelerating testicular maturation, leading to increased production of sperm.

1. Introduction

Many studies have reported the opposing effects that 5-HT and DA have on crustacean reproduction. For example, the administration of 5-HT into male freshwater crayfish, *Procambarus clarkii*, induces testicular maturation and development of androgenic glands (Sarojini et al., 1994), while in females it stimulates ovarian maturation and ovulation (Fingerman, 1997). In contrast, DA can inhibit testicular maturation in the fiddler crab, *Uca pugilator* (Sarojini et al., 1993, 1995a), and the crayfish, *P. clarkii* (Sarojini et al., 1995b, 1996), and also inhibit ovarian maturation in *P. clarkii* (Sarojini et al., 1995c, 1995d). In the freshwater prawn, *Macrobrachium rosenbergii*, treatment with 5-HT significantly increases the vitellogenin level in the hemolymph at ovarian stage IV, whereas DA has an opposite effect (Tinikul et al., 2008). In addition, females injected with 5-HT exhibit significantly shorter periods of ovarian maturation and embryonic development, whereas injections with DA result in a longer period of ovarian maturation, embryonic period and decrease of oocyte diameters (Meeratana et al., 2005, 2006; Tinikul et al., 2009). The effects of 5-HT and DA on reproduction in male *M. rosenbergii* have not been reported.

GnRHs are ancient decapeptides that are present in both vertebrate and invertebrates (Gorbman and Sower, 2003; Tsai, 2006). In vertebrates, GnRH is a key neuroendocrine factor that controls the synthesis and release of luteinizing hormone (LH) and follicle-stimulating hormone (FSH) from the pituitary gland, thereby regulating steroidogenesis and gametogenesis (Blazquez et al., 1998; Schulz et al., 2001; Sower et al., 2009; Tsai, 2006; Zohar et al., 2010). In invertebrates, GnRHs that have been described so far appear to be both structurally and functionally homologous to vertebrate GnRHs, and exhibit reproduction-related functions (Adams et al., 2003; Gorbman and Sower, 2003; Powell et

* Corresponding author. Tel.: +66 2 201 5406; fax: +66 2 354 7168.
E-mail addresses: scpso@mahidol.ac.th, puijar655@yahoo.com (P. Sobhon).

0044-8486/$ – see front matter © 2011 Elsevier B.V. All rights reserved.
doi:10.1016/j.aquaculture.2011.08.022

al., 1996; Terakado, 2001). GnRHs have been detected in a protochordate, *Ciona intestinalis* (Adams et al., 2003), a gastropod, *Aplysia californica*, (Zhang et al., 2008), a cephalopod, *Octopus vulgaris* (Iwakoshi et al., 2002), and an annelid, *Capitella teleta* (Rastogi et al., 2002; Tsai and Zhang, 2008). Although a GnRH-like gene or peptide has not yet been identified in crustaceans, immunoreactivities against octopus GnRH- and lamprey GnRH-like molecules have been detected in the central nervous system and ovaries of *Penaeus monodon* (Ngernsoungnern et al., 2008a, 2008b), *M. rosenbergii* (Ngernsoungnern et al., 2008c), and *Litopenaeus vannamei* (Tinikul et al., 2011). Furthermore, in *P. monodon*, treatment of female broodstock with three exogenous isoforms of GnRHs, namely, mammalian GnRH, salmon GnRH, and lamprey GnRH-I, significantly shortened ovarian maturation time (Ngernsoungnern et al., 2008b). Similarly, in *M. rosenbergii*, the ovarian maturation period of female broodstock treated with octopus GnRH, lamprey GnRH-I, and lamprey GnRH-III, is significantly shorter than those untreated (Ngernsoungnern et al., 2009). Thus, GnRH-like peptides may be present in decapod crustaceans and play an important role in inducing ovarian maturation. However, the roles of GnRH-like peptides in testicular maturation and spermatogenesis of *M. rosenbergii*, have not yet been studied.

Crz is a neuropeptide that was first identified as a potent cardioaccelerator in the American cockroach (Veenstra, 1989), and belongs to a family of peptides, including crustacean red pigment concentrating hormone, adipokinetic hormone, and possibly GnRH (Boerjan et al., 2010; Gade and Maco, 2009; Veenstra, 2009). It has been suggested that Crz in insects may have a reproduction-related function in addition to its role in metabolism and stress regulation (Boerjan et al., 2010; Veenstra, 2009). In crustaceans, Crz has been identified as one of the neuropeptides present in the pericardial organs of the Jonah crab, *Cancer borealis* (Huybrechts et al., 2003; Li et al., 2003), the nervous system and neuroendocrine organs of the American lobster, *Homarus americanus* (Ma et al., 2008), and the CNS of *L. vannamei* (Ma et al., 2010). In addition, Crz is known to be involved in the migration of pigments in the crayfish, *P. clarkii* (Porras et al., 2003). There is no evidence concerning the effect of Crz on reproduction in decapod crustaceans. So, we investigated the effects of 5-HT, DA, GnRH isoforms and Crz, on testicular maturation and spermatogenesis in *M. rosenbergii*.

1. Materials and methods

2.1. Animals

Sexually mature small male prawns, *M. rosenbergii*, weighing 33.10 ± 3.2 g ($X \pm$SD), were obtained from a commercial farm in Chachoerngsao province, Thailand. The animals were held in circular concrete tanks of 1.50 m diameter and water at a depth of 0.8 m. Approximately 30% of the water was changed every 2 days and the prawns were fed with a commercial diet (Charoen Pokphand Group, Thailand). The photoperiod was on a 12:12 h light:dark cycle. Plastic cages were added to each tank for molting prawns to hide, thus minimizing loss from the cannibalistic behavior of this species.

2.2. Bioassays of 5-HT, DA, GnRHs and Crz

The small male prawns were separated into 12 groups, each with 35 prawns. The effects of the neurotransmitters and neurohormones were compared with two control groups; group 1 (NC) was a no-injection control, and group 2 was a vehicle-injected control (VIC), injected with 100 µl of crustacean physiological saline (CPS; 29 g NaCl, 0.71 g KCl, 2.38 g $CaCl_2$, $2H_2O$, 3.16 g $MgSO_4$, $7H_2O$, 0.5 g $NaHCO_3$, 0.17 g $MgCl_2$, $6H_2O$, and 4.76 g HEPES, in 100 ml of distilled water). The neurotransmitters and neurohormones were dissolved in CPS. The prawns in the experimental groups 3–4 were injected with 100 µl of CPS containing 5-HT and DA (Sigma Chemical Company, St. Louis, MO), at doses of 2.5×10^{-7} and 2.5×10^{-6} mol/prawn (effective doses according to Alfaro et al., 2004; Chen et al., 2003; Tinikul et al., 2008). Groups 5–10 were injected with 100 µl of CPS containing l-GnRH-III, oct-GnRH and Crz, at doses of 50 and 500 ng/g body weight (BW) (effective doses according to Ngernsoungnern et al., 2008b). The l-GnRH-III (pGlu-His-Trp-Ser-His-Asp-Trp-Lys-Pro-Gly-NH_2), oct-GnRH (pGlu-Asn-Tyr-His-Phe-Ser-Asn-Gly-Trp-His-Pro-Gly-NH_2) and Crz (pGln-Thr-Phe-Gln-Tyr-Ser-Arg-Gly-Trp-Thr-Asn-NH_2), were custom synthesized by Genscript Corp, Piscataway, NJ, USA. Hormone preparations were administered on days 0, 4, 8 and 12. The injections were performed via an intramuscular route at the lateral aspect of the second abdominal segment of the prawn. Five animals from each of the control and experimental groups were randomly selected and sacrificed on days 0, 4, 8, 12, and 16 (i.e., at 4-day intervals) for analyses of testicular histology and spermatogenesis. Testis development was estimated based on the presence of various seminiferous tubules stages at day 12 after injections. The percentages of tubular stages were determined from 10 non-consecutive slides of each testis by counting at least 40 tubules per section.

2.3. Histology of testis

Testes were dissected out from prawns in each experimental group at days 0, 4, 12, and 16. They were fixed overnight in 4% paraformaldehyde in 0.1 M PBS (pH 7.4), then dehydrated in increasing concentrations of ethanol, and then embedded in paraffin. Sections were cut at 5 µm thickness and stained with hematoxylin and eosin (H&E; Sigma Aldrich) for histological observations.

2.4. Testicular development indices

The testis-somatic index (TSI) was calculated for each group of prawns according to the standard formula: TSI = weight of the testes (g) × 100/weight of prawn (g). A mean diameter of seminiferous tubules (DST) was determined by measuring the diameters of 50 seminiferous tubules (µm) in the testes of each prawn, according to Sarojini et al. (1995b).

2.5. Estimation of male germ cell proliferation using 5-bromo-2′-deoxyuridine (BrdU) labeling

To investigate germ cell proliferation in the testes, 5 prawns per group were randomly sampled and injected with 5 mg of 5-bromo-2′-deoxy-uridine (BrdU) per 100 g of body weight (0.5% BrdU in distilled water), 8 h prior to sacrifice, and testes collected at days 0, 4, 12, and 16. Testes were prepared for histological observations and estimation of cell proliferation using the BrdU assay for cell proliferation as described in the Detection Kit II (Roche, Mannheim, Germany) with modifications described previously (Lee et al., 2003). Paraffin sections of BrdU-labeled testes were cut at 5 µm and then rehydrated by washing 3 times in washing buffer (0.1 M phosphate buffered saline, PBS). They were then immersed in methanol containing 1% hydrogen peroxide to block endogenous peroxidase activity. Sections were immersed in 1% glycine diluted with 0.1 M PBS to block free aldehyde groups. Sections were then washed with 0.1 M PBS plus 0.4% Triton-X 100 pH 7.4 (PBST), and non-specific bindings of proteins blocked with 4% normal goat serum in 0.1 M PBST, pH 7.4, for 2 h at room temperature. After washing three times with PBS, the sections were incubated overnight with anti-BrdU (mouse monoclonal antibody, at 1:20 dilution in PBS) at room temperature. They were washed three times with PBS and then incubated with anti-mouse Ig-alkaline phosphatase (1:200) for 2 h at room temperature. The antigen–antibody complexes were visualized by incubating with color-substrate solution (NBT/BCIP solution; Roche, Mannheim, Germany), for 45 min at 25 °C. After washing three times, sections were mounted with mounting medium (Permount). Negative controls were performed by omitting the primary antibody.

Photomicrographs were taken using a Nikon eclipse E600 microscope equipped with a digital camera (Nikon DXM1200). The numbers of dividing cells (BrdU-labeled nuclei) were counted from stages I and II of 5 non-consecutive sections of each testis from 5 animals per group. The germ cell proliferation was expressed as number of BrdU-labeled nuclei per mm^2.

2.6. Statistical analyses

TSI, DST, and OL were calculated, and compared between the experimental and control groups. Measurements of cell numbers and proliferation indices were performed twice and the results analyzed with an SPSS program using one-way analysis of variance (ANOVA) and Tukey's post hoc test. A probability value less than 0.05 ($P<0.05$) indicated a statistical significance.

3. Results

3.1. Histology of testes in small male prawns

Based on cellular associations, the seminiferous tubules in each testis of an untreated small male were divided into 9 stages (i.e., stages I to IX) (Fig. 1). In all stages, groups of spermatogonia were always present close to the basement membrane. Nurse cells, which were present in all stages, were located on the basement membrane between the spermatogonia (Fig. 1A). Independently of spermatogonia, each stage of the testicular cycle (I to IX) was defined accordingly with the homogenous population of cells present, each at a given stage of prophase I. Stage I tubule contained mostly leptotene spermatocytes (Fig. 1A); stage II contained mostly zygotene and pachytene spermatocytes (Fig. 1B); stage III contained mostly diplotene spermatocytes (Fig. 1C); stage IV contained mostly diplotene and metaphase spermatocytes (Fig. 1D); stage V contained mostly metaphase spermatocytes (Fig. 1E); stage VI contained mostly early and mid-stage developing spermatids (Fig. 1F); stage VII contained mostly late-stage spermatids (Fig. 1G); stage VIII contained mostly mature sperm with condensed chromatin (Fig. 1H); and stage IX contained mostly mature sperm with decondensed chromatin (Fig. 1I).

3.2. Effects of neurotransmitters and hormones on histology of the testes of small males

There were no obvious histological changes in the small male testes (N = 5) of the NC and VIC control groups sampled at days 0, 4, 12,

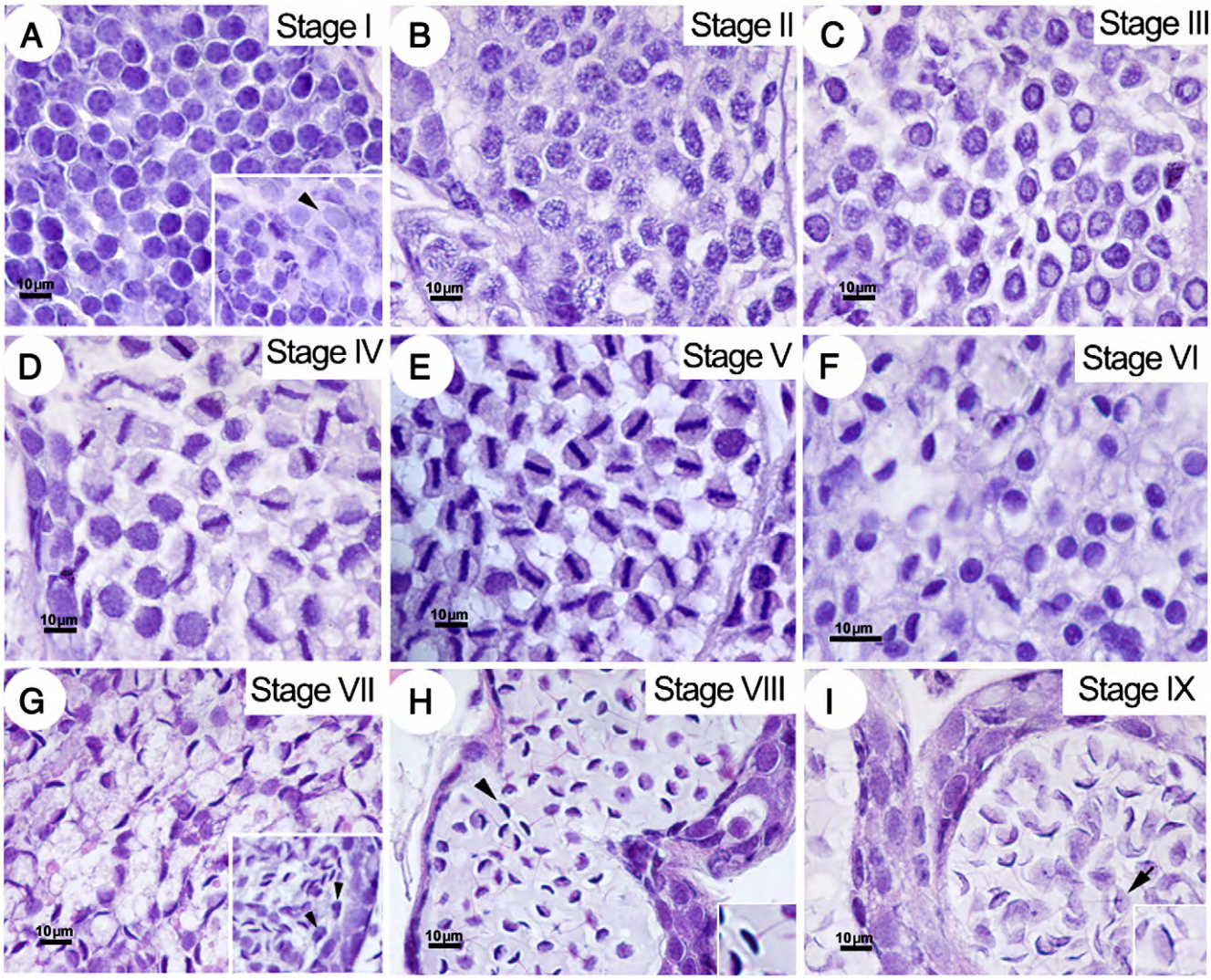

Fig. 1. Light micrographs showing the 9 stages (I–IX) of development of germ cells in seminiferous tubules (H&E staining). (A) Stage I contain mostly leptotene spermatocytes, with a layer of spermatogonia located at the basement membrane of the tubule (inset; arrowhead). (B) Stage II contains mostly zygotene and pachytene spermatocytes. (C) Stage III contains mostly diplotene spermatocytes. (D) Stage IV contains mostly diakinesis and metaphase spermatocytes. (E) Stage V contains mostly metaphase spermatocytes. (F) Stage VI contains mostly early and mid-spermatids. (G) Stage VII contains mostly late spermatids. Nurse cells are located at the periphery of a seminiferous tubule (inset; arrowheads). (H) Stage VIII contains mostly premature sperm with condensed chromatin in crescent-shaped nuclei (inset; arrowheads). (I) Stage IX contains mature sperm with decondensed chromatin in crescentic nuclei (inset; arrowheads).

Table 1
Testis development in small male prawns (N = 5) based on the presence of various seminiferous tubules stages at day 12 after injections with biogenic amines 5-HT and DA, GnRHs, and Crz. The numbers were determined from 5 non-consecutive slides from the testes of each prawn by counting at least 40 tubules per section.

Test group	Maturation stage (%) based on tubules present								
	I	II	III	IV	V	VI	VII	VIII	IX
Non-injection control (NC)	30	20	5	0	0	5	15	15	10
Vehicle-injected control (VIC)	35	15	5	5	5	5	10	5	15
5-HT 2.5×10^{-7} mol/prawn	25	30	15	0	5	10	0	10	5
5-HT 2.5×10^{-6} mol/prawn	60	15	0	0	0	10	5	10	0
DA 2.5×10^{-7} mol/prawn	0	0	0	5	10	5	15	40	25
DA 2.5×10^{-6} mol/prawn	0	0	0	0	0	0	5	40	55
l-GnRH-III 50 ng/gBW	40	25	10	0	10	5	10	0	0
l-GnRH-III 500 ng/gBW	50	35	5	0	0	5	5	0	0
Oct-GnRH 50 ng/gBW	60	30	5	0	0	0	5	0	0
Oct-GnRH 500 ng/gBW	55	40	0	0	0	0	5	0	0
Crz 50 ng/gBW	6	12	0	0	0	0	6	36	40
Crz 500 ng/gBW	0	0	0	0	0	0	0	36	64

and 16 after injection. However, animals treated with 5-HT at doses of 2.5×10^{-7} and 2.5×10^{-6} mol/prawn, and both types of GnRH (l-GnRH-III and oct-GnRH) at doses of 50 and 500 ng/gBW, showed obvious histological changes compared with controls at day 12 by having higher numbers of seminiferous tubules at stages I, II, III (Table 1). In contrast, prawns treated with the two doses of DA and Crz showed mostly seminiferous tubules at stages VIII and IX. Therefore, with treatment of 5-HT and GnRHs, the seminiferous tubules tended to increase in number at early and proliferative stages (stages I–III) which possessed more spermatogonia and spermatocytes, whereas the testes of the prawns injected with DA and Crz tended to increase in number at terminal stages (stages VIII–XI), which contained mostly mature sperm and only a few layers of spermatogonia (Table 1).

3.3. Effects of neurotransmitters and hormones on TSI and DST values

TSI values of all groups of prawns are shown in Fig. 2, with the NC and VIC groups showing no significant changes over the course of the experiment. However, the experimental groups treated with 2.5×10^{-7} and 2.5×10^{-6} mol/prawn of 5-HT showed significantly greater TSIs at days 12 and 16 (as well as at day 4 for the higher dose), compared with controls ($P<0.05$). In contrast, the TSIs of the prawns treated with DA at doses of 2.5×10^{-7} and 2.5×10^{-6} mol/prawn showed significant decreases by days 4, 12 and 16, compared with control groups ($P<0.05$). At day 4, the prawns treated with l-GnRH-III at doses of 50 and 500 ng/gBW, showed significantly increased TSIs, compared with the control groups ($P<0.05$). At days 12 and 16, experimental groups treated with l-GnRH-III and oct-GnRH, at doses of 50 and 500 ng/gBW, showed significantly greater TSIs compared with the control groups ($P<0.05$). At day 12, the experimental groups treated with Crz at 50 and 500 ng/gBW showed significant decreases in TSI values compared with the control groups ($P<0.05$). There was progressive death of animals in both Crz-treated groups between days 12 to 16.

DST values of all groups of prawns are shown in Fig. 3. The control groups showed no significant changes over the course of the experiment. However, at days 4, 12 and 16, the DST values of prawns treated with both doses of 5-HT showed significant increases, compared with the control groups ($P<0.05$). In contrast, prawns treated with DA at both doses showed significant decreases in DST compared with control groups ($P<0.05$). Experimental groups injected with both doses of l-GnRH-III and oct-GnRH (at dose of 500 ng/gBW) showed significantly increased DSTs at days 4, 12 and 16 ($P<0.05$), whereas, the testes of prawns treated with Crz (50 and 500 ng/gBW) showed significant decreases in DST. There was progressive death of animals in both Crz-treated groups between days 12 and 16.

Growth of prawns over the experimental period, as determined by increments of the OLs, was recorded for both controls and experimental groups. There was no significant difference between the groups (data not shown).

3.4. Determination of cell proliferation in the seminiferous tubules of normal and hormone-treated small males

In NC and VIC control sections at day 0, numerous BrdU-labeled nuclei were found in seminiferous tubules of small males at stages I (Fig. 4A) and II (Fig. 4B). Considerably fewer BrdU-labeled nuclei were observed in seminiferous tubules at stages III, IV and V (Fig. 4C–E), and they were reduced further in stages VI, VII and VIII (Fig. 4F–H). There were no BrdU-labeled nuclei observed in the seminiferous tubules at stage IX (Fig. 4I). The negative control sections of seminiferous tubules at stages I, II, and IX did not show any stained nuclei (Fig. 4J–L).

The numbers of BrdU-labeled nuclei observed in stages I and II seminiferous tubules of the NC and VIC control sections, showed no differences over the experimental period of 16 days (NC—Fig. 4A, and VIC data not shown). However, there were greater numbers of dividing germ cells in the stages I and II tubules in testes of prawns at day 12 after treatment with both doses of 5-HT (Fig. 5A–B), l-GnRH-III (Fig. 5E–F), and oct-GnRH (Fig. 5G–H). Most intensely labeled nuclei occupied the same position as spermatogonia close to the basement membranes, while other less intensely labeled nuclei were located at a more inner zone at the same location with early spermatocytes (Fig. 5B, E, H). This implied that most of the dividing cells were spermatogonia and early spermatocytes. In contrast, after

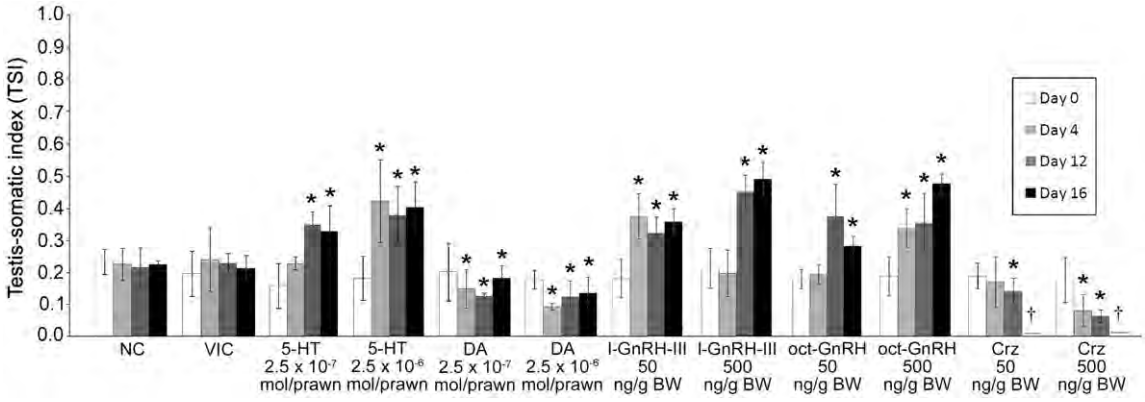

Fig. 2. Histograms showing the mean testis-somatic index (TSI) ± SD of prawns under the different treatments, at days 0, 4, 8, 12 and 16, compared with the control groups (NC, VIC). Asterisks indicate significant changes of TSI values ($P<0.05$), compared with the control groups (N = 5). †, treated prawns had died.

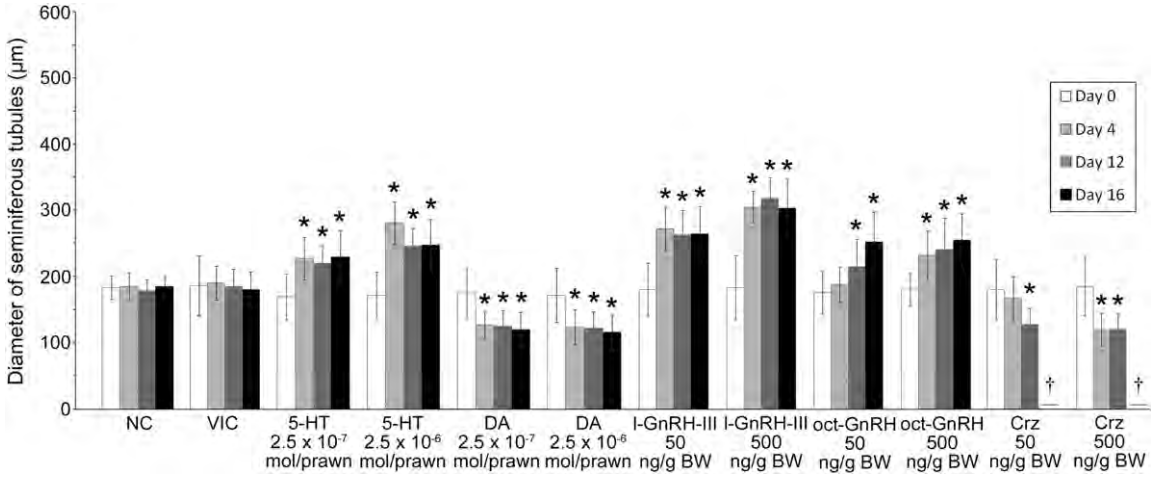

Fig. 3. Histograms showing the mean diameters of seminiferous tubules (DST) ± SD of prawns under the different treatments, at days 0, 4, 8, 12 and 16, compared with the control groups (NC, VIC). Asterisks indicate significant changes of DST values ($P<0.05$) compared with the control groups (N = 5). †, treated prawns had died.

treatments with DA (Fig. 5C–D) and Crz (Fig. 5I–J) the numbers of labeled nuclei had notably decreased.

A histogram of the numbers of BrdU-labeled nuclei (per mm^2) in the seminiferous stages I and II of the prawns is shown in Fig. 6. At days 0 to 16, the numbers of BrdU-labeled nuclei showed no significant differences within the NC and VIC control groups (range of 89 ± 12.6 to 110 ± 12.6 labeled nuclei/mm^2). However, the numbers of BrdU-labeled nuclei were significantly greater in the prawns injected with 5-HT at day 12 for the lower dose, and at days 12 and 16 for the higher dose (123 ± 13.6 and 133.4 ± 5.8 nuclei/mm^2, respectively), compared with the control groups ($P<0.05$). There were also significantly greater numbers of labeled nuclei at days 12 and 16 in prawns injected with l-GnRH-III at doses of 50 and 500 ng/gBW (132.3 ± 5.8 and 219.5 ± 1.81 nuclei/mm^2, respectively), and oct-GnRH at doses of 50 and 500 ng/gBW (151 ± 14.9 and 188.8 ± 16.9 nuclei/mm^2, respectively; $P<0.05$). In contrast, at day 4, there was a significant decrease in the numbers of BrdU-labeled nuclei in testes of prawns treated with DA at the dose of 2.5×10^{-6} mol/prawn (26.7 ± 6.0 nuclei/mm^2). At days 12 and 16, there were also significant decreases of labeled nuclei at both doses of DA, compared with the control groups ($P<0.05$). Treatment with 500 ng/gBW of Crz also resulted in a significant decrease of labeled nuclei at days 4 and 12 (46 ± 5.5 and 0 nuclei/mm^2), compared with the control groups ($P<0.05$). Also, there was a significant decrease in number of labeled nuclei at day 12 after treatment with Crz at the dose of 50 ng/gBW (50 ± 5.5 nuclei/mm^2) ($P<0.05$). There was progressive death of animals in both Crz-treated groups between days 12 to 16.

4. Discussion

The aim of this study was to investigate the effects of biogenic amines (5-HT and DA), gonadotropin-releasing hormones (GnRHs) and corazonin (Crz) on spermatogenesis in the small male freshwater prawns, *M. rosenbergii*. The major findings of this study were : 1) animals administered with 5-HT and GnRH isoforms, show significantly higher TSI, DST, and germ cell proliferation values than untreated controls ($P<0.05$), and 2) animals administered with DA and Crz, show significantly lower TSI, DST, and germ cell proliferation values than untreated controls ($P<0.05$).

The treatment of small males with 5-HT and GnRHs showed observable histological changes, with the majority of seminiferous tubules at early (proliferative) stages (I, II, and III). In contrast, prawns treated with DA and Crz showed mostly seminiferous tubules at terminal stages (VIII and IX), compared with saline controls. These findings demonstrated that treatments with 5-HT and GnRHs stimulated, whereas DA and Crz inhibited testicular development and tubules transformation.

Previous studies in decapods crustaceans, including *P. clarkii*, *U. pugilator*, *Litopenaeus stylirostris*, *L. vannamei* and *P. monodon*, have shown that 5-HT is stimulatory while DA is inhibitory to gonadal development in both males and females (Alfaro et al., 2004; Fingerman, 1997; Fingerman and Nagabhushanam, 1992; Fingerman et al., 1994; Sarojini et al., 1995a, 1995b, 1995c; Wongprasert et al., 2006). As well, in female *M. rosenbergii*, administration of 5-HT resulted in shortening the period of the ovarian development, as well as increased gonado-somatic index and oocyte diameters (Meeratana et al., 2006; Tinikul et al., 2009). 5-HT also significantly increased hemolymph vitellogenin (Vg) level, whereas DA had the opposite effect. In addition, the levels of 5-HT in the CNS and ovary gradually increased up to ovarian stage IV, whereas level of DA decreased (Chen et al., 2003; Tinikul et al., 2008). It was, therefore, suggested that these two biogenic amines play opposite roles in controlling ovarian development and oocyte maturation in this prawn. We have now shown for the first time that 5-HT also stimulated testicular development and male germ cell proliferation while DA had opposite effects.

Our study is the first to investigate the effects of GnRHs on spermatogenesis and testicular development in *M. rosenbergii*. GnRHs have not yet been characterized in decapod crustaceans, however, there has been accumulating studies implicating their existence in several physiological and immunohistochemical studies. We have shown that administration of l-GnRH-III, a primitive vertebrate isotype, and oct-GnRH, a mollusc isotype, could significantly increase TSI and DST values, and germ cell proliferation. This is supported by our previous studies showing that these heterologous GnRHs, l-GnRHs (I, II) and oct-GnRH, cause stimulatory effects on female reproduction, including ovarian maturation (Ngernsoungnern et al., 2008b, 2009). Moreover, GnRH-like immunoreactivity has been detected in the CNS and ovary of *M. rosenbergii* (Ngernsoungnern et al., 2008c). The identification and characterization of crustacean GnRH(s) in males, and females, and its relationships with 5HT and DA, as well as mechanism of action in *M. rosenbergii*, require further studies.

It was suggested that Crz can bind to a receptor belonging to the GnRH receptor family (Cazzamali et al., 2002; Park et al., 2002). Furthermore, a bioinformatic analysis indicated that Crz belongs to the GnRH family as it shares some amino acid similarity with GnRHs, particularly at the N-terminal region (Christie et al., 2010). We proposed that by binding to GnRH receptor, Crz could block the activity of GnRH, hence negating its action. Indeed, we have found for the first time, that administration of multiple doses of Crz inhibits germ cell

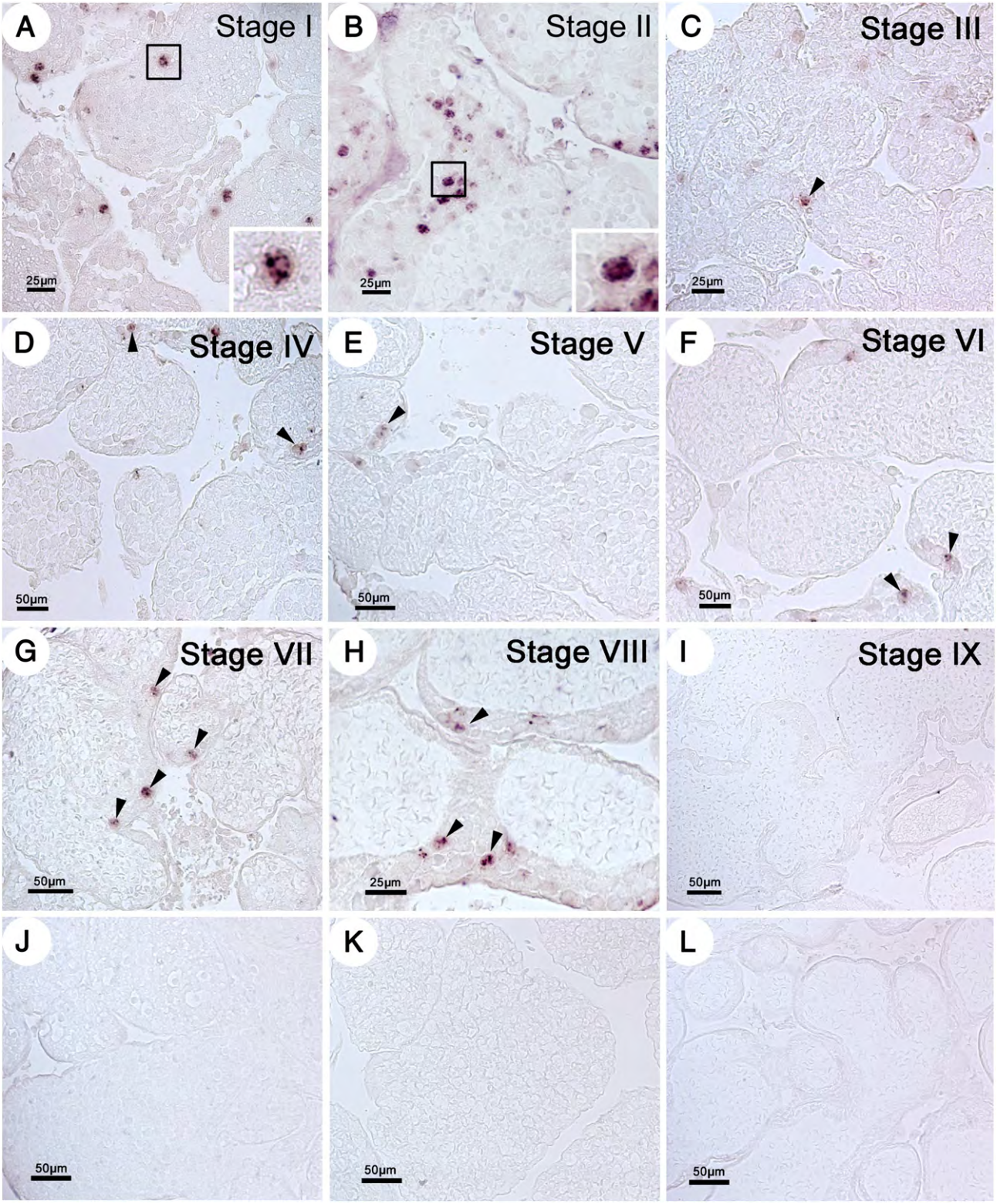

Fig. 4. Representative medium power light micrographs of the testes of small males showing BrdU-labeled nuclei in the seminiferous tubule stages I–IX. Relatively high numbers of BrdU-labeled nuclei (insets) are present in tubules at stages I and II (A–B). In contrast, very few labeled nuclei (arrowheads) are present in stages III–VIII (C–H), and there were no labeled nuclei in seminiferous tubules at stage IX (I). The negative control sections of tubules at stages I, II, and IX (J–L).

proliferation in a decapod crustacean. The male prawns injected with Crz showed decreased TSI values, DST, and germ cell proliferation in the testes, and eventually death. The latter event was probably elicited by the stress-induced action of Crz that occurred following multiple administrations of this hormone.

In addition to controlling heart beat in insects (Predel et al., 2007; Slama et al., 2006), Crz also acts as a stress hormone that mobilizes sugar (trehalose) and fatty acids to allow them to cope with stress situations (Boerjan et al., 2010; Predel et al., 2007). These data corroborate that Crz acts as a stress hormone, and may block the release of

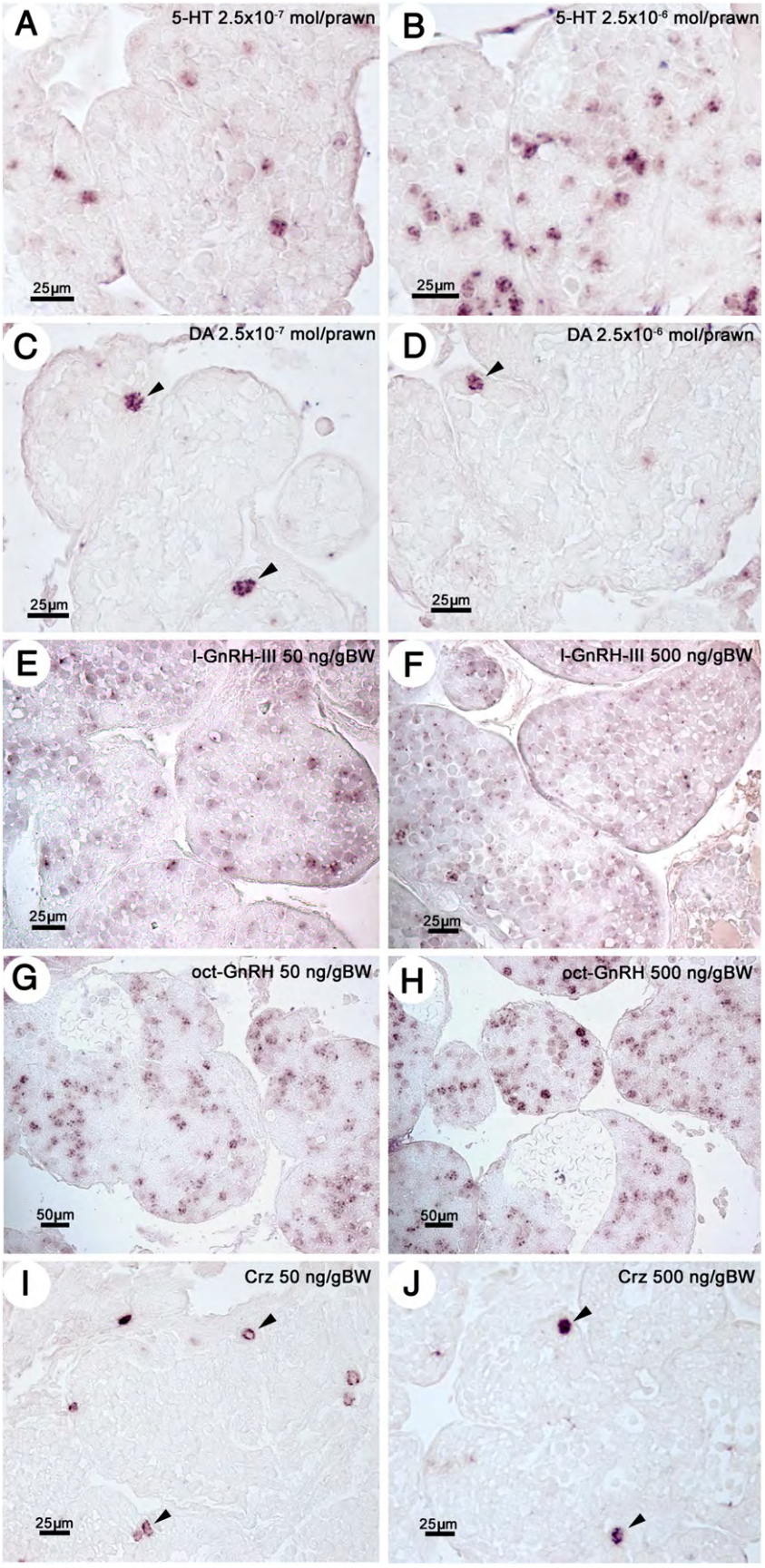

Fig. 5. Representative medium power micrographs showing BrdU-labeled nuclei (arrowheads) in seminiferous tubules at stages I and II of the testes of prawns 12 days after injections with 5-HT at doses of 2.5×10^{-7} and 2.5×10^{-6} mol/prawn (A and B), DA at doses of 2.5×10^{-7} and 2.5×10^{-6} mol/prawn (C and D), l-GnRH-III at doses of 50 and 500 ng/gBW (E and F), oct-GnRH at doses of 50 and 500 ng/gBW (G and H), and Crz at doses of 50 and 500 ng/gBW (I and J).

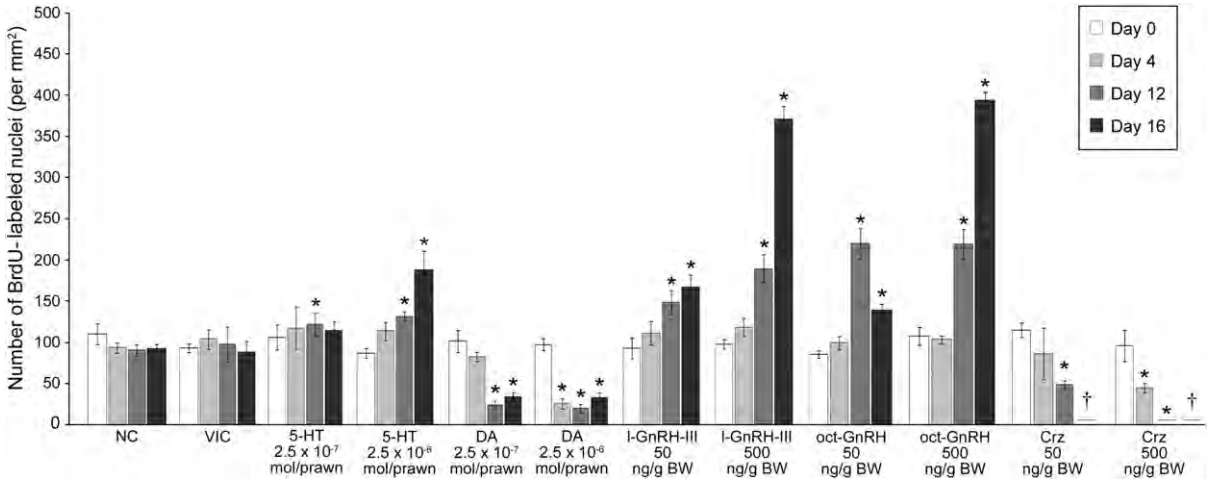

Fig. 6. Histograms showing the mean number ± SD of BrdU-labeled nuclei (per mm^2) in the seminiferous tubules stages I and II in testes of small male prawns under the different treatments, at days 0 to 16. Asterisks indicate significant changes ($P<0.05$), compared with the control groups (NC, VIC). †, treated prawns had died.

GnRH, thereby suppressing germ cell proliferation and testicular development in *M. rosenbergii*. Alternatively, Crz may bind to the GnRH receptors at the target organ levels (i.e. testicular cells), and block the action of GnRH at the testicular level, thereby inhibiting germ cell proliferation and differentiation. This is supported by the finding in a mammalian study, where hypothalamic GnRH cells express the receptors for corticotrophin-releasing factor, which is involved in the stress-induced suppression of GnRH release (Li et al., 2004). The Crz mechanisms of actions on the induction of stress, and its possible relation with the suppression of crustacean gonadal maturation need further investigations.

In summary, we have found that in *M. rosenbergii*, 5-HT and GnRHs have a stimulating effect on testicular maturation and spermatogenesis, while DA and Crz have inhibitory effects. The use of 5-HT and GnRH in stimulating male broodstock reproduction in farm situations now needs further work to determine an effective doses and means of administration. It is possible that this measure could be applied to accelerate testicular maturation, leading to the enhancement of sperm quantity and quality, as well as fertilizability. However, these sperm parameters and the reproductive performance of the treated prawns need to be studied further.

Acknowledgments

This research was supported by a Distinguished Research Professor Grant (jointly funded by the Thailand Research Fund (TRF), Office of Higher Education Commission (OHEC) and Mahidol University) to Prasert Sobhon, and a grant from OHEC under National Research University Projects to Prasert Sobhon and Prapee Sretarugsa, a Research Grant for a New Scholar (TRF, OHEC, and Mahidol University) to Yotsawan Tinikul, and a TRF-Royal Golden Jubilee (RGJ) Ph.D. scholarship to Jaruwan Poljaroen.

References

Adams, B.A., Tello, J.A., Erchegyi, J., Warby, C., Hong, D.J., Akinsanya, K.O., Mackie, G.O., Vale, W., Rivier, J.E., Sherwood, N.M., 2003. Six novel gonadotropin-releasing hormones are encoded as triplets on each of two genes in the protochordate, *Ciona intestinalis*. Endocrinology 144, 1907–1919.

Alfaro, J., Zu´n˜iga, G., Komen, J., 2004. Induction of ovarian maturation and spawning by combined treatment of serotonin and a dopamine antagonist, spiperone in *Litopenaeus stylirostris* and *Litopenaeus vannamei*. Aquaculture 236, 511–522.

Blazquez, M., Bosma, P.T., Fraser, E.J., Van Look, K.J.W., Trudeau, V.L., 1998. Fish as models for the neuroendocrine regulation of reproduction and growth. Comparative Biochemistry and Physiology. C 119, 345–364.

Boerjan, B., Verleyen, P., Huybrechts, J., Schoofs, L., De Loof, A., 2010. In search for a common denominator for the diverse functions of arthropod corazonin: a role in the physiology of stress? General and Comparative Endocrinology 166, 222–233.

Cazzamali, G., Saxild, N., Grimmelikhuijzen, C., 2002. Molecular cloning and functional expression of a *Drosophila* corazonin receptor. Biochemical and Biophysical Research Communications 298, 31–36.

Chen, Y.N., Fan, H.F., Haieh, S.L., Kuo, C.M., 2003. Physiological involvement of DA in ovarian development of the giant freshwater prawn, *Macrobrachium rosenbergii*. Aquaculture 228, 383–395.

Christie, A.E., Christopher, S., Niko, H.D., Ohno, P., Lenz, P.H., 2010. Bioinformatic analyses of the publicly accessible crustacean expressed sequence tags (ESTs) reveal numerous novel neuropeptide-encoding precursor proteins, including ones from members of several little studied taxa. General and Comparative Endocrinology 167, 164–178.

Fingerman, M., 1997. Roles of neurotransmitters in regulating the reproductive hormone release and gonadal maturation in decapod crustaceans. Invertebrate Reproduction and Development 31, 47–54.

Fingerman, M., Nagabhushanam, R., 1992. Control of the release of crustacean hormones by neuroregulators. Comparative Biochemistry and Physiology. C 102, 343–352.

Fingerman, M., Nagabhushanam, R., Sarojini, R., Reddy, P.S., 1994. Biogenic amines in crustaceans: identification, location and roles. Journal of Crustacean Biology 14, 413–437.

Gade, G., Maco, G.H., 2009. Peptides of the adipokinetic hormone/red pigment-concentrating hormone family with special emphasis on Caelifera: primary sequences and functional considerations contrasting grasshoppers and locusts. General and Comparative Endocrinology 162, 52–68.

Gorbman, A., Sower, A.S., 2003. Evolution of the role of GnRH in animal (Metazoan) biology. General and Comparative Endocrinology 134, 207–213.

Huybrechts, J., Nusbaum, M.P., Vanden Bosch, L.V., Baggerman, G., De Loof, A., Schoofs, L., 2003. Neuropeptidomic analysis of the brain and thoracic ganglion from the Jonah crab, *Cancer borealis*. Biochemical and Biophysical Research Communications 308, 535–544.

Iwakoshi, E., Takuwa, K., Fujisawa, Y., Hisada, M., Ukena, K., Tsutsui, K., Minakata, H., 2002. Isolation and characterization of a GnRH-like peptide from *Octopus vulgaris*. Biochemical and Biophysical Research Communications 291, 1187–1193.

Lee, J.K., Park, J.H., Kim, H.S., Chung, S.T., Eom, J.H., Nam, K.T., Oh, H.Y., 2003. Evaluation of cell proliferation in ear lymph node using BrdU immunohistochemistry for mouse ear swelling test. Environmental Toxicology and Pharmacology 14, 61–68.

Li, L.J., Kelley, W.P., Billimoria, C.P., Christie, A.E., Pulver, S.R., Sweedler, J.V., Marder, E., 2003. Mass spectrometric investigation of the neuropeptide complement and release of the pericardial organs of the crab, *Cancer borealis*. Journal of Neurochemistry 87, 642–656.

Li, X.F., Bowe, J.E., Mitchell, J.C., Brain, S.D., Lightman, S.L., O'Byrne, K.T., 2004. Stress induced suppression of the gonadotropin-releasing hormone pulse generator in the female rat: a novel neural action for calcitonin gene-related peptide. Endocrinology 145, 1556–1563.

Ma, M., Chen, R., Sousa, G.L., Bors, E.K., Kwiatkowksi, M.A., Goiney, C.C., Goy, M.F., Christie, A.E., Li, L., 2008. Mass spectral characterization of peptide transmitters/hormones in the nervous system and neuroendocrine organs of the American lobster *Homarus americanus*. General and Comparative Endocrinology 156, 395–409.

Ma, M., Gard, A.L., Xiang, F., Wang, J., Davoodian, N., Lenz, P.H., Malecha, S.R., Christie, A.E., Li, L., 2010. Combining in silico transcriptome mining and biological mass spectrometry for neuropeptide discovery in the Pacific white shrimp *Litopenaeus vannamei*. Peptides 31, 27–43.

Meeratana, P., Sobhon, P., Damrongphol, P., Wongprasert, K., Somapha, S., Suseangtham, A., Withyachumnarnkul, B., 2005. Possible mechanism of serotonin induces ovarian maturation in giant freshwater prawn broodstock, *Macrobrachium rosenbergii*, De Man. 31st Congress on Science and Technology of Thailand, Suranaree University of Technology, Nakhonrajasrima, Thailand.

Meeratana, P., Withyachumnarnkul, B., Damrongphol, P., Wongprasert, K., Suseangtham, A., Sobhon, P., 2006. Serotonin induces ovarian maturation in giant freshwater prawn broodstock, *Macrobrachium rosenbergii* de Man. Aquaculture 260, 315–325.

Ngernsoungnern, P., Ngernsoungnern, A., Kavanaugh, S., Sobhon, P., Sower, S., Sretarugsa, P., 2008a. The presence and distribution of gonadotropin-releasing hormone-liked factor in the central nervous system of the black tiger shrimp, *Penaeus monodon*. General and Comparative Endocrinology 155, 613–622.

Ngernsoungnern, A., Ngernsoungnern, P., Weerachatyanukul, W., Chavadej, J., Sobhon, P., Sretarugsa, P., 2008b. The existence of gonadotropin-releasing hormone (GnRH) immunoreactivity in the ovary and the effects of GnRHs on the ovarian maturation in the black tiger shrimp *Penaeus monodon*. Aquaculture 279, 197–203.

Ngernsoungnern, A., Ngernsoungnern, P., Kavanaugh, S., Sower, S.A., Sobhon, P., Sretarugsa, P., 2008c. The identification and distribution of gonadotropin-releasing hormone-like peptides in the central nervous system and ovary of the giant freshwater prawn, *Macrobrachium rosenbergii*. Invertebrate Reproduction and Development 8, 49–57.

Ngernsoungnern, P., Ngernsoungnern, A., Sobhon, P., Sretarugsa, P., 2009. Gonadotropin-releasing hormone (GnRH) and a GnRH analog induce ovarian maturation in the giant freshwater prawn, *Macrobrachium rosenbergii*. Invertebrate Reproduction and Development 53, 125–135.

Park, Y., Kim, Y.J., Adams, M.E., 2002. Identification of G protein-coupled receptors for *Drosophila* PRXamide, CCAP, corazonin, and AKH supports a theory of ligand receptor coevolution. Proceedings of the National Academy of Sciences of the United States of America 99, 11423–11428.

Porras, M.G., De Loof, A., Breuer, M., Archiga, H., 2003. Corazonin promotes tegumentary pigment migration in the crayfish *Procambarus clarkii*. Peptides 24, 1581–1589.

Powell, J.F., Reska-Skinner, S.M., Prakash, M.O., Fischer, W.H., Park, M., Rivier, J.E., Craig, A.G., Mackie, G.O., Sherwood, N.M., 1996. Two new forms of gonadotropin-releasing hormone in a protochordate and the evolutionary implications. Proceedings of the National Academy of Sciences of the United States of America 93, 10461–10464.

Predel, R., Neupert, S., Russell, W.K., Scheibner, O., Nachman, R.J., 2007. Corazonin in insects. Peptides 28, 3–10.

Rastogi, R.K., Di Fiore, M.M., D'Aniello, A., Iela, L., Fiorentino, M., 2002. GnRH in the invertebrates: an overview. Progress in Brain Research 141, 19–29.

Sarojini, R., Nagabhushanam, R., Fingerman, M., 1993. *In vivo* evaluation of 5-hydroxytryptamine stimulation of the testes in the fiddler crab, *Uca pugilator*, a presumed action on the neuroendocrine system. Comparative Biochemistry and Physiology. C 106, 321–325.

Sarojini, R., Nagabhushanam, R., Fingerman, M., 1994. 5-hydroxytryptaminergic control of testes development through the androgenic gland in the red swamp crayfish, *Procambarus clarkii*. Invertebrate Reproduction and Development 26, 127–132.

Sarojini, R., Nagabhushanam, R., Fingerman, M., 1995a. Evidence for opioid involvement in the regulation of ovarian maturation of the fiddler crab, *Uca pugilator*. Comparative Biochemistry and Physiology. A 111, 279–282.

Sarojini, R., Nagabhushanam, R., Fingerman, M., 1995b. In vivo effects of DA and DArgic antagonists on testicular maturation in the red swamp crayfish, *Procambarus clarkii*. Biology Bulletin 189, 340–346.

Sarojini, R., Nagabhushanam, R., Fingerman, M., 1995c. In vivo inhibition by DA of 5-hydroxytryptamine stimulated ovarian maturation in the red swamp crayfish, *Procambarus clarkii*. Experientia 51, 156–158.

Sarojini, R., Nagabhushanam, R., Fingerman, M., 1995d. Mode of action of the neurotransmitter-5-hydroxytryptamine in stimulating ovarian maturation in the red swamp crayfish, *Procambarus clarkii*: an in vivo and in vitro study. The Journal of Experimental Zoology 27, 395–400.

Sarojini, R., Nagabhushanam, R., Fingerman, M., 1996. In vitro inhibition by dopamine of 5-hydroxytryptamine-stimulated ovarian maturation in the red swamp crayfish, *Procambarus clarkii*. Experientia 52, 707–709.

Schulz, H.F., Vischer, J.E.B., Cavaco, E.M., Santos, C.R., Goos, H.T., Bogerd, J., 2001. Gonadotropins, their receptors, and the regulation of testicular functions in fish. Comparative Biochemistry and Physiology. B 129, 407–417.

Slama, K., Sakai, T., Takeda, M., 2006. Effect of corazonin and crustacean cardioactive peptide on heartbeat in the adult American cockroach (*Periplaneta americana*). Archives of Insect Biochemistry and Physiology 62, 91–103.

Sower, S.A., Freamat, M., Kavanaugh, S., 2009. The origins of the vertebrate hypothalamic–pituitary–gonadal (HPG) and hypothalamic–pituitary–thyroid (HPT) endocrine systems: new insights from lampreys. General and Comparative Endocrinology 161, 20–29.

Terakado, K., 2001. Induction of gamete release by gonadotropin releasing hormone in a protochordate, *Ciona intestinalis*. General and Comparative Endocrinology 124, 277–284.

Tinikul, Y., Mercier, A.J., Soonklang, N., Sobhon, P., 2008. Changes in the levels of serotonin and dopamine in the central nervous system and ovary, and their possible roles in the ovarian development in the giant freshwater prawn, *Macrobrachium rosenbergii*. General and Comparative Endocrinology 158, 250–258.

Tinikul, Y., Soonthornsumrith, B., Phoungpetchara, I., Poljareon, J., Meeratana, P., Duangsuwan, P., Soonklang, N., Mercier, A.J., Sobhon, P., 2009. Effects of serotonin, dopamine, octopamine, and spiperone on ovarian maturation and embryonic development in the giant freshwater prawn, *Macrobrachium rosenbergii* (De Man, 1879). Crustaceana 82, 1007–1022.

Tinikul, Y., Poljaroen, J., Nuurai, P., Anuracpreeda, P., Chotwiwatthanakun, C., Phoungpetchara, I., Kornthong, N., Poomtong, T., Hanna, P.J., Sobhon, P., 2011. Existence and distribution of gonadotropin-releasing hormone-like peptides in the central nervous system and ovary of the Pacific white shrimp, *Litopenaeus vannamei*. Cell and Tissue Research 343, 579–593.

Tsai, P.S., 2006. Gonadotropin-releasing hormone in invertebrates: structure, function, and evolution. General and Comparative Endocrinology 148, 48–53.

Tsai, P.S., Zhang, L., 2008. The emergence and loss of gonadotropin-releasing hormone in protostomes: orthology, phylogeny, structure, and function. Biology of Reproduction 79, 798–805.

Veenstra, J.A., 1989. Isolation and structure of corazonin, a cardioactive peptide from the American cockroach. FEBS Letters 250, 231–234.

Veenstra, J.A., 2009. Does corazonin signal nutritional stress in insects? Insect Biochemistry and Molecular Biology 39, 755–762.

Wongprasert, K., Asuvapongpatana, S., Poltana, P., Tiensuwan, M., Withyachumnarnkul, B., 2006. Serotonin stimulates ovarian maturation and spawning in the black tiger shrimp *Penaeus monodon*. Aquaculture 261, 1447–1454.

Zhang, L., Tello, J.A., Zhang, W., Tsai, P.S., 2008. Molecular cloning, expression pattern, and immunocytochemical localization of a gonadotropin-releasing hormone-like molecule in the gastropod mollusk, *Aplysia californica*. General and Comparative Endocrinology 156, 201–209.

Zohar, Y., Munoz-Cueto, J.A., Elizur, A., Kah, O., 2010. Neuroendocrinology of reproduction in teleost fish. General and Comparative Endocrinology 165, 348–365.